Microbial Engineering and Optimization Strategies for Polyhydroxyalkanoate (PHA) Synthesis

Minglong Li

A thesis submitted in partial fulfilment of the requirements

for the degree of

Doctor of Philosophy

The University of Sheffield

Department of Chemical and Biological Engineering

23/4/2025

Declaration

I, Minglong Li, confirm that the Thesis is my own work. I am aware of the University's Guidance on the Use of Unfair Means (www.sheffield.ac.uk/ssid/unfair-means). This work has not previously been presented for an award at this, or any other, university. Content from Chapter 5 of this thesis has been structured and submitted as a paper to a peer reviewed journal and is currently under review, titled "Microbial synthesis of polyhydroxyalkanoate blends with engineered *Pseudomonas putida*".

Acknowledgments

First and foremost, I would like to express my deepest gratitude to my primary supervisor, Dr. Kang Lan Tee, for her unwavering support and guidance throughout my PhD journey. From the fundamentals of experimental techniques to academic writing and scientific communication, Dr. Tee has provided meticulous training and encouragement. Her guidance was instrumental in helping me navigate the challenges of my research, and without her supervision, this project would not have been possible. I am deeply indebted to her for the skills I have acquired and the confidence I have gained under her mentorship.

I would also like to extend my sincere thanks to my second supervisor, Professor Tuck Seng Wong. His insightful advice, both academically and in terms of career development, has been invaluable. His practical suggestions have been a constant source of direction and support throughout my research.

I am incredibly grateful to Khalid Doudin for providing NMR analysis and technical support for the PHA samples in this project, and to Alan Burling for conducting GPC testing. I would also like to thank Sharon Spey for her assistance with GC-MS analysis, which was critical for the progression of my work. Additionally, I would like to acknowledge the help of Veer Shah and David Robins, who provided significant assistance with data collection and experimental execution.

I am fortunate to have been part of an exceptional research group, and I am thankful to all its members for their collaboration, advice, and support. Their insights and encouragement were instrumental in overcoming the challenges of the research process. I also extend my gratitude to the department and university staff, whose tireless efforts created a stable and conducive environment for research.

Finally, I want to express my heartfelt thanks to my family for their constant

encouragement and support throughout this long academic journey. Their love and belief in me have been my source of strength, especially my father, whose financial support allowed me to pursue my studies. I am also deeply thankful to Zhengxin Lin and my cat, Na Na, for their companionship, as well as my friends, whose presence and encouragement helped me persevere through the most challenging moments.

Abstract

This thesis presents an integrated approach to microbial strain engineering and process optimization for the sustainable production of polyhydroxyalkanoates (PHAs), a family of biodegradable and biocompatible polymers with significant potential to replace conventional plastics. The research focuses on enhancing PHA production, tailoring polymer composition, and evaluating the use of renewable feedstocks in industrially relevant microbial hosts.

A key outcome of this work is the successful construction of genetically engineered *Pseudomonas putida* capable of synthesizing short-chain-length (scl-) and medium-chain-length (mcl-) PHA copolymers through the heterologous expression of the *phaCAB* operon from *Cupriavidus necator*. By systematically evaluating promoter strength, PHA monomer composition was modulated from 17.9 mol% to 99.6 mol% 3-hydroxybutyrate (3HB), with polymer titers reaching up to 1.48 g/L and intracellular PHA content exceeding 42 wt% under glucose-supplemented conditions. Physicochemical characterization using gas chromatography–mass spectrometry (GC-MS), gel permeation chromatography (GPC), nuclear magnetic resonance (NMR), and differential scanning calorimetry (DSC) confirmed the production of structurally distinct polymer blends, with tunable molecular weights and thermal properties aligned with target applications.

In parallel, this thesis explored the integration of synthetic mcl-PHA biosynthetic pathways into native scl-PHA producers, including *Rhodococcus* and *C. necator*. Although functional expression was achieved in *E. coli*, no detectable mcl-PHA production was observed in the native hosts, revealing critical limitations in carbon flux and pathway compatibility. These findings highlight the importance of host-specific engineering strategies and underscore the metabolic rigidity of non-model organisms.

Furthermore, the potential of low-cost, renewable substrates was assessed using sugarcane molasses and potato peel hydrolysate (PPH). *Burkholderia* BCC 59163 achieved PHA accumulation up to 57.01 wt% from molasses, while the engineered *P. putida* demonstrated the ability to produce PHA blends from PPH. However, both substrates presented technical challenges related to nutrient variability, low titers, or process consistency, emphasizing the need for further feedstock optimization.

Overall, this thesis advances the field of sustainable biopolymer production by demonstrating how genetic control, host selection, and feedstock integration collectively determine polymer output and quality. The findings lay a foundation for the development of next-generation microbial platforms capable of producing application-specific PHAs with reduced environmental and economic costs.

Table of content

List of Tables

List of figures

Chapter 1: Introduction

This chapter introduces the motivation, background, and research objectives of this study, focusing on the growing need for sustainable alternatives to petroleum-based plastics. It outlines the potential of polyhydroxyalkanoates (PHAs) as biodegradable polymers and highlights the role of microbial strain engineering in overcoming production challenges. The chapter also defines five specific research objectives that guide the work presented in the subsequent chapters, including strain development, process optimization, substrate utilization, and product characterization.

1.1 Background:

In the face of escalating environmental concerns associated with synthetic plastic pollution, the quest for sustainable alternatives has become imperative. PHAs, a family of biodegradable polymers produced by various microorganisms, emerge as a promising solution. These naturally occurring biopolymers not only offer a biodegradable option but also reduce reliance on non-renewable fossil fuels, as they can be derived from renewable biomass. The significance of PHAs extends beyond their environmental benefits, encompassing diverse applications ranging from biodegradable packaging materials to medical devices such as sutures and drug delivery systems, highlighting their potential to revolutionize the materials industry.

However, the widespread adoption of PHA is hindered by challenges related to production efficiency and cost-effectiveness. These obstacles underscore the necessity of strain engineering—leveraging advanced genetic and metabolic engineering techniques to enhance microbial pathways that synthesize PHAs. By optimizing these biological routes, it is possible to significantly increase the titer of PHA production and improve the physical properties of the polymers, tailoring them to meet specific industrial requirements.

Moreover, the engineering of microbial strains to produce PHAs can lead to improved scalability and economic viability, crucial factors for the transition from laboratory research to industrial application. Strain engineering also offers the opportunity to expand the range of substrates used for PHA production, including the utilization of waste products, thereby promoting a more sustainable and circular approach to biopolymer manufacturing.

This thesis aims to contribute to this burgeoning field by developing enhanced microbial strains capable of efficient PHA production. Through this research, we seek to address the dual challenges of environmental sustainability and material innovation, setting the stage for a future where biodegradable plastics align with the principles of a circular economy and lessen the environmental impact of global plastic use.

1.2 Research objectives

This research project is centered on advancing the field of biopolymer production through comprehensive strain engineering. The primary focus is on utilizing microbial hosts, primarily *Pseudomonas putida* and other engineered strains, to optimize PHA production. The specific objectives that guide this research endeavor are as follows:

1.2.1 Broadening strain engineering

To enhance PHA production capabilities by engineering various microbial strains. This includes introducing and optimizing biosynthetic pathways to improve PHA titer, as well as producing PHAs with varying monomer compositions, thereby influencing the polymer's properties to meet diverse application needs.

1.2.2 Optimization of PHA composition

Producing PHAs with different compositions by modifying metabolic pathways and cultivation conditions of various strains. The aim is to tailor the material properties of PHAs—such as molecular weight, mechanical strength, and thermal stability—to

extend their potential uses across a wider range of industries.

1.2.3 Influence of substrates on PHA production

To systematically assess how different carbon and nitrogen sources affect the titer and quality of PHA in the engineered strains. This objective explores the metabolic adaptability of the strains to various substrates, which could lead to more cost-effective and efficient production processes.

1.2.4 Utilization of sustainable feedstocks

To investigate the feasibility of using sustainable and economically viable feedstocks for PHA production. This includes evaluating agricultural residues and industrial by-products as potential raw materials, aiming to reduce the overall production costs and enhance the environmental sustainability of the process.

1.2.5 Characterization of PHAs

To thoroughly characterize the produced PHAs in terms of their chemical composition and physical properties. Methods such as Gas Chromatography-Mass Spectrometry (GC-MS), Nuclear Magnetic Resonance (NMR), Differential Scanning Calorimetry (DSC), and Thermogravimetric Analysis (TGA) will be employed. These analyses will help in understanding how variations in monomer composition affect the material properties of PHAs.

These objectives are designed to tackle the key challenges in PHA production, focusing on improving the titer, cost-effectiveness, and application range of PHAs through innovative strain engineering. This research aims to contribute significantly to the development of sustainable biopolymers, aligning with global efforts to mitigate the environmental impact of traditional plastics.

In summary, this chapter presented the environmental context motivating this research

and defined the key objectives underpinning the investigation. These objectives form the foundation for the technical strategies explored in the following chapters. In particular, the next chapter provides a detailed review of current literature on PHA biosynthesis, properties, and engineering approaches, thereby establishing the scientific framework for the experimental work that follows.

Chapter 2: Literature review

This chapter reviews the current state of knowledge on PHA and their potential as sustainable alternatives to conventional plastics. It begins with an overview of synthetic plastic pollution and the drivers behind the search for biodegradable materials. The chapter then delves into the structural and functional properties of PHA, their biosynthetic pathways, microbial hosts, and extraction techniques. Emphasis is also placed on metabolic engineering strategies and the influence of substrate selection on polymer titer and composition. Finally, the applications of PHA in various sectors are discussed, and research gaps relevant to this study are identified, forming the basis for the experimental investigations in subsequent chapters.

2.1 Conventional plastics

2.1.1 Introduction to conventional plastics

Conventional plastics, primarily derived from petrochemical industry, encompass a range of synthetic polymers including polyethylene (PE), polypropylene (PP), and polyvinyl chloride (PVC) (Geyer et al., 2017). These materials are prized for their durability, lightweight, and resistance to degradation, characteristics that make them indispensable in a variety of applications. From packaging materials and household goods to components in the automotive and construction industries, the versatility of conventional plastics underpins their widespread use around the world (Moharir and Kumar, 2019, Schmaltz et al., 2020). The global production of plastics has escalated over the past several decades, reaching 400.3 million tons annually and over 90% of it was fossil based (Plastics Europe, 2023). This increase reflects not only the material's utility but also the increasing reliance of human society on plastics as a material, which brings about a series of issues such as the disposal of plastic waste, the dangers plastics pose to humans and the environment.

2.1.2 Environmental and human health impact

Plastic pollution has become one of the most visible and pressing environmental issues worldwide, largely driven by the rapid increase in plastic production and consumption (Schmaltz et al., 2020). Despite the known durability of plastics being a desirable property for industrial applications, it significantly hinders their degradation, thereby leading to long-term environmental persistence (Andrady, 2015). Existing waste management strategies have proven insufficient to mitigate this issue on a global scale.

As of 2015, only about 21% of plastic waste had been effectively processed through recycling or incineration. The remaining 79% typically ends up in landfills or leaks into natural ecosystems, where it can remain for centuries and fragment into microplastics (Afrin et al., 2020, Geyer et al., 2017, Jacques and Prosser, 2021). These microplastics are now pervasive across terrestrial and aquatic ecosystems, raising concerns about their long-term ecological effects (Schmaltz et al., 2020). Furthermore, while incineration offers a method for reducing waste volume, it often results in the emission of hazardous by-products, such as dioxins and furans, especially in facilities with limited pollution control infrastructure (Moharir and Kumar, 2019). This poses significant risks to both environmental and human health.

The full impact of microplastic pollution on human health is not yet fully understood, but emerging evidence indicates a growing concern. Microplastics can accumulate in the food chain, ultimately being ingested by humans (Barboza et al., 2018). Current estimates suggest that humans consume approximately 39,000 to 52,000 microplastic particles annually through food and water intake (Cox et al., 2019). Moreover, these particles can act as vectors for harmful substances such as residual additives and heavy metals used in plastic manufacturing, further increasing health risks (Lusher et al., 2018). Collectively, these issues highlight a complex and deeply rooted challenge that cannot be solved by waste management alone but requires material-level innovation and systemic change.

2.1.3 Solutions and alternatives

In response to the growing environmental and health concerns associated with plastic pollution, various policy and grassroots efforts have been introduced over the past two decades (Adam et al., 2020, Karasik et al., 2020), although most are effective only in certain countries (Dauvergne, 2018). These policies seek to reduce plastic usage through restrictions or taxation. Additionally, local governments and non-governmental organizations are actively promoting the prohibition and reduction of single-use plastic products (Schnurr et al., 2018). Volunteer groups also advocate for reducing the reliance on plastic products. Despite the implementation of numerous initiatives and policies, plastic pollution on a global scale remains largely uncontrolled (Karasik et al., 2020).

Considering the ineffectiveness of numerous measures to mitigate global plastic pollution, the utilization of sustainable and biodegradable alternatives represents a promising avenue for exploration and development. For instance, considerable research has been devoted to biopolymers such as polylactic acid (PLA), polyhydroxyalkanoate (PHA), starch, and lignocellulose (Moshood et al., 2022, Kabir et al., 2020). These biopolymers are capable of biodegradation and exhibit material properties comparable to those of conventional plastics (Chen, 2010). Furthermore, their production and waste management processes exert a relatively lower environmental impact compared to traditional plastics (Sid et al., 2021).

However, the transition to bioplastics is accompanied by a distinct set of technical and economic challenges that limit their widespread adoption. Many alternatives, such as PLA, require specific industrial composting conditions for effective degradation. Others, like starch-based plastics, may lack the mechanical strength needed for certain applications. Moreover, production scalability and economic feasibility remain significant hurdles. As such, biopolymers are not yet a complete substitute for conventional plastics but rather represent a promising and evolving field of research. These challenges emphasize the need for further innovation in both microbial platform

development and process optimization—an area where PHA-based materials offer considerable potential.

2.2 Polyhydroxyalkanoates

2.2.1 Introduction to PHA

PHA is biopolymer synthesized by microorganisms as intracellular storage compound (Poli et al., 2011). These PHA-producing microorganisms are widely distributed in nature, with over 90 identified genera of bacteria known to synthesize these biopolymers (Kim et al., 2007). The initial discovery of PHA dates back to 1926, when French scientist Lemoigne identified a lipid-like intracellular substance in *Bacillus megaterium*, which was later confirmed to be polyhydroxybutyrate (PHB) (Lemoigne, 1926). Subsequent research has built upon this foundational discovery, leading to the identification of two additional monomers, 3-hydroxyvalerate (3-HV) and 3-hydroxyhexanoate (3-HHx), in 1973 (Wallen, 1973). To date, over 150 distinct PHA monomers have been identified, characterized by carbon chain lengths ranging from 3 to 20, with a variety of structures and functional groups (phenoxy, epoxy, cyano, chloro, bromo, and phenyl groups) (Chen, 2010, Choi et al., 2020b). This extensive array of monomers highlights the chemical diversity and the wide range of physicochemical properties intrinsic to PHAs.

2.2.2 Structure of PHAs

PHAs are polyesters composed of 3-hydroxy fatty acid monomers, which are connected through ester bonds. The general chemical structure of PHAs can be represented by the formula [O-CH(R)-CH2-CO]n, where R is a variable side chain that can range from hydrogen to more complex alkyl groups (Raza et al., 2018). **Figure 2.1** shows structure of common PHA monomers (Tan et al., 2014). This side chain variability is what gives PHAs their diverse properties and functionalities (Choi et al., 2020b).

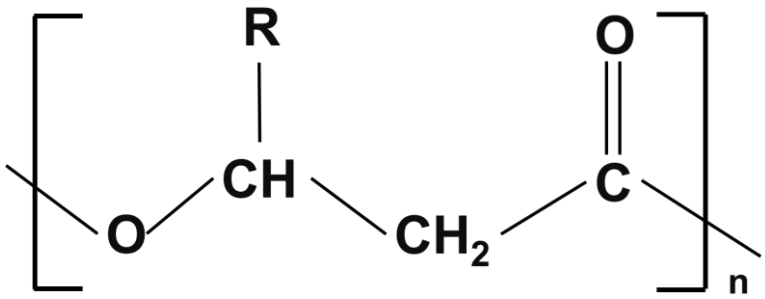

Figure 2.1. The general structure of PHA, side-chin R represents different groups. When the R group is methyl (CH_3), the polymer is named poly(3-hydroxybutyrate); When the R group is propyl (C_3H_7), it is called poly(3-hydroxyhexanoate).

2.2.3 Classification of PHAs

PHA can be categorized based on the number of carbon atoms in their monomer units, which influences their physical and mechanical properties (Anjum et al., 2016, Raza et al., 2018). This classification mainly encompasses short-chain-length PHA (scl-PHA) and medium-chain-length PHA (mcl-PHA), with common monomers shown in **Figure 2.2**. scl-PHA consists of monomers with 3 to 5 carbon atoms while mcl-PHA is composed of monomers containing 6 to 14 carbon atoms. There are studies categorizing PHAs with monomer units containing more than 14 carbon atoms as long-chain-length-PHA (lcl-PHA) but these types of PHAs are relatively rare and less studied (Kunasundari and Sudesh, 2011).

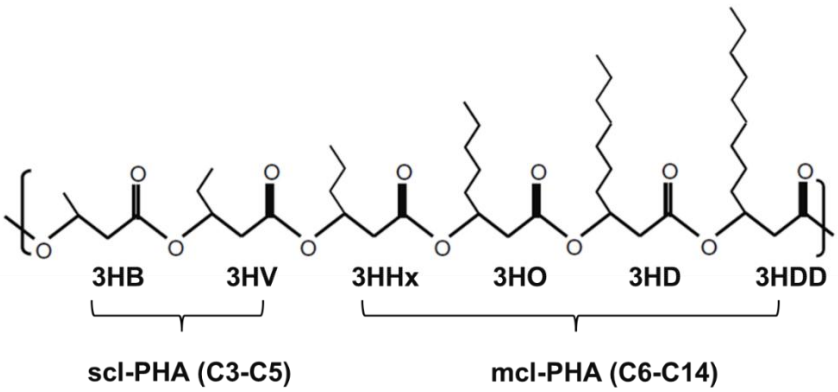

Figure 2.2. PHA structure with common monomer. 3HB (C4), 3-hydroxybutyrate; 3HV (C5), 3-hydroxyvalerate; 3HHx (C6), 3-hydroxyhexanoate; 3HO (C8), 3-hydroxyoctanoate; 3HD (C10), 3-hydroxydecanoate; 3HDD (C12), 3-hydroxydodecanoate.

Additionally, based on the types of monomers, PHAs can also be classified into homopolymers and copolymers (McChalicher and Srienc, 2007, Chen, 2010). PHAs consisting of a single type of monomer are referred to as homopolymers, whereas copolymers are composed of multiple distinct monomers. As mentioned before, the first homopolymer was PHB discovered by Lemoigne in 1926 (Lemoigne, 1926). Subsequent investigations have identified several other homopolymers, including poly(4-hydroxybutyrate) (P4HB), poly[(R)-3-hydroxyvalerate] (PHV), and poly[(R)-3-hydroxyoctanoate] (PHO) (Chen, 2010). Beyond homopolymers, various bacterial species are capable of synthesizing copolymers by incorporating different short-chain-length monomers. Examples include poly[(R)-3-hydroxypropionate-co-(R)-3-hydroxybutyrate], poly[(R)-3-hydroxybutyrate-co-4-hydroxybutyrate], and poly[(R)-3-hydroxybutyrate-co-(R)-3-hydroxyvalerate] (PHBV) (Zhao and Chen, 2007).

2.2.4 Natural PHA producer

It has been nearly a century since the initial discovery of PHA. Currently, 92 bacterial species have been reported as capable of producing PHA (Vicente et al., 2023). *Bacillus megaterium*, the first recognized PHA producer, served as one of the earliest model organisms in research endeavors (Macrae and Wilkinson, 1958). *Cupriavidus necator* is notable for its exceptional capacity to synthesize substantial amounts of PHA and has been extensively utilized in studies aimed at optimizing PHA production (Reinecke and Steinbüchel, 2008). The *Pseudomonas* species is particularly renowned and widely applied due to its ability to utilize diverse carbon sources for the production of mcl-PHA (Mohanrasu et al., 2021). Numerous studies have highlighted its capability to produce PHA with variable monomer compositions (Takase et al., 2004, Wang et al., 2009).

In addition, there are other natural PHA producers, such as *Rhodococcus*, which, although less efficient in PHA production compared to the aforementioned bacteria, are deemed promising due to their broad substrate specificity and environmental

adaptability (Hernandez et al., 2008, Indest et al., 2016). The diversity and existence of these natural PHA producers provide indispensable insights and foundational data for scientific research. **Table 2.1** summarizes the common natural PHA producers and the substrates they utilize.

Although these natural PHA-producing organisms offer valuable insights into microbial biosynthesis, it is essential to critically assess their applicability as hosts for metabolic engineering. Accordingly, the following section provides an in-depth comparative analysis of the bacterial strains selected for this study, with emphasis on their metabolic flexibility, genetic accessibility, and industrial potential.

Table 2.1. Examples of natural PHA producer and different substrates used.

Bacteria Strain	**Substrate**	**PHA type**	**PHA titer (% DCW)**	**Reference**
Bacillus megaterium	Cheese whey	PHB	51.6	(Obruca et al., 2011)
Bacillus megaterium	Lactate	PHB	64.7	(Lee et al., 2022)
Cupriavidus necator	glucose	PHB	80.0	(Ahn et al., 2015)
Cupriavidus necator	Waste glycerol	PHB	50.0	(Cavalheiro et al., 2009)
Pseudomonas putida	glucose	mcl-PHA	16.9	(Huijberts et al., 1992)
Pseudomonas putida	glucose	mcl-PHA	1.7	(Wang and Nomura, 2010)
Rhodococcus ruber	glucose	PHB-co-HV	40.0	(Anderson et al., 1995)
Rhodococcus jostii	gluconate	PHB-co-HV	7.6	(Hernandez et al., 2008)

2.2.5 Bacterial hosts selected in this thesis

A variety of bacterial species have been employed as hosts for PHA biosynthesis, each with distinct metabolic characteristics, environmental resilience, and suitability for genetic engineering. In recent years, increased efforts have been made to move beyond traditional producers and investigate more robust, versatile organisms for sustainable and high-titer biopolymer production. This section critically examines several key bacterial platforms considered in this study.

Cupriavidus necator (formerly *Ralstonia eutropha*) remains one of the most extensively studied organisms for scl-PHA, particularly PHB, accumulation. It demonstrates high PHA titer, efficient carbon conversion, and scalability in industrial fermentation processes (Morlino et al., 2023, Choi et al., 2020b). Its ability to metabolize a broad spectrum of carbon sources, including sugars, organic acids, and industrial by-products, makes it attractive for low-cost production. Importantly, *C. necator* can grow autotrophically using hydrogen and CO_2 as energy and carbon sources, respectively (Jawed et al., 2022), offering a promising route for carbon-neutral production processes. Additionally, it exhibits considerable stress tolerance under suboptimal environmental conditions (Morlino et al., 2023). Its robustness makes it suitable for industrial-scale applications, where conditions are often less controlled than in laboratory environments. These features justify its frequent designation as a model chassis for PHA synthesis. However, its natural PHA synthesis is limited to scl-PHAs unless extensively engineered, potentially restricting its use in tailoring material properties without further metabolic modification.

Another promising platform is *Pseudomonas putida*, a natural producer of mcl-PHA that has attracted growing interest due to its wide metabolic scope and robustness. Capable of utilizing low-cost substrates such as industrial waste streams, *P. putida* supports economically feasible production processes (Loeschcke and Thies, 2015). Its innate tolerance to oxidative and osmotic stress further increases its applicability in large-scale, non-sterile environments (Weimer et al., 2020). Furthermore, the

availability of advanced genetic engineering tools, including CRISPR-based genome editing and efficient plasmid systems, allows for precise modulation of PHA biosynthesis pathways (Loeschcke and Thies, 2020). Notably, *P. putida* is classified as a biosafety level 1 organism, enhancing its utility in laboratory and industrial settings. Its flexibility in redirecting carbon flux towards mcl-PHA synthesis makes it an ideal platform for engineering efforts aimed at improving PHA accumulation and compositional control.

In contrast to these conventional chassis, *Rhodococcus* species offer a unique set of advantages that have only recently begun to be fully explored in the context of PHA biosynthesis. This genus is well-known for its metabolic versatility, with the ability to degrade and utilize a broad range of compounds, including recalcitrant organics like hydrocarbons and aromatic chemicals (Krivoruchko et al., 2019, Martinkova et al., 2009). Their robustness under extreme environmental stresses, such as high solvent concentrations, salinity, and acidic conditions, makes them especially suitable for utilizing waste-derived feedstocks (Cappelletti et al., 2016). Their resilience enhances their applicability in industrial processes that often take place under suboptimal conditions. Given that raw materials like molasses or cellulose hydrolysates often yield suboptimal nutrient profiles or contain residual acid, such traits are critical for strain performance in industrial contexts. Moreover, *Rhodococcus* strains are known for synthesizing a range of valuable products, including biosurfactants, bio-flocculants, carotenoids, and storage compounds such as triacylglycerols (TAG) and PHA (Hernandez et al., 2008). For example, *R. opacus* PD630 can accumulate up to 87% CDW as TAG, while *R. jostii* RHA1 can reach 55% CDW when grown on benzoate (Cappelletti et al., 2020). While the native lipid pathways may compete with PHA synthesis, the abundant intermediate pools offer an opportunity to redirect carbon flux toward PHA via metabolic engineering.

Additionally, species from the *Burkholderia* genus have been investigated for their adaptability and metabolic flexibility (Mendonça et al., 2014). Although less

characterized than *C. necator* or *P. putida*, they demonstrate potential as alternative hosts for PHA production. Notably, their ability to utilize molasses as a carbon source remains underexplored. This gap presents a valuable opportunity to assess their performance in converting industrial by-products into PHAs and expand the repertoire of microbial hosts for sustainable biopolymer synthesis.

Taken together, the selection of various strains in this thesis is grounded in a comparative assessment of metabolic versatility, environmental robustness, and genetic accessibility. This multi-strain strategy aims to exploit their complementary advantages to address current limitations in PHA titer, monomer composition control, and the use of low-cost, sustainable feedstock.

2.2.6 Biosynthesis pathway and key enzymes

PHA production involves multiple biosynthetic routes and a complex enzyme system, with the most common pathways illustrated in **Figure 2.3** and their associated enzymes summarized in **Table 2.2**. Among these, Pathway I enables microorganisms to synthesize PHB from carbohydrates. Sugar was firstly transferred into acetyl-CoA, then acetoacetyl-CoA to 3-hydroxybutyryl-CoA which would be polymerized by PHA synthase to produce PHB (Huisman et al., 1989, Chen, 2010, Meng et al., 2014). A PHA degradation pathway is commoned found in many organisms associated with the following enzymes: PHA depolymerase, dimer hydrolase, 3-hydroxybutyrate dehydrogenase, and acetoacetyl-CoA synthase. This degradation pathway was found in lots of strains such as *Aeromonas hydrophila*, *Cupriavidus necator*, and *Pseudomonas oleovorans* (Sudesh et al., 2000).

In Pathway II, fatty acids are first oxidized (β-oxidation) within the bacterial cells. PhaJ enzyme helps to convert precursors from β-oxidation pathway and to PHA production by transferring enoyl-CoA to R-3-Hydroxyacyl-CoA, which can be further used as substrate by PhaC. Pathway II is commonly existing in the bacteria with capability to

accumulate mcl-PHA such as *Pseudomonas* sp and *A. hydrophila* (Sudesh et al., 2000, Choi et al., 2020b). In pathway III, PhaG enzyme works by leading carbon flux from the fatty acid de novo synthesis to PHA production. Acetyl-CoA from pathway I first enters the fatty acid synthesis to supply R-3-Hydroxyacyl-ACP as substrate of PhaG, followed by polymerization of corresponding 3HA-CoA. NADH-dependent acetoacetyl-CoA reductase is used to oxidize (S)-3-hydroxybutyryl-CoA in pathway IV (Chen, 2010), with remaining reactions carried out by the PhaB and PhaC enzymes from Pathway I.

A critical enzyme in all PHA biosynthetic pathways is PHA synthase (PhaC), which catalyzes the polymerization of (R)-hydroxyalkanoate-CoA monomers. The presence of different PhaC enzymes in various microorganisms enables the production of PHA with diverse compositions (Bhubalan et al., 2011). PhaCs are currently grouped into four types based on their substrate specificity and preference for synthesizing either scl-PHA or mcl-PHA (Chek et al., 2019, Zher Neoh et al., 2022). Specifically, type I, III, and IV PhaCs primarily synthesize scl-PHA, whereas type II PhaCs preferentially produce mcl-PHA, incorporating monomers with more than five carbon atoms.

However, exceptions exist, such as the type II PhaCs from certain *Pseudomonas* species, which can synthesize $PHA_{scl\text{-}mcl}$ containing both scl and mcl monomers with varying chain lengths (Sudesh et al., 2000). Significant efforts have been made to manipulate the composition formula of mcl and scl monomers or to broaden the substrate range for producing $PHA_{scl\text{-}mcl}$ (Shen et al., 2011). From the perspective of PhaC enzyme research, it is possible to produce customized PHA with targeted properties (Zher Neoh et al., 2022).

Table 2.2. Major enzymes involved in different PHA synthesis pathways.

Pathway	Abbreviation	Enzyme	Species	Reference
Pathway I	PhaA	β-Ketothiolase	*C. necator*	(Huisman et al., 1989, Meng et al., 2014, Chen, 2010)
	PhaB	NADPH dependent acetoacetyl-CoA reductase		
	PhaC	PHA synthase		
PHA degradation	PhaZ	PHA depolymerase	*A. hydrophila*	(Sudesh et al., 2000)
		Dimer hydrolase	*P. stutzeri*	
		(R)-3-Hydroxybutyrate dehydrogenase	*C. necator*	
		Acetoacetyl-CoA synthase	*P. oleovorans*	
Pathway II	FadD	acyl-CoA synthetase	*P. aeruginosa*	(Choi et al., 2020b)
	FadE	acyl-CoA dehydrogenase;		
	FadB	3-hydroxyacyl-CoA dehydrogenase		
	FadA	3-ketoacyl-CoA thiolase		
	PhaJ	enoyl-CoA hydratase		
Pathway III	FabD	malonyl-CoA:ACP transacylase	*P. mendocina*	(Choi et al., 2020a, Klinke et al.,

Pathway	Abbreviation	Enzyme	Species	Reference
	FabB	β-ketoacyl-ACP synthase I		1999)
	FabF	β-ketoacyl-ACP synthase II		
	FabG	3-ketoacyl-ACP reductase		
	FabA	3-hydroxyl-ACP dehydrase		
	FabI	enoyl-ACP reductase		
	PhaG	3-Hydroxyacyl-ACP-CoA transferase		
Pathway IV		NADH-dependent acetoacetyl-CoA reductase	*Rhizobium (Ciser)* sp.	(Meng et al., 2014)

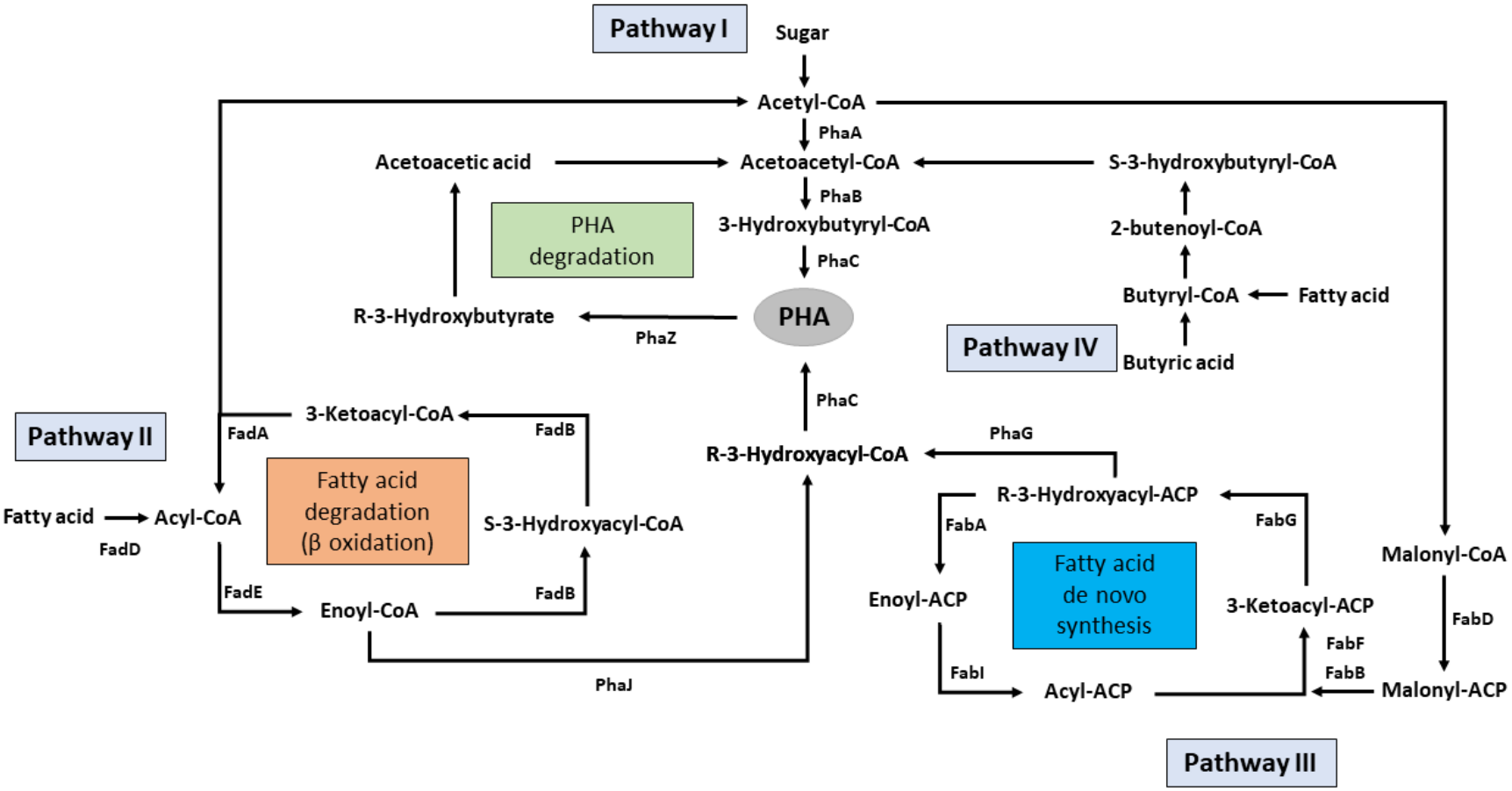

Figure 2.3. Four common biosynthesis pathways for PHA production (Salvachua et al., 2020, Choi et al., 2020a).

2.3 Properties of PHAs

2.3.1 General properties

Although the diversity of monomers imparts a wide range of properties to PHAs, these polymers still share many common characteristics. In general, PHAs exhibit properties analogous to those of petroleum-based plastics (Keskin et al., 2017). PHAs are characterized by their insolubility in water and solubility in chlorinated solvents such as chloroform. They demonstrate excellent gas barrier properties and are resistant to ultraviolet radiation (Raza et al., 2018). A particularly significant attribute of PHAs is their biodegradability, which enables their decomposition in natural environments (Bugnicourt et al., 2014). Furthermore, PHAs exhibit notable biocompatibility. This combination of biodegradability and biocompatibility positions PHAs as promising materials for sustainable and biomedical applications (Chen, 2010).

However, despite these advantages, PHAs are not universally suitable for all industrial applications. Their relatively high production cost, brittleness (particularly in PHB), and thermal instability have limited their competitiveness compared to petroleum-based plastics in large-scale, low-cost uses. Moreover, while the gas barrier properties are advantageous in packaging, the moisture sensitivity and slower degradation in non-composting environments remain concerns for broad commercialization. These factors necessitate further composition and structural tuning, such as PHA blending and copolymerization to enhance their performance and expand their applicability.

2.3.2 Molecular weight

As with other polymeric materials, the molecular weight (Mw) of PHA plays a crucial role in determining its mechanical and thermal properties. Table 2.3 lists representative molecular weights of various PHA types. Interestingly, the same chemical composition does not always yield identical molecular weights, and substantial variability exists depending on microbial strain, cultivation conditions, and carbon source. For example, PHB synthesized by different bacterial species can vary widely in molecular weight

(Myshkina et al., 2008, Chanprateep et al., 2010), while *Pseudomonas* species produce mcl-PHAs with notably different molecular weights depending on the substrate provided (Ashby et al., 2002, Liu et al., 2011).

The molecular weight of PHA exhibits significant variation (0.5×10^5 to 35×10^5), with its polydispersity index (PDI) ranging from 1.1 to 6.0 (Kumar et al., 2013). The PDI is a critical parameter indicating the distribution of molecular weights within a polymer sample, calculated as the ratio of the weight-average molecular weight (M_w) to the number-average molecular weight (M_n). This index is pivotal in determining the heterogeneity of polymer mixtures concerning molecular size. A broad PDI range complicates the determination of copolymer uniformity, particularly for copolymers with substantial discrepancies between M_w and M_n. This variability arises due to the uncertain patterns in their thermal and mechanical properties (Singh et al., 2015). The performance characteristics of polymeric compounds, including plasticity, crystallinity, elastic behavior, and mechanical resistance, are profoundly influenced by their composition and molecular weight. Studies have shown that PHAs with higher average molecular weights exhibit greater mechanical strength, making them more suitable for use as high-strength materials (Iwata, 2005).

Table 2.3. Molecular weight and polydispersity index of various PHA.

Strains and Substrate	**PHA Composition (mol%)**	**Mw ($\times 10^5$ Da)**	**PDI**	**Reference**
Azotobacter Glucose	PHB	12-16	-	(Myshkina et al., 2008)
Aeromonas Lauric acid + valeric acid	3HB:66, 3HV:21, 3HHx:13	12.7	2.3	(Zhang et al., 2009)
Pseudomonas Glucose	3HHX:3, 3HO:13, 3HD:42, 3HTD, 3HDD:5, 3HDDE:37	3.4	3.7	(Ashby et al., 2002)

Strains and Substrate	PHA Composition (mol%)	Mw ($\times 10^5$ Da)	PDI	Reference
Pseudomonas Dodecanoic acid	3HHx:15, 3HO:40, 3HD:30, 3HDD:15	1.0	1.2	(Liu et al., 2011)
Cupriavidus Fructose	PHB	6.5	1.8	(Chanprateep et al., 2010)
Cupriavidus valeric acid + 4HB-Na	3HB:10, 3HV:40, 4HB: 50	11	1.1	(Chanprateep and Kulpreecha, 2006)
Bacillus Fatty acids	3HB:100-59, 3HV:0-48	8.4	3.9	(Tajima et al., 2003)
Enriched mixed culture Acetic acid	3HB:98.4, 3HV:1.6	4.9	1.9	(Jiang et al., 2009)

Current literature offers varied reports on optimal molecular weight ranges for different applications—ranging from medical implants to biodegradable films—but there is no standardized benchmark for application-specific requirements. This inconsistency highlights a gap in understanding how to tailor molecular weight during biosynthesis. Furthermore, studies exploring the link between carbon source modulation and PDI control remain relatively limited, presenting a potential avenue for improving the quality and predictability of PHA-based materials.

2.3.3 Thermal properties

The thermal properties of PHA polymers are critical in determining the optimal thermal conditions in terms of processing and application. The melting temperature (T_m) of a polymer defines the point at which it transitions from a crystalline phase to an amorphous solid phase. For effective polymer processing, a substantial difference

between the T_m and the degradation temperature (T_d) is essential (Singh et al., 2015). The glass transition temperature (T_g) signifies the transformation of the polymer from a glassy, brittle state to a soft, pliable state above T_g. The T_g of PHA typically ranges from -53°C to 10°C, while the T_m ranges from 37°C to 179°C (**Table 2.4**), both of which are influenced by the monomer composition of the PHA (Dai et al., 2008, Bengtsson et al., 2010).

The T_m of PHA is primarily influenced by the 3-hydroxybutyrate (3HB) component and is also affected by the incorporation of medium-chain-length monomers (Chanprateep et al., 2010, Zhang et al., 2009, Ashby et al., 2002). Homopolymer PHB exhibits a higher melting point (171-179°C) compared to other homopolymers such as poly(3-hydroxyvalerate) [P(3HV), 103°C] and poly(4-hydroxybutyrate) [P(4HB), 53°C]. Consequently, when PHB forms copolymers with other monomers like 3HV, the T_m of the copolymer PHBV decreases relative to that of the homopolymer PHB. As the mole fraction of the 3HV monomer increases from 5% to 70%, the melting point of the PHA copolymer decreases from 170°C to 87°C (Chanprateep et al., 2010).

A similar trend is observed for the glass transition temperature. For example, the T_g of PHB (2.5-10°C) is significantly higher than that of a PHBV copolymer containing 90% 3HV. mcl-PHA exhibits substantially lower T_m and T_g compared to PHB. When medium-chain monomers are incorporated into the PHB backbone, both Tg and Tm decrease. For instance, even with just 10-12% of the 3-hydroxyhexanoate (3HHx) monomer, the T_m of the PHA copolymer decreased to 96-127°C, and T_g decreased to -1.2°C (Zhang et al., 2009). A similar effect is observed in PHA composed of more complex monomer compositions (Bengtsson et al., 2010). In the terpolymer P(3HB-co-3HV-co-3HHx), as the molar content of 3HB decreases from 75% to 48%, T_m decreases from 101°C to 54°C, and T_g decreases from -1.9°C to -5.1°C. This demonstrates the profound influence of monomer composition on the thermal properties of PHA polymers.

Nevertheless, despite this tunability, limitations remain in achieving thermal stability

comparable to that of conventional plastics. Narrow processing windows between Tm and Td constrain PHA utility in high-temperature applications. Moreover, the variability in thermal properties across different microbial production systems introduces challenges in reproducibility and standardization. Current research often focuses on empirical modification of monomer composition but lacks a comprehensive understanding of the molecular-level mechanisms dictating thermal transitions. Addressing this knowledge gap is critical for advancing PHA performance in thermally demanding sectors.

2.3.4 Mechanical properties

The mechanical properties of PHA polymers, including crystallinity, elongation, and tensile strength, are critical indicators of their processability and end-use performance. These properties are inherently linked to the polymer's molecular structure and composition, which can be tailored through microbial synthesis and post-synthetic modifications. Within bacterial cells, PHAs exist as spherical granules with diameters typically ranging from 50 to 500 nanometers, providing a natural, intracellular storage form. The crystallinity of PHA, which significantly affects its thermal stability and biodegradability, is influenced by factors such as molecular weight and monomer composition (Tsuge et al., 2009, Ashby et al., 2002, Pan and Inoue, 2009). For instance, homopolymer PHB with lower molecular weight tends to exhibit higher crystallinity and increased brittleness, limiting its flexibility and processability.

Crystalline morphology also varies: PHB crystallizes into α-form lamellar structures and β-form zigzag conformations. The β-form, associated with higher molecular weight polymers, contributes to improved mechanical strength and thus offers enhanced suitability for film and fiber applications (Pan and Inoue, 2009, Iwata, 2005). However, such binary classification may oversimplify the structural complexity of PHAs, as intermediate or mixed-phase behavior is often observed but insufficiently characterized in the literature—suggesting a need for more nuanced crystallographic analysis.

Crystallinity values range from 0% to 70%, largely depending on the 3HB content. Homopolymer PHB demonstrates higher crystallinity than its copolymer counterparts (Patel et al., 2009). When the 3HV monomer content increases from 8% to 15-18%, the crystallinity of PHBV polymers decreases from 57.3% to 44%. Researchers have successfully produced a range of PHA polymers with varying properties, including brittle and flexible types, by altering the 4HB monomer content in copolymers (Chanprateep et al., 2010). Additionally, the incorporation of longer carbon chain monomers, such as 3HHx, results in PHA becoming more amorphous, thereby reducing its crystallinity (Zhao and Chen, 2007).

The elastic modulus (**Table 2.4**) is an indicator of the rigidity of PHA. Common mcl-PHA (elastic modulus: 0.002 GPa) tends to be flexible, whereas scl-PHA (elastic modulus: 3.5 GPa) is typically brittle (Singh et al., 2015). The elongation at break measures the ability of a material to be stretched without breaking. The wide range of elongation values endows PHA with diverse characteristics, ranging from low-elongation rigid materials to high-elongation flexible materials. Tensile strength, which represents the pressure required to stretch a material until it ruptures, varies between 0.9 and 190 MPa for PHA (Singh et al., 2015). The changes in T_m, T_g, and crystallinity due to variations in chemical composition also manifest in the mechanical performance of PHA. For example, as the 4HB content in copolymers increases, the elastic modulus of PHA decreases, and the elongation increases, making the polymer more flexible (Akaraonye et al., 2010, Chanprateep et al., 2010).

While these findings underscore the tunability of PHA, current literature tends to emphasize compositional effects without sufficiently exploring how such tunability can be strategically harnessed to design materials with both performance and sustainability. Therefore, further research is needed to bridge the gap between composition-property relationships and application-specific requirements.

2.3.5 Comparison with traditional plastics

Table 2.4 summarizes the mechanical properties of several commonly used traditional plastics. Compared to these materials, PHAs exhibit a broader and more tunable range of elastic moduli, primarily due to their variable monomer composition. In contrast, traditional plastics typically possess fixed mechanical profiles—for instance, polystyrene (PS) and polyvinyl chloride (PVC) are known for their high rigidity, while polyethylene (PE) offers greater flexibility but limited strength variation. This compositional rigidity restricts the adaptability of traditional plastics for multifunctional applications.

In terms of elongation at break and tensile strength, PHAs and traditional plastics demonstrate overlapping ranges. However, this similarity can be misleading if not considered alongside the structural origins of these properties. While synthetic polymers rely on chemical additives or copolymer blending to modify performance, PHA properties can be inherently tailored through biosynthetic pathways, offering a more integrated and potentially less toxic alternative.

Overall, PHAs can match the performance of traditional plastics in many applications. However, the key differentiator lies in their compositional flexibility and biological origin. The ability to biosynthetically engineer PHAs with specific mechanical profiles introduces a new paradigm in polymer design. Despite these advantages, current literature tends to focus more on biodegradability than on performance-based comparisons, indicating a gap in studies that rigorously benchmark PHAs against conventional plastics under standardized processing and usage conditions. Addressing this would strengthen the case for PHAs as viable commercial alternatives beyond ecological benefits.

2.3.6 Property modifications

The diversity of monomer types and compositions is a significant factor contributing to

the varying properties of PHA. However, this natural variability alone does not fully meet the diverse performance requirements for broader industrial or biomedical applications. Therefore, deliberate control and enhancement of PHA properties are essential. Over the years, researchers have attempted to modify and improve the properties of PHA through various approaches. Physical modification methods, such as blending, and chemical methods, such as incorporating different functional groups, have been explored to achieve these improvements (Li et al., 2016).

Blending is an effective, simple method to produce polymer with altered properties by adjusting materials, conditions, and compositions of blending. It is particularly attractive due to its low cost and scalability. An effective way to generate PHA blend is to mix it with synthetic biodegradable polymers and natural raw materials, resulting in interesting properties with low-cost. Cellulose derivatives have attracted considerable research attention due to their broad application range and compatibility with PHA (Sharma et al., 2021). In a study on blends of PHB and ethyl cellulose, the blend with varying glass transition temperature was observed to increase as the PHB content decreased (Zhang et al., 1997). El-Shafee et al. (El-Shafee et al., 2001) found that when cellulose acetate butyrate (CAB) was distributed within the crystalline structure of PHB, the mechanical strength of the blend improved, with elongation increasing from 2.2% to 7.3%. Another significant finding by Mousavioun's team showed that the addition of lignin enhanced the thermal stability of PHB (Mousavioun et al., 2012), increasing its potential for use in temperature-sensitive applications. Further study has explored how blending with synthetic biodegradable polymers, such as polylactide (PLA), affects the properties of PHA (Takagi et al., 2004), confirming that blending is an effective method to modify PHA properties.

Table 2.4. Thermal and mechanical properties of PHA and petroleum-based polymers.

Polymer type	Monomers	T_m (°C)	T_g (°C)	Elastic modulus (GPa)	Elongation to break (%)	Tensile strength (MPa)	Reference
PHA							
homopolymer	3HB	171-179	2.5-10	1.1-3.5	0.4-5.0	19-40	(Chanprateep and Kulpreecha, 2006, Chanprateep et al., 2010, Zhang et al., 2009, Ashby et al., 2002)
homopolymer	4HB	53	-48	149	1000	104	(Akaraonye et al., 2010)
copolymer	3HB, 3HV	87-170	-13-2.2	0.8-1.37	30-100	20-70	(Chanprateep et al., 2010)
copolymer	3HB, 4HB	150-169	-10 to -2	0.66-1.23	10.7-48	0.87-2.98	(Chanprateep et al., 2010)
copolymer	3HB, 3HHx	96-127	-1.2	0.5	113-400	9.4-21	(Zhang et al., 2009)
copolymer	3HB, 3HV, 3HHx	54-101	-5.1 to -1.9	0.07-0.1	740-833	12.8-14.3	(Bengtsson et al., 2010, Zhang et al., 2009)
mcl-PHA	3HHx, 3HO,	37-40	-53 to -49	-	-	-	(Ashby et al., 2002)

Polymer type	Monomers	T_m (°C)	T_g (°C)	Elastic modulus (GPa)	Elongation to break (%)	Tensile strength (MPa)	Reference
	3HD, 3HDD, 3HTD						
petrol-based							
polyethylene	ethylene	88-132	-36	0.05-1.0	12-700	10-78	(Singh and Mallick, 2009, Castilho et al., 2009, Chanprateep et al., 2010)
polyvinylchloride	Vinyl chloride	100-260	82	3.4	20-80	10-60	(Castilho et al., 2009)
polypropylene	propylene	170-176	-10	0.6-1.7	400-900	27-38	(Singh and Mallick, 2009, Akaraonye et al., 2010)
polystyrene	styrene	110-240	100	3.0-3.1	3-4	50	(Castilho et al., 2009, Akaraonye et al., 2010)

Another type of method for improving PHA properties is through chemical modification, which typically involves introducing different functional groups into the monomer structure. Although more complex than blending, this approach can impart unique properties to PHA. For example, incorporating carboxyl groups can enhance the hydrophilicity of PHA, thereby improving its water permeability (Kai and Loh, 2014). Halogenation is another method to modify PHA by inserting or substituting halogen atoms (chlorine, bromine and fluorine) into the polymer, altering its properties. Chlorination of PHA can be obtained when passing chlorine gas through a solvent containing unsaturated PHA, which has been found to increase both the melting and glass transition temperature (Arkin et al., 2000). Epoxidation is also a significant strategy for modifying PHA properties. Using m-chloroperoxybenzoic acid (m-CPBA), Bear et al. (Bear et al., 1997) successfully conducted epoxidation on mcl-PHA, incorporating epoxy groups and increasing the thermal stability of the polymer.

In summary, both blending and chemical modification have proven effective in tailoring PHA properties, yet each approach has notable limitations that restrict its full industrial translation. A significant research gap remains in understanding how structurally diverse PHA particularly those engineered via metabolic and genetic tools, responding to these modification strategies in a predictable and controllable manner. This thesis aims to address this gap by combining strain engineering, promoter modulation, and downstream characterization to enable more rational design of PHA materials with tunable performance.

2.4 Substrate utilization

2.4.1 PHA composition influenced by carbon sources

Carbon sources are a critical consideration in PHA production, reported to constitute approximately 50% of the overall production cost (Kim, 2000). The utilization of carbon sources by various strains is influenced by their distinct physiological and biochemical characteristics, which then affects the composition of the produced PHA (Raza et al.,

2018). For example, *Pseudomonas putida* has been demonstrated to synthesize PHA with diverse functional groups in the side chains, including phenyl, phenoxy, olefin, halogens, alkyls, and esters (Kim et al., 2000). This diversity is observed when cultivating cells on substrates with different specific chemical structures.

A study found that *Pseudomonas* species DR2 cultivated on various carbon sources (such as glucose, citrate, glycerol, acetate, and corn oil) can accumulate PHA with different titer. The highest PHA production (37.3% w/w of cell dry weigh, CDW) was detected when using corn oil as the sole carbon source, followed by 23.5% using waste fried oil (Song et al., 2008). Therefore, selecting an appropriate carbon source is crucial as it significantly impacts both the titer and the monomer composition of the produced PHA.

2.4.2 Impact of carbon-to-nitrogen ratio

Numerous studies have demonstrated that the carbon/nitrogen (C/N) ratio in the medium significantly affects PHA production and cell growth (Ahn et al., 2015, Cui et al., 2017). The C/N ratio serves as a key regulatory factor in microbial metabolism, influencing the partitioning of resources between biomass formation and polymer storage. Generally, an elevated C/N ratio in the medium enhances PHA accumulation within cells, while a reduction in the C/N ratio has been shown to adversely impact cell growth.

A research conducted by Basaket found that more PHA can be produced after cultivating cells under nitrogen-limited conditions (chemical oxygen demand/nitrogen: 100/2) (Basak et al., 2011). They reported a maximum PHA accumulation of 43.3% (w/w) CDW when cultivation of cells was performed with activated sludge as carbon source. Another study revealed that varying the C/N ratio in the medium significantly influences PHA production and composition in *P. nitroreducens* (Yao et al., 1999). The research indicated that increasing the C/N ratio resulted in a decrease in 3-

hydroxybutyrate (3HB) content from 100% to 7% in the produced PHA, while the total produced PHA surged from 0.5% to 33.5% of CDW, even though cell growth was negatively affected. Understanding the interplay between the C/N ratio, PHA accumulation, and cell growth provides valuable insights for managing these variables. In the fermentation process, one strategy is to keep an excess carbon source in the medium during cultivation to boost PHA production (Preusting et al., 1993).

These findings underscore the complex trade-off between maximizing PHA accumulation and maintaining sufficient cell biomass for sustainable production. A high C/N ratio typically induces a stress response that triggers intracellular carbon storage in the form of PHA, but may also suppress essential growth processes, especially when nitrogen becomes critically limiting. However, optimizing the C/N ratio in the context of genetically modified organisms and mixed substrates requires further investigation. This research seeks to bridge this gap by integrating cultivation condition optimization with strain engineering to achieve higher PHA titers with controllable composition.

2.4.3 Sustainable carbon feedstock

Numerous carbon feedstocks have been explored to produce PHA; however, the production or preparation of these carbon sources often incurs high costs. Especially the expense of pure carbon sources, such as glucose, remains a significant limitation. Consequently, there is a need for more economic and sustainable alternatives. Research has investigated the utilization of waste materials, including sugar cane molasses, hydrolysate from sunflower stalks, lignocellulosic hydrolysate, and hydrolysate from waste office paper (Van-Thuoc et al., 2008, Choi et al., 2020b, Huang et al., 2006). These waste materials are byproducts of other industrial processes and are more cost-effective than traditional feedstock like glucose. Beyond cost efficiency, their use also contributes to circular bioeconomy principles by valorizing waste streams and reducing the environmental footprint of PHA production.

Wheat is extensively cultivated worldwide, and its hard outer layer, known as bran, is rich in proteins, carbohydrates, and minerals that are potentially valuable for microbial utilization. Employing wheat bran as a feedstock can significantly reduce PHA production costs while addressing the issue of bran waste disposal. Research has demonstrated the viability of using wheat bran as a carbon source. For example, the cultivation of *Halomonas boliviensis* LC1 with wheat bran resulted in a PHB titer of 1.08 g/L (Van-Thuoc et al., 2008). Additionally, another study reported a PHA content of 55.6% (w/w) CDW from *Haloferax mediterranei* when strain was cultured with rice bran and corn starch as substrates (Huang et al., 2006). These findings highlight promising strategies to lower production costs and mitigate the environmental impact of agricultural waste.

Starch is an economical material for feedstock; however, its accessibility is limited because many microorganisms lack the ability to produce starch α-amylase. Consequently, an external supply of this enzyme is necessary for these microbes to hydrolyze and utilize starch as a carbon source. The strain *Haloferax mediterranei* can accumulate PHA up to 43% (w/w) of CDW when cultivated on enzymatically extruded starch (Chen et al., 2006). Alternatively, starch can be pre-converted into a form that cells can absorb. For instance, when *C. necator* utilizes saccharified waste potato starch as the sole carbon source in a high cell density fed-batch cultivation system, PHA production can reach 55% (w/w) of CDW (Haas et al., 2008). These studies demonstrate the potential of carbohydrate-rich waste, although the need for enzymatic pretreatment can offset cost savings.

Molasses, a viscous byproduct of the sugar cane extraction industry, contains nutrients conducive to microbial growth, such as sucrose, glucose, fructose, iron, magnesium, calcium, and vitamins (Shasaltaneh et al., 2013). One study reported that *Bacillus* sp. strain COL1/A6 produced 6.0 g/L of PHA when utilizing sugar-cane molasses for cultivation (Raza et al., 2018). Furthermore, *Pseudomonas fluorescens* A2a5, cultivated on a medium with inexpensive sugar cane liquor, yielded PHA constituting

70% (w/w) of CDW, significantly lowering production costs (Jiang et al., 2008). Another investigation demonstrated that the pH of the culture medium influenced PHA composition when sugar cane molasses was used, and noted that high ammonia concentrations negatively impacted PHA biosynthesis, consistent with the previously discussed low C/N ratio (Albuquerque et al., 2007). Additionally, research regarding growing *Pseudomonas aeruginosa* EBN-8 mutant in clarified molasses based medium achieved 1.67 g/L biomass and 1.45 g/L rhamnolipids, though PHA accumulation was not specified; this species is also widely reported for PHA production (Raza et al., 2007). Although these studies are on the laboratory scale, the findings highlight the potential of sugar-cane molasses as an economical feedstock for PHA production. While molasses is widely available and affordable, its complex composition may introduce variability, necessitating process optimization.

Waste vegetable oils are also considered a promising carbon source for bacterial production of rhamnolipids and PHA (Haba et al., 2007, Marsudi et al., 2008). Numerous microorganisms already have been explored for PHA biosynthesis from these waste oils. Haba and his colleagues cultivating *Pseudomonas aeruginosa* 47T2, successfully producing 7.6 g/L of PHA and 10 g/L of rhamnolipids (Haba et al., 2007). During the characterization of PHA from waste oils, seven congeners were identified, with the most abundant monomeric units being C10:0 and C12:0. This suggests that oils promote the production of mcl-PHA monomers, as they inherently contain long-chain fatty acids.

Wastewater, which contains numerous pollutants and heavy metal ions, is typically unsuitable for biological growth. However, when properly treated, many microorganisms can thrive in wastewater environments. A prime example is the activated sludge process in wastewater treatment, which utilizes microbes to degrade contaminants. The *Azotobacter vinelandii* UWD strain has been observed to synthesize PHA up to 58% (w/w) of CDW when grown in swine wastewater (Ryu et al., 2008). Additionally, a combination of acetate and paper pulp wastewater as carbon

sources resulted in a PHA accumulation of 43% (w/w) of CDW (Yan et al., 2006), with the microbes for this study being sourced directly from activated sludge. Furthermore, the development of biorefinery technology has led to studies on producing PHA from gases like CO, CO2, and CH4 (Durre and Eikmanns, 2015, Lee et al., 2021). Utilizing greenhouse gases in microbial processes not only offers the potential for ultra-low-cost PHA production but also presents a strategy for mitigating global warming if implemented on a large scale.

Transforming waste into valuable products can address both economic and environmental related issues but there are challenges remaining to be overcome. Despite the advantages of waste utilization, PHA production remains unstable due to impurities and the changing chemical composition in waste materials. As discussed above, the use of various waste materials as substrates results in differing levels of PHA accumulation. PHA content ranges from 8% (w/w) to 89.1% of CDW from waste feedstocks such as whey, corn starch, wheat bran, sugar-cane molasses, bean curd waste, and waste frying oils (Kim, 2000, Teresa Cesario et al., 2014, Obruca et al., 2014). To manage these variations, optimizing PHA production at the laboratory scale is crucial. These optimization processes, however, require time and financial investment.

While producing PHA from waste can significantly alleviate the environmental burden associated with waste management, the resulting PHA often contains numerous impurities that limit its direct application in various fields, particularly those requiring non-toxic products, such as the medical sector. Additionally, biological contaminants like viruses, bacteria, or plasmids may be present in PHA derived from waste, further restricting its medical use (Koller et al., 2013b, Koller et al., 2013a). Impurities such as endotoxins, proteins, lipids, and DNA have been identified from PHA produced with waste feedstocks. Effective removal of these contaminants necessitates downstream recovery and washing processes, which incur additional expenses. Similar purification expense must be taken into account when using many waste materials as feedstocks,

including the separation of PHA from wastewater (Volova et al., 2003).

In conclusion, although sustainable carbon sources offer a promising route to low-cost and environmentally friendly PHA production, their effective application is hindered by substrate inconsistency, impurity burden, and the need for strain-specific process adjustments. Current research largely focuses on demonstrating feasibility at lab scale, with limited translation into robust, scalable systems. A major research gap remains in developing engineered strains and adaptive bioprocesses capable of tolerating substrate heterogeneity while maintaining high titer and polymer quality. This work addresses that gap by integrating metabolic engineering with feedstock flexibility to support scalable PHA production using sustainable carbon sources.

2.5 PHA extraction method

Since PHA is primarily an intracellular inclusion, extracting it from microbial cells is both complex and expensive. Over the years, scientists have developed and summarized numerous PHA extraction methods through extensive experimentation. Each method has its own set of advantages and disadvantages. The choice of method often depends on the downstream application, desired purity, polymer integrity, and environmental impact. This section critically reviews major extraction techniques, highlighting their efficiencies, limitations, and relevance to scalable, sustainable production systems.

2.5.1 Extraction using solvent

Solvent extraction is the most employed method for PHA recovery due to its simplicity and ease of operation. The process involves several key steps: breaking down the cell membrane to access PHA granules, dissolving the granules in an appropriate solvent, and precipitating them in a non-solvent. Based on the properties of PHA, chlorinated solvents such as chloroform, 1,2-dichloroethane, acetone, and ethylene carbonate are ideal for solubilizing PHA from cell debris (Bugnicourt et al., 2014). To precipitate PHA from these solvents, chilled methanol or ethanol can be used as non-solvents. Solvent

extraction is particularly advantageous for purifying PHA for applications like medical use because it preserves the integrity of the polymer and effectively removes cell endotoxins (Jacquel et al., 2008).

In a study examining various solvents, including tetrahydrofuran (THF), 2-propanol, n-hexane, acetone, ethyl acetate, and methylene chloride, for the extraction of PHA at room temperature, methylene chloride yielded the highest recovery rate at 86% (w/w) (Furrer et al., 2007). When acetone and ethyl acetate were utilized, the presence of 10% impurities was noted; however, the purity of the PHA significantly increased to nearly 100% after precipitation with methanol. The results indicated that all tested solvents, except for 2-propanol, could nearly achieve 100% recovery of low-endotoxin-contaminated mcl-PHA from biomass. Although n-hexane demonstrated effective PHA extraction at 50°C, the recovery rate decreased at 40°C, albeit with a reduction in endotoxin content in the final product (Furrer et al., 2007).

The researchers also explored a modified solvent extraction incorporating a self-floatation step. During this process, cell biomass was mixed with chloroform at 30°C for 72 hours, followed by an overnight period at room temperature to allow for self-floatation of the cell debris (Ibrahim and Steinbuechel, 2009). This method achieved an 85% recovery efficiency and highly purified (98%) product. Despite these results, solvent-based methods suffer from high solvent toxicity, safety concerns, and environmental burdens, which significantly limit their scalability and sustainability.

2.5.2 Extraction using digestion method

In this method, digestion is employed to disrupt the cell membrane and release the intracellular PHA. Digestion can be categorized into chemical and enzymatic types, both targeting the degradation of cellular components other than PHA. In terms of chemical digestion, 2 commonly used chemicals are sodium hypochlorite, to facilitate PHA recovery from cells. Additional chemicals such as palmitoyl carnitine, sodium

dodecyl sulfate, and betaine have been investigated for their effectiveness when used in conjunction with sodium hypochlorite (Koller, 2016). Using sodium hypochlorite or surfactants alone has been found to generate suboptimal results, with sodium hypochlorite alone causing up to 50% degradation of the PHA polymer. Therefore, a combination of sodium hypochlorite and surfactants is employed for improved performance (Dong and Sun, 2000).

While many solvents like chloroform and propylene carbonate can extract nearly pure PHA, their toxicity is a significant drawback. A study demonstrated a much higher recovery efficiency of PHB (5.6 g/L) using the digestion method compared to chloroform extraction (0.63 g/L) (Sayyed et al., 2009). Enzymatic digestion involves several steps, including heat treatment of samples, followed by enzymatic hydrolysis and surfactant washing. The primary advantage of enzymatic digestion lies in its high efficiency of PHA recovery, a result of high enzymes specificity(Jacquel et al., 2008). However, enzymatic processes often remain cost-prohibitive due to enzyme price and require careful optimization to avoid unintended polymer degradation.

2.5.3 Extraction using supercritical fluid

Extraction using supercritical fluid is a recently developed technique for PHA extraction, noted for its low toxicity and cost-effectiveness. Supercritical carbon dioxide (CO_2) is a prominent example used to extract PHA from cell biomass due to its moderate temperature and pressure requirements. The low viscosity and minimal surface tension of supercritical fluids enable rapid percolation, resulting in more efficient diffusion compared to liquid extraction agents (Hejazi et al., 2003). Precise control of temperature and pressure is crucial during this process, as excessive levels can alter the cell membrane, complicating PHA extraction (Khosravi-Darani et al., 2003). Using this method, a high recovery rate of 89% PHA has been achieved from *Ralstonia eutropha* cells (Hejazi et al., 2003). Beyond CO_2, other gases such as ammonia and methanol have also been utilized in their supercritical states to extract PHA

(Kunasundari and Sudesh, 2011). For instance, combining supercritical CO_2 with chloroform extraction allowed for a 42.4% (w/w) recovery of mcl-PHA from freeze-dried *Pseudomonas resinovorans* cells (Hampson and Ashby, 1999).

A notable advantage of supercritical fluid extraction is its ability to produce pure PHA, a level of purity not achievable with traditional solvent extraction. However, heat-resistant impurities like endotoxins in the final product can induce inflammatory reactions (Koller et al., 2013a, Koller et al., 2013b). For applications requiring high purity PHA, such as medical uses, supercritical fluid extraction is ideal, as it can extract PHA with 100% purity (Williams and Martin, 2005). Yet, the requirement for specialized equipment and process control currently restricts its adoption to laboratory or pilot-scale operations.

2.5.4 Aqueous two-phase extraction

Aqueous two-phase extraction (ATPE) is regarded as an environmentally friendly alternative to traditional solvent extraction method, as it employs a system comprising two phases, typically water and a non-volatile phase. This technique utilizes water for the isolation, purification, and recovery of PHA (Kepka et al., 2003). ATPE is particularly noted for its efficacy in removing impurities from the final product. In one study, when using ATPE with 12% (w/v) polyethylene glycol and 9.7% (w/v) potassium phosphate, 51% of PHA was recovered from *Bacillus flexus* cells (Divyashree et al., 2009). During the process, as the disrupted cells settled to the bottom layer, PHA was transferred to the polyethylene glycol phase. This demonstrates that ATPE, although not a solvent-based method, is an effective approach for recovering PHA from microbial cells.

2.5.5 PHA purification by animals

A novel biological method for purifying PHA has been developed using Tenebrio molitor, commonly known as the mealworm. This approach involves mealworms consuming lyophilized *C. necator* cells and subsequently excreting the PHA granules as whitish

feces. Subsequent purification steps involving water, detergent, and heat treatment yielded nearly 100% pure PHA granules (Ong et al., 2018, Murugan et al., 2016). This method simplifies the subsequent purification steps, eliminates the reliance on chemical solvents, and allows the intracellular fats and other proteins to be utilized as nutrients for the growth of mealworms. Despite its novelty, the scalability, consistency, and regulatory acceptability of such biologically assisted recovery methods remain to be fully validated. However, for non-critical applications such as agriculture, this approach may offer an unconventional, low-cost alternative.

Overall, each extraction method presents trade-offs between recovery efficiency, purity, cost, environmental sustainability, and scalability. No single technique fully satisfies all industrial criteria. A critical research gap remains in integrating upstream strain engineering with downstream recovery processes to create streamlined and sustainable PHA production pipelines.

2.6 Engineering strategy

2.6.1 Engineering metabolic flux for PHA synthesis

Metabolic engineering is an effective method for controlling biosynthetic processes, primarily by increasing metabolic flux to the pathway toward the target product, thereby achieving the goals of enhancing PHA accumulation or modifying the chemical composition of PHA. A common approach is the overexpression of genes related to the PHA synthesis pathway. For instance, in the PHB synthesis pathway, the three most critical genes are *phaA*, *phaB*, and *phaC*. When *phaC* is overexpressed alone, the PHB titer in *C. necator* is increased to 1.4 times that of the wild type (Barati et al., 2021). When these three genes are simultaneously overexpressed in depolymerase gene disrupted *Rhodobacter sphaeroides*, the PHB titer is increased by up to 3.9 times (Kobayashi and Kondo, 2019). In *Pseudomonas* species, the fatty acid synthesis pathway is the basis to produce mcl-monomers. Overexpression of the *phaG*, *alkK*, and *phaC* genes in *P. putida* can promote carbon flux towards the mcl-PHA synthesis

(Salvachua et al., 2020). The fatty acid degradation pathway can also provide a carbon source for mcl-PHA; when the enoyl-CoA hydratase gene (*phaJ*) and *phaC* are simultaneously overexpressed in *Pseudomonas chlororaphis*, higher mcl-PHA titers are achieved (Li et al., 2021a).

Another method to increase carbon flux in the PHA production pathway is to inhibit or knock out competing pathways, thereby allowing more resources to be allocated to PHA production. Many bacteria consume glucose as a carbon source, and the TCA cycle competes with the PHA synthesis pathway for acetyl-CoA (Lütke-Eversloh and Steinbüchel, 1999, Heinrich et al., 2015). Research has shown that weakening the TCA cycle can enhance PHB titer (Tao et al., 2017). In the production of PHBV, propionate is added to the medium to supply carbon chin for the 3HV monomer. However, propionate is consumed by the methylcitrate cycle. When the gene *prpC*, which encodes the key enzyme in this cycle, is knocked out, the conversion efficiency of propionate to 3HV is greatly improved (Fu et al., 2014). As an intracellular storage material, PHA is inevitably utilized by the cell, leading to a reduction in PHA accumulation. A direct method to address this is to intervene in the PHA degradation pathway. Knocking out the PHA depolymerase gene (*phaZ*) has been proven to increase the intracellular accumulation of PHA (Zhao et al., 2019a, Salvachua et al., 2020).

Control of metabolic flux can not only increase PHA titer but also regulate the monomer composition of PHA. Numerous examples in this regard come from modifications to the beta-oxidation pathway, as many bacteria can utilize fatty acids as a carbon source and provide precursors for PHA synthesis (Chung et al., 2011, Liu et al., 2011, Green et al., 2002). When genes related to the beta-oxidation pathway are inhibited or knocked out, fatty acid substrates enter the cell but cannot be degraded due to incompleteness of beta-oxidation pathway, allowing the production of PHA with specific monomer chain lengths (Liu et al., 2011). This method has been successfully applied to different bacteria, enabling the production of various mcl-PHA homopolymers. For

example, P3HHx, P(3-hydroxyheptanoate), and P(3-hydroxydecanoate) have all been produced by *P. putida* mutants (Wang et al., 2011, Liu et al., 2011). However, this approach has certain drawbacks, as cell growth and PHA titer can be adversely affected in the absence of other non-fatty acid substrates (Green et al., 2002, Ward and O'Connor, 2005). Therefore, research has also explored the use of mixed carbon sources as substrates to ensure both cell density and PHA titer (Jiang et al., 2013).

In summary, while metabolic flux engineering has been instrumental in improving PHA titer and tailoring polymer composition, current strategies often rely on overexpression or deletion of individual genes without fully accounting for the broader metabolic context. This reductionist approach may fail to address complex regulatory feedback, redox imbalances, and resource allocation trade-offs that emerge during large-scale cultivation or under stress conditions. Moreover, strain-specific metabolic responses and limitations in precursors supply further complicate universal applications of these methods. As such, a more holistic and dynamic engineering framework is required—one that integrates flux balancing, cofactor regeneration, and strain-specific constraints. The research presented in this thesis addresses this need by combining metabolic rewiring with regulatory tuning, targeting robust PHA production even under nutrient variability and using low-cost feedstocks.

2.6.2 Engineering of promoters

Promoter engineering typically includes screening and optimization of promoters to control the transcription levels of PHA biosynthesis related genes, thus also regulating expression. Constitutive promoters can provide stable expression for genes (Xu et al., 2019), such as the strong constitutive promoter pTEF, which can promote the expression of PhaC in *Yarrowia lipolytica* to produce copolymers from fatty acids (Rigouin et al., 2019). The advantage of inducible promoters is that their expression levels are highly controllable. For example, Patricia Calero (Calero et al., 2016) and colleagues tested the strength of various inducible promoters in *P. putida*, facilitating

the engineering efforts for this bacterium . There are also studies that directly increased PHA production in *P. putida* by using the strong inducible promoter PxylA (Wang et al., 2018).

The genetic background of the host bacterium often influences the strength of the promoter, with endogenous promoters typically performing better than exogenous or synthetic ones (Wang et al., 2023). One study screened numerous strong endogenous promoters in *P. putida* and used them to enhance the transcription levels of *phaC1* and *phaC2*, with three promoters significantly increasing PHA production (Zhang et al., 2021). Native promoters from *Pseudomonas mendocina* were also selected to strengthen the transcription of PhaC, and a P16 promoter successfully increased mcl-PHA titer (Zhao et al., 2019b).

To more precisely regulate gene expression, it is necessary to use promoters of varying strengths, highlighting the importance of establishing a promoter library (Xu et al., 2019). A library of promoters with different strengths was created for PHA production, achieving transcription levels ranging from 40 to $1.4x10^5$ in *H. bluephagenesis* and *E. coli*, and increasing the content of P(3HB-co-4HB) copolymers to 80% (w/w) CDW (Shen et al., 2019). When promoter engineering is combined with other biotechnological modifications, such as ribosome binding site optimization and genome streamlining, the production efficiency of PHA can also be enhanced (Sindhu et al., 2021, Liu et al., 2022).

In conclusion, promoter engineering offers a powerful means to fine-tune gene expression and optimize PHA biosynthesis. However, current applications often focus on promoter strength in isolation, without considering dynamic host responses, metabolic burden, or the interplay with downstream regulatory elements. Furthermore, promoter libraries remain underdeveloped in many non-model PHA producers, limiting the transferability of tools between strains or environmental conditions. Inducible systems also face limitations in industrial scalability due to cost and process complexity.

This thesis addresses these challenges by integrating promoter strength characterization with host-specific optimization, aiming to establish a flexible and predictable regulatory platform for efficient PHA production.

2.6.3 Enlarging cell size by morphology engineering

Since PHA (Polyhydroxyalkanoates) are intracellular inclusions produced in confined spaces within cells, the quantity and size of PHA granules are constrained by the size of these spaces, which hardly increased by altering metabolic flux (Jiang and Chen, 2016). Therefore, much scientific effort has focused on increasing the size of bacteria that produce PHA (Jiang et al., 2015, Elhadi et al., 2016). Studies have shown that when the expression of the fission ring protein FtsZ is inhibited, *E. coli* cells grow longer, enlarging the intracellular space and enabling the accumulation of more PHA granules (Wang et al., 2014). Similar studies have also been conducted where weakening the skeleton protein MreB increased the cell diameter by 2-5 times, allowing *E. coli* cells to store more PHA (Jiang et al., 2015).

Further research revealed that when the expression of both proteins MreB and FtsZ was simultaneously inhibited using CRISPRi, the rod-shaped morphology of *E. coli* was lost, resulting in diverse shapes including gourd-shaped, oval, spindle-shaped, and other forms, leading to an even greater accumulation of PHA compared to single protein inhibition (Elhadi et al., 2016). Additionally, this result, achieved in *E. coli*, was successfully transferred to another bacterium with higher industrial production potential, *Halomonas campaniensis*, also enhancing its PHA titer (Jiang et al., 2017).

To summarize, morphology engineering presents a promising strategy to increase PHA storage capacity by physically enlarging the intracellular space. While effective, this approach can disrupt normal cell division and morphology, potentially impairing cellular fitness, viability, or downstream processing behavior. Moreover, the long-term stability and scalability of these engineered morphologies under industrial fermentation

conditions remain largely unexplored.

2.6.4 Enhancing NADH/NADPH supply for synthesis

By raising the availability of NADH or NADPH in bacteria, PHA production can be enhanced (Zheng et al., 2017). In the process of PHA synthesis, acetyl-CoA serves as a vital precursor for PHA production and requires the participation of NADPH as a cofactor. NADPH with low levels can cause acetyl-CoA to be converted into acetate, thereby reducing its entry into the PHA synthesis pathway (Koller, 2018, Koller, 2019). One method to increase NADPH levels is to overexpress the gene *gapN* encoding glyceraldehyde 3-phosphate dehydrogenase. Concurrently, knocking out the *ackA-pta* gene, which is responsible for acetate production, allows more acetyl-CoA to flow into PHA production (de las Heras et al., 2016). In another study, researchers found that *Halomonas bluephagenesis* requires more NADH rather than NADPH as a cofactor, and under oxygen-limited conditions, increasing the NADH/NAD+ ratio can enhance PHA production (Ling et al., 2018).

Enhancing intracellular NADH/NADPH availability is a critical lever for improving PHA biosynthesis, especially in strains where redox balance is tightly coupled with metabolic flux. However, current strategies often rely on static gene overexpression or knockout approaches, which may not adapt well to fluctuating environmental or metabolic conditions during fermentation.

2.6.5 Engineering of PHA synthase (PhaC)

As the most crucial enzyme for PHA synthesis, research on PhaC has been ongoing for many years (Chek et al., 2019). Scientists have enhanced the polymerization capability of PhaC through modifications, including mutations and the fusion of functional domains from different PhaC enzymes (Shen et al., 2011, Tsuge et al., 2004). Of course, these modifications are achieved only when there is a clear understanding of PhaC structures. Studies have shown that PhaC from *C. necator* is a dimer

composed of N-terminal and C-terminal regions (Kim et al., 2017). Further research has combined the C-terminal of $PhaC_{AC}$ from *Aeromonas caviae* with the N-terminal of $PhaC_{Cn}$ from *Cupriavidus necator* to create a hybrid PhaC, resulting in the production of copolymers containing 2-hydroxybutyrate (2HB) monomers (Sudo et al., 2020).

Approach involves site-directed mutagenesis of PhaC can also improve the performance. When $PhaC_{61\text{-}3}$ and $PhaC_{1437}$ from different *Pseudomonas* species were mutated, their substrate specificity broadened, enabling them to polymerize both scl and mcl monomers (Yang et al., 2010). Another example proving that modifications to PhaC can effectively enhance monomer diversity is demonstrated when site-directed saturation mutagenesis is applied to PhaC from *C. necator*. Fifteen mutants were able to polymerize lactic acid, resulting in the production of the copolymer P(LA-co-3HB) (Ochi et al., 2013).

Overall, enzyme engineering of PhaC has significantly expanded the diversity and tailor ability of PHA monomers through domain fusion and site-directed mutagenesis. However, engineered synthases are frequently tested under ideal laboratory conditions, and their stability, catalytic efficiency, and polymer specificity under industrial or mixed-substrate environments are poorly characterized.

2.6.6 Adaptive laboratory evolution (ALE) for PHA production

ALE is a relatively uncommon method in PHA research. The key aspect of ALE is to exert environmental pressures on microorganisms to obtain advantageous variants (Sandberg et al., 2019). In the context of PHA production, this approach is primarily applied to evolve strains with enhanced utility and capability to utilize specific substrates. For example, a common PHA producer, *Cupriavidus necator*, has a variant, v6C6, obtained through adaptive evolution, which exhibits a 9.5-fold increase in growth rate and an enhanced PHB production capacity when using glycerol as a substrate compared to the wild type (Gonzalez-Villanueva et al., 2019). A genome-streamlined

strain *Pseudomonas putida* KTU-U27 has undergone adaptive evolution, resulting in significantly improved utilization of xylose or cellobiose (Liu et al., 2023). This advancement is particularly beneficial for addressing the cost issue associated with substrates in PHA production. Another study focused on the effects of gradually increasing sodium acetate concentrations on *Halomonas bluephagenesis*. After 71 transfers, an evolved strain, B71, was successfully isolated, showing enhanced tolerance and utilization of acetate, along with improved PHB production compared to the parental strain (Zhang et al., 2022).

In conclusion, ALE provides a valuable route to obtain strains with enhanced substrate utilization and stress tolerance, especially when rational engineering is limited by incomplete metabolic knowledge. However, ALE is inherently time-consuming and unpredictable, and the underlying genetic mechanisms driving observed improvements are often unclear without comprehensive omics analysis.

2.6.7 Summary of engineering strategies

The engineering strategies described in this section represent a multi-dimensional approach to enhancing PHA biosynthesis. Each strategy—ranging from metabolic flux redirection and promoter optimization to cell morphology manipulation, redox cofactor balancing, enzyme modification, and adaptive evolution—addresses a specific bottleneck in the PHA production pathway. While these methods have demonstrated significant improvements in titer, monomer composition, and substrate flexibility, they also reveal inherent limitations, such as lack of dynamic control, host-specific variability, and challenges in industrial scalability. Most notably, existing studies often treat these strategies in isolation, with limited integration into holistic design frameworks. This thesis builds upon these foundational efforts by developing a systems-level engineering platform that combines multiple strategies tailored to strain-specific context.

2.7 Application of PHA

PHA possesses properties similar to synthetic plastics, offering versatility in applications ranging from packaging and agriculture to medical devices and pharmaceuticals. As industries increasingly seek to reduce their environmental footprint, the development and application of PHAs represent a significant step forward in creating sustainable materials that meet both ecological and economic demands. This section explores the diverse applications of PHAs, their benefits, and widespread adoption.

2.7.1 PHA for biofuel applications

The monomers of PHA are connected by ester bonds, and the methyl esterification reaction can convert PHA into the corresponding methyl esters. These esters have properties similar to biodiesel, making them suitable as additives for gasoline or biodiesel (Gao et al., 2011). For example, biofuel butanol can be synthesized using glucose as a raw material by combining metabolic pathways with an improved PHB production pathway (Bond-Watts et al., 2011). The application of PHA as raw material for biofuels holds great potential because it does not require highly purified PHA. These PHAs can be produced from activated sludge or wastewater, which means lower feedstock and purification costs (Johnson et al., 2009). With the development of related research, the most common PHB has been successfully converted into various biofuels. For instance, by heating PHB in sulfuric acid solution at 200-240°C, it can be converted into hydrocarbon oils (Kang and Yu, 2014).

2.7.2 PHA for medical applications

The biocompatibility and biodegradability of polyhydroxyalkanoates (PHA) provide this polymer with the potential for drug delivery applications. Reports suggest that PHA is a superior material for drug delivery compared to polymers such as polylactic acid (PLA) and polyglycolic acid (PGA) (Patel et al., 2016, Kumar et al., 2018, Brigham and Sinskey, 2012). Additionally, the structural diversity of PHA allows for modifications in

its physical and thermal properties, which can influence drug loading and release (Kumar et al., 2015). Drug release from polymer primarily occurs through mechanisms such as permeation, diffusion, or biodegradation. PHA can be processed into various forms such as nanoparticles, microspheres, and fiber-like shapes, enhancing the efficiency of drug delivery for different releasing mechanisms (Brigham and Sinskey, 2012).

PHA possess the notable ability to promote cell proliferation and attachment, which underpins their extensive use in medical applications (Adeleye et al., 2020). Additionally, PHA can be combined with a variety of organic or inorganic substances, making it highly suitable for uses such as wound care, tissue engineering, and neural repair (Gregory et al., 2022). Encapsulating anti-inflammatory agents like diclofenac and dexamethasone within PHA has been found to enhance wound healing and accelerate skin repair (Murueva et al., 2014). In particular, 3HB/4HB monomers have shown promise in skin regeneration when processed into films and electrospun membranes, which foster improved vascularization and wound healing (Shishatskaya et al., 2016). Furthermore, the copolymer P(3HB-3HHx), produced via microbial fermentation, has been effectively employed as a scaffold for the repair of tarsal bones in rat (Zhou et al., 2010).

2.7.3 PHA for agricultural applications

In agriculture, conventional plastic materials such as seedling bags and films play a crucial role in maintaining soil temperature and moisture, as well as in packaging fertilizers and nutrients (Rajdeep and Naithani, 2013). Low-density polyethylene (LDPE) is the most commonly used material; however, the environmental concerns surrounding plastic waste have sparked global action, resulting in taxes and bans in numerous regions (Adane and Muleta, 2011). PHA, due to their biodegradability, has emerged as a promising eco-friendly alternative to traditional plastics. In addition to being biodegradable, PHA's application in agriculture requires lower purity standards,

thereby simplifying the purification process and reducing costs (Adeleye et al., 2020).

Fertilizer release is a key factor in agriculture, with excessive or uncontrolled fertilization leading to both economic losses and soil contamination (Wu, 2008). Bioplastic-based fertilizers have been employed in agriculture and horticulture for decades, with slow-release fertilizers considered a significant advancement in agricultural technology due to their efficient nutrient delivery and control over product longevity (Harmaen et al., 2016). PHA can be used to create slow-release fertilizers by providing a biodegradable plastic coating. For example, fertilizers coated with PHA have been applied in oil palm plantations, where nutrients are released gradually as the PHA degrades (Ivanov et al., 2015).

2.7.4 PHA for construction applications

To mitigate and prevent the environmental impacts associated with construction waste, the construction industry is increasingly adopting the use of emerging biodegradable materials. Bio-based polymeric materials, composed of biopolymers and natural plant fibers, are the subject of growing research interest due to their potential to reduce the environmental footprint of traditional construction materials (Ahmad et al., 2022). PHA-based bioplastic foams, for instance, can be employed as wall insulation or non-structural components, thus reducing the production of hazardous plastic foams and enabling efficient post-use disposal (Adeleye et al., 2020). In a study on PHA-based bio-based composites, PHB matrices reinforced with hemp fibers exhibited mechanical properties comparable to construction-grade timber (Christian and Billington, 2011). Consequently, PHA-based bio-based composites hold significant potential as a direct substitute for timber in construction applications and could also be utilized in the production of wood-based products, such as furniture or shelving (Christian and Billington, 2011).

2.7.5 PHA for packaging applications

The biodegradability of polyhydroxyalkanoates (PHA) has significantly contributed to its commercialization across a wide range of sectors, with particular emphasis on packaging materials. PHA has been successfully processed into various commercial packaging products, including cosmetic containers, shampoo bottles, milk cartons, garbage bags, food packaging, disposable garment bags, and even combs (Ramesh et al., 2010, Bugnicourt et al., 2014). Despite its relatively high production costs, which have constrained large-scale manufacturing, PHA is widely recognized as a promising alternative to conventional non-degradable plastics, which are associated with environmental degradation (Muhammadi et al., 2015). The blending of PHA with other substances offers the potential to tailor its properties for specific applications. For example, research by Muizniece-Brasava and Dukalska demonstrated that the use of dioctylsebacate and bisoflex as plasticizers improved the suitability of PHB for sour cream packaging, generating preservation results comparable to traditional graphite-coated polyethylene materials (Muizniece-Brasava and Dukalska, 2006). Furthermore, studies have indicated that gamma radiation, commonly employed for sterilizing food packaging, has negligible effects on the properties of PHB (Hermida et al., 2008). These findings collectively highlight the practicality and scientific viability of PHA as a sustainable packaging material.

2.8 Research gaps to be addressed

Although considerable advancements have been made in microbial PHA research over the past decades, multiple technical and scientific bottlenecks remain that hinder the transition of PHA technologies from bench to market. This thesis builds upon a critical evaluation of the current literature and identifies five interrelated research gaps that persist in the state-of-the-art. These gaps directly inform the design of the experimental strategies in this work, which aim to bridge them through targeted genetic engineering, substrate optimization, and in-depth polymer characterization.

2.8.1 Limited integration of multiple biosynthetic pathways

Contemporary PHA research is heavily divided between scl and mcl PHA production systems, often involving either *C. necator* or *P. putida* as dedicated hosts. Notably, *Rhodococcus* species can synthesize large amounts of intracellular lipids rich in long-chain fatty acids. These endogenous lipid synthesis pathways have the potential to serve as internal precursor pools for mcl-PHA biosynthesis, thereby reducing the need for costly exogenous long-chain fatty acid supplementation. However, the potential of these organisms to synthesize hybrid PHA or customized copolymers by integrating both fatty acid de novo synthesis and β-oxidation pathways remains underexploited.

Attempts at pathway integration have been largely limited by metabolic burden, cross-pathway inhibition, or incompatible regulatory systems (e.g., conflicting cofactor demands, unbalanced precursor pools) (Choi et al., 2020b). As such, very few studies have successfully demonstrated the simultaneous and tunable production of scl- and mcl-PHA fractions in a single engineered chassis. This thesis directly addresses this gap by constructing and testing dual-pathway plasmids in multiple host backgrounds, enabling co-polymer production with controllable composition.

2.8.2 Insufficient promoter-level regulation for monomer control

While recent developments in synthetic biology have enabled enzyme overexpression for enhanced PHA titers, fine-grained regulation of gene expression remains underdeveloped, particularly at the promoter level. Most PHA studies still rely on strong, constitutive promoters without systematically evaluating how promoter strength affects metabolic flux and polymer architecture.

Moreover, the effect of promoter driven expression on monomer ratios, polymer distribution, and final material performance is seldom quantified. This thesis pioneers the use of a promoter library with varying expression strengths to dynamically modulate the expression of the *phaCAB* operon in *P. putida*, directly linking promoter activity to

changes in monomer composition and polymer properties.

2.8.3 Underutilization of sustainable, complex feedstocks

The economic and ecological rationale for using industrial and agricultural waste streams as carbon sources for PHA production is well recognized. However, most engineered strains are tested with glucose, fatty acids, or pure carbon precursors under idealized lab conditions. The metabolic adaptability of engineered strains to real-world feedstocks, such as molasses or potato peel hydrolysates, is rarely investigated in depth.

Challenges such as impurities, inconsistent composition, or the presence of inhibitory compounds are often neglected, leaving a critical knowledge gap regarding the true industrial applicability of PHA-producing microbes. This thesis systematically evaluates the performance of *Burkholderia* and engineered strains on sugarcane molasses and starch-rich waste, quantifying growth kinetics, product titer, and monomer distribution in the context of feedstock complexity.

2.8.4 Incomplete characterization of engineered polymers

Most studies on PHA production emphasize titer and monomer composition but provide limited analysis of physicochemical properties such as molecular weight, thermal behavior, and crystallinity. These parameters are critical for assessing polymer functionality and application potential yet are often underreported.

Moreover, in cases where both scl- and mcl-PHA are produced simultaneously, it is rarely clarified whether the resulting materials are true copolymers or physical blends. This distinction is crucial, as blends and copolymers exhibit fundamentally different structural and mechanical properties. The lack of systematic characterizations such as detailed NMR analysis or DSC profiling leaves the material identity ambiguous.

This thesis addresses this gap by employing a comprehensive set of analytical techniques to confirm polymer structure and composition, and to distinguish between copolymer formation and physical blending.

2.8.5 Limited evaluation of strain robustness under industrial conditions

Many engineered strains perform well under controlled laboratory conditions, but their stability and productivity often decline in industrially relevant environments characterized by nutrient variability, osmotic stress, or the presence of inhibitory compounds. The resilience of promising microbial hosts such as *P. putida* and *C. necator* under such conditions remains inadequately studied, raising concerns about their suitability for real-world applications.

Considering these gaps, the research presented in this thesis aims to develop novel microbial platforms that address the limitations identified above. By combining pathway integration, promoter engineering, sustainable feedstock utilization, and advanced polymer characterization, this work seeks to contribute a more holistic and application-driven strategy for advancing the field of microbial PHA production.

2.9 Summary

This literature review has provided a comprehensive overview of the current state of PHA research, with a particular focus on strain engineering as a strategy for optimizing microbial production. PHA is biopolymer synthesized by various microorganisms and represents a promising class of biodegradable alternatives to petrochemical plastics due to their material diversity and environmental compatibility.

The review has outlined the molecular structure, biosynthesis pathways, and classification of PHAs, highlighting the central role of enzymes such as PHA synthase. It further examined genetic and metabolic engineering strategies aimed at enhancing PHA titer and tailoring polymer composition, including metabolic flux control, cofactor

balance (NADH/NADPH), and regulated gene expression.

Several microbial hosts, including *P. putida* and *C. necator*, have been widely studied for their ability to produce various types of PHA. However, challenges remain in integrating multiple biosynthetic pathways within a single organism to enable the production of customizable PHA blends. Similarly, while the use of sustainable feedstocks has been proposed to reduce production costs, achieving high PHA titer under complex substrate conditions still requires further strain optimization.

Additionally, the literature emphasizes the importance of advanced analytical techniques such as NMR, GC-MS and GPC for characterizing the physicochemical properties of PHAs. These tools are essential for understanding how genetic modifications influence the final material properties and for guiding their application in industrial contexts.

In summary, this chapter has outlined the key developments and challenges in the field of PHA research, from biosynthesis and strain engineering to substrate utilization and downstream processing. While significant progress has been made, several limitations remain, including the integration of multiple biosynthetic pathways, precise control over monomer composition, and the use of low-cost, sustainable feedstocks. These limitations highlight the need for innovative strain design and process optimization strategies. The next chapter introduces the experimental materials and methods developed to address these challenges and systematically investigate the objectives defined in **Chapter 1**.

Chapter 3: Materials and methods

This chapter details the experimental design, biological materials, and analytical techniques employed in this study. It outlines the microbial strains and plasmids used for genetic engineering, the cloning strategies implemented for pathway construction, and the cultivation conditions optimized for PHA production. In addition, the methodologies for PHA extraction and characterization are described, including gas chromatography, nuclear magnetic resonance, and thermal analysis. These methods provide the foundation for assessing the performance of engineered strains and the physicochemical properties of the produced polymers.

3.1 Bacterial strains, plasmids and culture media

All strains used in this project are listed in **table 3.1**. *Escherichia coli* DH5α was used for all molecular cloning, plasmid propagation, and maintenance. *Rhodococcus*, *Cupriavidus necator*, *Pseudomonas putida* mt-2 and *Burkholderia* strains were used for engineering and (or) PHA production. All plasmids are listed in **Table 3.2**. Plasmid pDD56 was obtained from Addgene plasmid repository (DeLorenzo et al., 2018). Plasmids carrying 4 constitutive promoters (P_{phaC1}, P_{rrsC}, P_{j5}, and P_{g25}) were in lab stock and previously reported (Johnson et al., 2018). Plasmid pPS85 and pPS87 were obtained from pSEVA-SIB collection (Calero et al., 2016).

E. coli was grown in Luria–Bertani (LB) medium (10 g/L tryptone, 5 g/L yeast extract, 10 g/L NaCl). Other PHA producing strains were grown in either LB medium or mineral salt medium (MSM) supplemented with 1% glucose as sole carbon source unless stated otherwise. MSM was prepared as previously described (Schlegel et al., 1961) with reduced concentration of nitrogen (0.5 g/L NH_4Cl). Solid media used is TYE agar (10 g/L tryptone, 5 g/L yeast extract, 8 g/L NaCl, 15 g/L agar). Chloramphenicol (25 µg/mL), Kanamycin (50 µg/mL) and gentamicin (20 µg/mL) were used as needed.

Sugar cane molasses (lab stock) was dissolved in deionized water to obtain 20% (w/v) solution before mix with MSM medium to final concentration of 2% (w/v), sterilized by either syringe filtration or autoclave. Potato peel hydrolysate (PPH) was prepared using an enzymatic method. In brief, 20 g of potato peels were mixed with 200 mL of deionized water, and the pH was adjusted to 6 using NaOH. After adding 2 mL of BAN 480L (Sigma Aldrich) and mixing thoroughly, the mixture was incubated at 80°C for 30 minutes. The pH was then adjusted to 4 with acid, followed by the addition of 2 milliliters of AMG 300L (Sigma Aldrich) and further mixing. After incubation at 60°C for 30 minutes, the liquid phase was separated, and the pH was adjusted to 7. Subsequent impurities were removed by filtration and centrifugation.

High-performance liquid chromatography (HPLC) analysis, conducted by Kang Lan Tee and David Robins, revealed the final PPH contained 3.11% (w/w) glucose and 0.41% (w/w) fructose. Other components were not quantified in this study. PPH was mixed with autoclaved deionized water or MSM medium at a volume ratio of 1:1 for cultivation.

Table 3.1. Strains used in this project.

Strain	**Description**	**Source or reference**
Escherichia coli DH5α		Lab stock
Rhodococcus jostii RHA1		Lab stock
Rhodococcus opacus PD630	DSM 44193	DSMZ
Rhodococcus ruber N361	DSM 43338	DSMZ
Cupriavidus necator H16	ATCC 17699	ATCC
Pseudomonas putida mt-2	DSM 6125	DSMZ
Burkholderia tropica	TBRC 1718	Lab stock
Burkholderia bannensis	TBRC 4635	Lab stock
Burkholderia acidipaludis	TBRC 4970	Lab stock
Burkholderia contaminans	BCC 81317	Lab stock
Burkholderia soli	BCC 59163	Lab stock

Table 3.2. Plasmids used in this project.

Plasmid	Description	Source or reference
pBBR1c-PhaC	oriV(pBBR1); *P. putida phaC*1. Cam^R	Lab stock
pBBR1c-CAG	oriV(pBBR1); *P. putida phaC*1, *alkK* and *phaG*. Cam^R	This study
pDD56	oriV(pBR322); araC-ParaB-enhanced YFP. Km^R	(DeLorenzo et al., 2018)
pDD56-CAG	pDD56 derived, *P. putida phaC*1, *alkK* and *phaG*. Km^R	This study
pDD56-CJ	pDD56 derived, *P. putida phaC*1and *phaJ4*. Km^R	This study
pBBR1-MCS2	Broad-host-range vector, Km^R	(Kovach et al., 1995)
pBBR1c-phaCAB	oriV(pBBR1); *C. necator phaCAB* operon. Cam^R	Lab stock
PphaC1-phaCAB	PphaC1-RFP derived, *C. necator phaCAB* operon. Km^R	This study
ParaB-phaCAB	pPS85 derived, *C. necator phaCAB* operon. Gm^R	This study
PrhaB-phaCAB	pPS87 derived, *C. necator phaCAB* operon. Gm^R	This study
pPS85	oriV(pBBR1); araC-ParaB-gfp(Mut3). Gm^R	(Calero et al., 2016)
pPS87	oriV(pBBR1); rhaS-rhaR-PrhaB-gfp(Mut3). Gm^R	(Calero et al., 2016)
Pj5-RFP	oriV(pBBR1); P_{j5}-rfp. Cam^R	(Johnson et al., 2018)
Pg25-RFP	oriV(pBBR1); P_{g25}-rfp. Cam^R	(Johnson et

Plasmid	Description	Source or reference
		al., 2018)
PrrsC-RFP	oriV(pBBR1); P_{rrsC}-rfp. Cam^R	(Johnson et al., 2018)
PphaC1-RFP	oriV(pBBR1); P_{phaC1}-rfp. Cam^R	(Johnson et al., 2018)
Pj5K-RFP	Pj5-RFP derived, P_{j5}-rfp. Km^R	This study
Pg25k-RFP	Pg25-RFP derived, P_{g25}-rfp. Km^R	This study
PrrscK-RFP	PrrsC-RFP derived, P_{rrsC}-rfp. Km^R	This study
Pc1K-RFP	PphaC1-RFP derived, P_{phaC1}-rfp. Km^R	This study

3.2 Molecular cloning and strain transformation

All oligonucleotide primers used for PCR reaction are listed in **Table 3.3** and synthesized by Eurofins (Ebersberg, Germany). All restriction endonucleases used for molecular cloning were purchased from New England Biolabs.

3.2.1 Molecular cloning plasmids for scl-PHA producer engineering

Gene *alkK* and *phaG* were PCR amplified from *P. putida* KT2440 genomic DNA with primer AlkK-F, AlkK-R, PhaG-F and PhaG-R. Plasmid backbone was obtained by restriction digesting pBBR1c-PhaC with BamhI and XhoI enzymes. To generate pBBR1c-CAG plasmid, three DNA fragments were assembled by NEBuilder HiFi DNA Assembly Master Mix (New England Biolabs) according to the manufacturer's protocols. In the subsequent construction of the pDD56-CAG plasmid, *phaC*, *alkK*, and *phaG* were PCR amplified as whole fragment from plasmid pBBR1c-CAG with primer CAG-F and CAG-R. Backbone was PCR amplified from plasmid pDD56 with primer pDD56-BK-F and pDD56-BK-R, assembled with fragment CAG by HiFi DNA Assembly Master Mix. PhaC containing backbone was then PCR amplified with primer pDD56-C-F and pDD56-C-R using pDD56-CAG as template. *PhaJ4* was PCR amplified from

P. putida KT2440 genomic DNA with primer PhaJ-F and PhaJ-R. Two DNA fragments were restricted digested with enzymes XbaI and HindIII before connected by ligation using T4 DNA ligase (New England Biolabs), forming plasmid pDD56-CJ.

Table 3.3. Primers used for PCR reaction in this project.

Primer name	Sequence (5' to 3')
AlkK-F	TGTGCATGAGCGGTAAGGATCCTTTAAGAAGGAGATATACAATGTTGCAGACACGCATC
AlkK-R	TCATCTAGTATTTCCCCTCTTTCTCTAGATTACAACGTGGAAAGGAACG
PhaG-F	AGAAAGAGGGGAAATACTAGATGAGGCCAGAAATCGCTGTACTTG
PhaG-R	TGATGCCTGGAGATCCTTACTCGAGTCAGATGGCAAATGCATGCTGC
CAG-F	GAAGGAGGTTAGGACATATGTCGAACAAGAACAACGACG
CAG-R	GCTCTAGTAGAATTCAAGCTTCAGATGGCAAATGCATGCTG
pDD56-BK-F	AGCTTGAATTCTACTAGAGCCAGGCATCAAATAAAACG
pDD56-BK-R	CATATGTCCTAACCTCCTTCTCTTTGCTAC
pDD56-C-F	TGATAAGCTTGAATTCTACTAGAGCCAGGCATC
pDD56-C-R	TAAATCTAGATTACCGCTCATGCACATACGTG
PhaJ-F	GTAATCTAGATTTAAGAAGGAGATATACCATGCCCCATGTACCGGTTAC
PhaJ-R	AGTAGAATTCAAGCTTATCAGACAAAACAGAGCGACAGCGAC
Km-F	GCATGCATAATCAGAAGAACTCGTCAAG
Km-R	GGAAGCTAAAATGATTGAACAAGATGGATTGC
PB-F	TTGTTCAATCATTTTAGCTTCCTTAGCTCCTG
PB-R	GTTCTTCTGATTATGCATGCGCCCAATAC
phaCAB-F	ATGGCGACCGGCAAAGGCGC
phaCAB-R	TCAGCCCATGTGCAGGCCGC

Primer name	Sequence (5' to 3')
Pc1K-BK-F	CGCCTTTGCCGGTCGCCATGATTTGATTGTCTCTCTG
Pc1K-BK-R	CGGCCTGCACATGGGCTGAGGATCCAAACTCGAG
pPS85-BK-F	CGGCCTGCACATGGGCTGATCTTGGACTCCTGTTGATAG
pPS85-BK-R	CGCCTTTGCCGGTCGCCATGGTATATTCCTCCTATCG
pPS87-BK-F	GGCCTGCACATGGGCTGATCTTGGACTCCTGTTG
pPS87-BK-R	CGCCTTTGCCGGTCGCCATGGTATATTCCTCCTATC

3.2.2 Molecular cloning plasmids for *P. putida* engineering

To test different constitutive promoters in *P. putida*, different RFP expression vectors were constructed. The selection marker CamR on original plasmids (PphaC1-RFP, PrrsC-RFP, Pj5-RFP and Pg25-RFP) was replaced with the kanamycin resistance gene. The backbones of 4 plasmids were obtained by PCR amplification using primer PB-F and PB-R (**Table 3.3**). Kanamycin resistance gene was PCR amplified from pBBR1-MCS2 plasmid with primer Km-F and Km-R. DNA purification was performed using Gel and PCR Clean-Up Kit (Macherey-Nagel). After purification, two DNA fragments were assembled by using NEBuilder HiFi DNA Assembly Master Mix.

To generate expression vector for PHB production, gene encoding GFP or RFP in original plasmid used for promoter test was replaced with *phaCAB* operon. PCR was employed to amplify *phaCAB* operon from pBBR1c-phaCAB plasmid using primer phaCAB-F and phaCAB-R. Backbone of different plasmids was PCR amplified using corresponding primers listed in **Table 3.3**. NEBuilder HiFi DNA Assembly Master Mix was used to assemble two purified DNA fragments.

3.2.3 DNA gel electrophoresis

DNA gel electrophoresis was adapted from standard molecular biology protocols and used routinely for the analysis of PCR products, restriction digestion fragments, and plasmid verification (Creager, 2020). DNA samples were separated using 1.0–1.5%

(w/v) agarose gels prepared in 1× TAE buffer (40 mM Tris-acetate, 1 mM EDTA, pH ~8.0). For visualization, gels were stained with ethidium bromide (EtBr). DNA loading dye (6×) was mixed with each sample prior to loading. A DNA molecular weight marker, GeneRuler™ 1 kb DNA Ladder (Thermo Scientific), was run alongside the samples to estimate fragment sizes. Electrophoresis was performed at a constant voltage of 100 V for around 45 minutes, depending on the size of the DNA fragments.

3.2.4 Bacterial transformation

E. coli DH5α transformation with plasmids was performed using the standard $CaCl_2$ method, plated on TYE agar. *C. necator* was transformed using 0.2 M sucrose solution as previously described (Tee et al., 2017). *P. putida* and *Rhodococcus* strains were transformed with plasmids using the electroporation protocol (Cho et al., 1995) with some changes. Briefly, one fresh colony was inoculated into 5 ml of LB for overnight culture at 30°C with shaking at 250 rpm. A total of 400 µL was transferred to 20 mL of LB and proceeded to culture to OD_{600}~0.6, cells were chilled on ice for 10 min and harvested by centrifugation (5000 g, 10 min and 4°C), then washed two times with ice-cold 10%(v/v) glycerol and resuspended in 1 ml of 10%(v/v) glycerol. Electroporation was conducted by adding DNA to 100 µL aliquot and shocked using pre-chilled 2 mm cuvette at 2.3 kV. 900 ul of LB was added for suspension, after 2 h of incubation at 30°C with shaking, cells were spread on TYE agar plate with appropriate antibiotic.

3.3 Cultivation conditions and optical density measurement

A single colony was pre-cultured in LB medium and then used to inoculate MSM medium in flasks to an initial OD_{600} of 0.2, with the medium volume being one-fifth of the flask or falcon tube volume. Except for *E. coli* (cultured at 37°C), all other strains were cultured at 30°C with shaking at 250 rpm. Induction of promoters was conducted by adding 0.4% of arabinose or 10 mM of rhamnose into MSM culture until OD_{600} around 0.6. Cells were harvested by centrifuging (8000 rpm, 10 min, RT) after cultivation. Cell pellet was washed twice with 1X Phosphate-buffered saline (PBS)

solution (137 mM NaCl, 2.7 mM KCl, 8 mM Na_2HPO_4, and 2 mM KH_2PO_4). Cell pellet was then stored at -80°C, followed by lyophilization to get dry cell and measure cell dry weight (CDW). Unless otherwise stated, all cultivations in this thesis were performed using shaker incubators under above conditions.

General monitoring of cell growth was conducted by measuring optical density at 600 nm (OD_{600}) using a WPA CO 8000 Cell Density Meter. For the experiments described in **Chapter 6** (OD_{850} measured), cell growth was monitored using RTS-1 Personal Bioreactor (Grant Instruments, UK). In this system, cultures were grown in TPP® TubeSpin Bioreactor tubes, which were mounted onto the rotating platform of the RTS-1 unit. The bioreactor continuously measured optical density at 850 nm through the wall of the cultivation tube at 15-minute intervals.

3.4 Analysis of total protein expression

Total protein expression was analyzed using sodium dodecyl sulfate-polyacrylamide gel electrophoresis (SDS-PAGE) (Laemmli, 1970, Gallagher, 2012). Cell pellet obtained from 24 hours cultivation (1 mL, MSM medium with 1% glucose) was resuspended in 200 µL of 50 mM phosphate buffer (pH 7.5), followed by the addition of 200 µL of 2× SDS reducing buffer supplemented with β-mercaptoethanol. Samples were denatured at 94 °C for 20 minutes using a heating block, centrifuged at maximum speed (⩾13,000 rpm) for 5 minutes, and 10 µL of the resulting supernatant was loaded onto a 10% polyacrylamide gel. A molecular weight marker, PageRuler™ Unstained Broad Range Protein Ladder (Thermo Scientific, catalog #26630), was loaded alongside the samples for molecular weight estimation.

Electrophoresis was carried out at a constant voltage of 200 V for approximately 35 minutes. After electrophoresis, gels were rinsed thoroughly with deionized water to remove residual SDS and stained using a Coomassie Blue-based staining solution. Gels were then rinsed with water, microwaved in water for 3–4 cycles to accelerate

destaining, and incubated in deionized water overnight for background clearance. The gel preparation, running, and staining procedures were adapted from standard protein electrophoresis protocols commonly used in molecular biology (Gallagher, 2012, Hames, 1998).

3.5 Promoter strength assay

To test the strength of different promoters in *P. putida*, single colony was inoculated into 50-mL falcon tube containing 5 mL of LB medium and incubated overnight at 30°C, 250 rpm. The overnight culture was then used to inoculate 5 mL MSM medium in a 50-mL falcon tube to an initial OD600 of 0.2 and cultivated at 30°C, 250 rpm. The induction of promoters was conducted by adding 0.4%(w/v) of arabinose or 10 mM of rhamnose into MSM culture until OD_{600} around 0.6.

After a certain time of cultivation (4h, 8h, 12h, 16h, 20h, 24h, 48h, 72h), 100 uL of culture was transferred into a well of 96-well clear bottom plate. Fluorescence of RFP (E_x 584 nm, E_m 607 nm; bottom read) and GFP (E_x 485 nm, E_m 528 nm; bottom read) were measured using SpectraMax M2e microplate reader [Molecular Devices (Wokingham, UK)].

3.6 PHA extraction using the Soxhlet

For PHA extraction, lyophilized cells were transferred to an extraction thimble and placed in extraction Soxhlet. Methanol was added to the round bottom flask and heated by heating mantel to reflux for 2 h. Then methanol was removed, and dichloromethane was added to round bottom flask, heated to reflux overnight (at least 12 h). After reflux, all dichloromethane was collected and heated to evaporate until volume reduced to around 5-10 mL. Pouring PHA containing dichloromethane to stirring pre-chilled methanol (10X the volume of dichloromethane) to precipitate the PHA. If necessary, re-dissolve the PHA in dichloromethane and precipitate again to further improve purity of PHA.

3.7 Gas chromatography analysis of PHA

The intracellular PHA content and monomer composition were analyzed using gas chromatography (GC) or gas chromatography–mass spectrometry (GC-MS).10 mg lyophilized cells were subjected to methanolysis in the presence of 1 mL dichloromethane (containing benzoic acid as internal standard) and 1 mL of methanol (15% sulfuric acid) for 3.5 h at 100°C. 1 mL of distilled water was added when the sample was cooled down on ice. The mixture was vortexed for 5 minutes and stood at room temperature. After phase separation, the organic phase (bottom layer) was transferred to another GC vial to be analyzed.

The GC system used was a Shimadzu GC2010 pro gas chromatograph (Kyoto, Japan) equipped with an AOC-20i auto-injector and an SH-Rtx-5MS column. Hydrogen was used as mobile phase with flow rate of 40 mL/min. The temperature program used was as follows: 80°C hold for 5 min, ramp from 80 to 180°C at 8°C per min and a final hold at 180°C for 12 min. For qualitative and quantitative analysis, commercially available 3-hydroxyalkanoate methyl ester standards (purchased from Cayman Chemical Company) were analyzed under the same conditions (**Figure S1**). Standard solutions at known concentrations were injected to generate calibration curves by plotting peak area versus monomer concentration (**Figure S2**). A representative GC chromatogram of a PHA blend sample (corresponding to **Figure 5.8**) is shown in **Figure S3**.

The system of GC-MS is Agilent 7200 Accurate Mass Q-ToF GC-MS equipped with an Agilent DB5-MS-UI Column. Helium was used as carrier gas with flow rate of 1.2 mL/min. The temperature program used was as follows: started at 60°C, ramp from 60 to 300°C at 10°C per min and a final hold at 300°C for 6 min. Mass Spectrometer was EI scan mode with range 35-500 m/z. Transfer line temperature is 200°C and source temperature is 230°C.

3.8 Characterizations of extracted PHA

3.8.1 Nuclear magnetic resonance (NMR)

^{1}H spectra were recorded on Bruker Avance AVIII 400 MHz NMR spectrometers equipped with a 5-mm solution state BBO probe with Z-gradient, the temperature was regulated at 25°C and no spinning was applied to the NMR tube. Standard ^{1}H experiments were measured at 400.13 MHz using a 30° pulse for excitation, 64 k acquisition points over a spectral width of 20 ppm with 16 transients and a relaxation delay of 1 s. Chemical shifts are given in ppm with respect to tetramethylsilane using the NMR solvent used as internal standards.

For diffusion ordered spectroscopy (DOSY), ^{1}H DOSY NMR spectra were recorded on Bruker Avance AVIII 400 MHz NMR spectrometers equipped with a 5-mm solution state BBO probe with Z-gradient at temperature 25˚C. Using the standard single-stimulated echo pulse sequence stebpgp1s, the pulsed-field gradients were incremented in 16 steps, from 5% to 95% of the maximum gradient strength (3.4 G/cmA) in a linear ramp and 32 scans at each step. The diffusion time ∆ (d20) and the gradient length δ (p30) were optimized for each sample. The DOSY spectra were multiplied with an exponential window function before Fourier transformation (xf2) and subsequently phase and baseline corrected.

Diffusion coefficient (D) for each sample was obtained using Diffusion in Dynamics Center software and fitting each curve using Eq. (1) below:

$$I = I_0 e^{\left[-D\gamma^2 g^2 \delta^2 (\Delta - \delta/3)\right]} \quad (1)$$

where, I is signal intensity, I_0 is the reference intensity, D is diffusion coefficient, γ is the gyromagnetic ratio of the observed nucleus, g is the gradient strength, the little delta δ is the length of the gradient and the big delta Δ is the diffusion time.

3.8.2 Gel permeation chromatography (GPC)

PHA extracted by Soxhlet was used for molecular weight determination through gel permeation chromatography (GPC). One hundred microliters of sample (1-3 mg/ml) were analysed on an Agilent 1260 Infinity LC system (Agilent, USA), equipped with a

refractive index and viscosity detector. Polymers were separated using two PLgel MIXED-C (7.5x300 mm, 5 µm; Agilent) columns with a PLgel guard column (7.5x50mm, 5um; Agilent), all connected in series. Chloroform was used as the mobile phase at a flow rate of 1 mL/min, with the columns maintained at 40°C. Low-polydispersity polystyrene standards with peak molecular weights ranging from $0.162x10^3$ to $1.014x10^6$ g/mol (InfinityLab EasiVial Standards, Agilent) were used as standards. All molecular weight standards and experimental samples contained toluene as an internal standard to normalize retention times. Calibration of the system and analysis of the experimental samples were performed using the Agilent GPC data analysis software package. The number-average molecular weight (Mn), weight-average molecular weight (Mw), and polydispersity (PD) were measured for each sample.

3.8.3 Thermal gravimetry analysis (TGA)

Thermal degradation of PHA blends was evaluated by using a Perkin Elmer PYRIS 1 TAG system. Measurement was conducted by heating 8 mg PHA sample under nitrogen atmosphere (flow rate of 20 mL/min). The heating process started from 30°C to 400°C at a rate of 10°C/min.

3.8.4 Differential scanning calorimetry (DSC)

The thermal properties of PHA were analyzed by differential scanning calorimetry (DSC), using the Perkin Elmer DSC4000 system under a nitrogen stream with a flow rate 20 mL/min. Each PHA sample (5-7 mg) was placed in an aluminum pan and held at -80°C for 1 min. In the first heating cycle, the sample was heated from -80°C to 200°C at 10°C/min and held at 200°C for 1 min. The sample was then cooled from 200°C to -80°C at 5°C/min and held at -80°C for 5 min. For the second heating, the sample was heated again from -80°C to 200°C at 10°C/min. The crystallization (Tc) temperature and the enthalpy of crystallization (ΔH_c) was obtained from the DSC curve of the cooling step. The melting temperature (T_m) and enthalpy of melting (ΔH_m) was obtained from the DSC curve of the second heating.

3.9 Definition of key fermentation metrics

In this study, the following standard fermentation metrics were used to evaluate PHA production performance:

Cell Dry Weight (CDW, g/L):

The total biomass concentration in the culture, determined by collecting, washing, and lyophilizing cells from a known volume of culture, and measuring the resulting dry mass.

PHA Content (wt% CDW):

The proportion of PHA accumulated within cells, expressed as a percentage of the cell dry weight. This was calculated by quantifying the intracellular PHA content via methanolysis followed by GC analysis and normalizing it to the CDW.

PHA Titer (g/L):

The final concentration of PHA produced per liter of culture medium. It represents the overall production level and is calculated as:

PHA titer = CDW × PHA content (% CDW) / 100

PHA Composition (mol%):

The relative molar ratio of individual 3-hydroxyalkanoate monomers (e.g., 3HB, 3HHx, 3HO, 3HD) present in the PHA polymer. Monomer composition was determined by GC analysis after methanolysis and expressed as a percentage of the total molar amount of monomers detected.

3.10 Data collection and expression

The data presented in this thesis were collected from the experiments described in this chapter. Each data generated represents the average of at least two independent measurements, ensuring accuracy and consistency. Data were visualized using various graphs, charts, and plots to provide clear insights into trends and patterns

observed throughout the research.

Quantitative results, except for **Chapter 4** (derived from single experiment for each sample), are expressed as the mean ± standard error of mean (SEM) from three independent biological replicates, reflecting the biological variation across experiments. The standard error of the mean (SEM) was used to highlight the precision of the data, while statistical significance was determined where applicable using tests such as ANOVA. The careful processing and expression of data, combined with statistical analysis, ensured that the results presented are both reliable and scientifically rigorous.

In summary, this chapter established the technical framework used to investigate PHA biosynthesis and engineering. The described protocols enable precise manipulation of genetic constructs, controlled cultivation of microbial hosts, and comprehensive characterization of PHA products. These methods are applied in the following chapters to engineer microbial strains for enhanced PHA production and to evaluate the impact of genetic and process variables on polymer titer and composition. The next chapter focuses on the metabolic engineering of scl-PHA producing strains and the introduction of mcl-PHA biosynthetic pathways.

Chapter 4: Engineering of scl-PHA Producer

This chapter describes the engineering of native scl-PHA producing strains, with a focus on the integration of mcl-PHA biosynthetic pathways. *Rhodococcus* species and *C. necator* were selected as model hosts due to their metabolic versatility and known capacity for PHA accumulation. Two distinct mcl-PHA synthesis routes were evaluated—via fatty acid de novo synthesis and β-oxidation—requiring the identification and heterologous expression of key enzymes. Expression vectors were constructed and introduced into the selected strains to enable functional pathway analysis. The results of plasmid construction, protein expression, and PHA production are presented and discussed in this chapter.

4.1 Enzymes needed for different pathways

As mentioned in **Section 2.2.5** of the literature review, there are two common biosynthetic pathways for mcl-PHA, as shown in **Figure 4.1**. The following section will briefly explain the composition of each pathway and the enzymes selected for constructing these pathways.

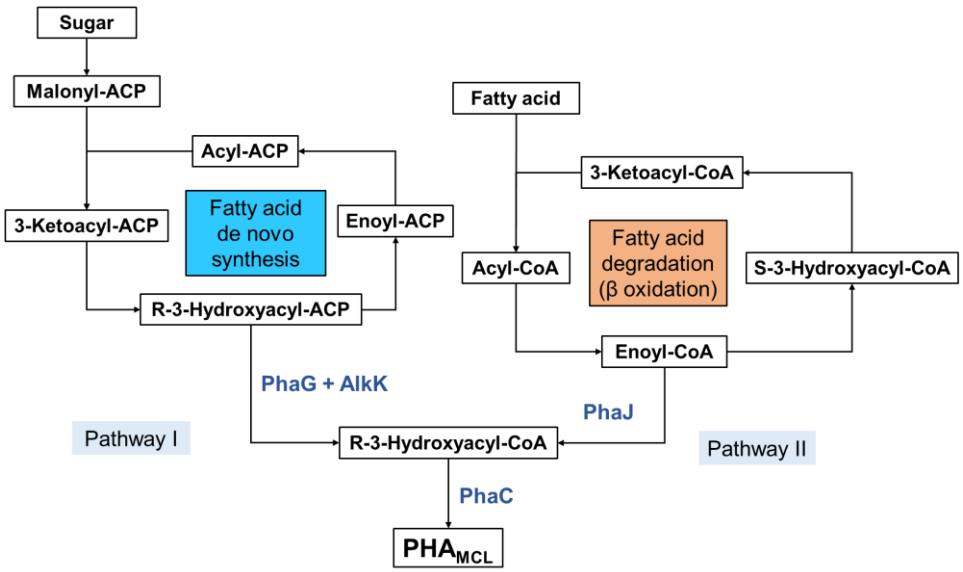

Figure 4.1. Common synthesis pathways for mcl-PHA and key enzymes required (Choi et al., 2020a, Salvachua et al., 2020). PhaG: ydroxyacyl-ACP acyltransferase; AlkK: acyl-CoA-synthase; PhaJ; enoyl-CoA hydratase; PhaC: PHA polymerase.

4.1.1 Pathway I through fatty acid de novo synthesis

Pathway I relies on the synthesis of fatty acids within the microorganism. Short-chain carbon sources enter the Fatty Acid de novo synthesis pathway through metabolic routes, where R-3-Hydroxyacyl-ACP is converted into free fatty acids by the action of the thioesterase PhaG, which are then converted into the corresponding 3HA-CoA by fatty acid-CoA ligase AlkK. The 3HA-CoA can subsequently be polymerized by PHA synthase to form PHA.

In this pathway, the three key enzymes are PhaG, AlkK, and PhaC, as mentioned above. These three enzymes are commonly found in mcl-PHA producers such as *P. putida*. Heterologous expression of the genes encoding these enzymes from *P. putida* enabled successful production of mcl-PHA copolymers in *E. coli* and *P. putida* (Wang et al., 2012, Wang et al., 2018). Inspired by these results, this project aims to use the genes from *P. putida* to express the corresponding proteins in the selected model strain, thereby constructing a complete mcl-PHA production pathway.

4.1.2 Pathway II through fatty acid degradation (*β*-oxidation)

Pathway II requires carbon flux from fatty acid degradation. Medium- and long-chain fatty acids enter the β-oxidation pathway, generating Enoyl-CoA, which is then converted to 3HA-CoA by an essential enzyme, PhaJ, and subsequently polymerized into PHA by PhaC. Therefore, the key enzymes for constructing this pathway are PhaJ and PhaC. Similarly, this pathway is found in many mcl-PHA producers and has been successfully used to produce mcl-PHA in *Escherichia coli* and even *C. necator* (Flores-Sanchez et al., 2020, Sato et al., 2011). Therefore, PhaJ and PhaC from *P. putida* were selected to achieve the mcl-PHA production only in *Rhodococcus* strains.

4.2 Results and discussion

This section covers all experimental results and discussions related to the engineering of scl-PHA producers. Including assessing the feasibility of plasmid-mediated protein

expression across various bacterial strains, using molecular cloning to construct expression vectors for the relevant proteins, which were used to transform the target bacteria. After obtaining successful transformants, they were utilized for PHA production.

4.2.1 Construction of expression vectors

To express the three enzymes AlkK, PhaG, and PhaC simultaneously, they were cloned into a single plasmid. This process began with the lab stock plasmid pBBR1c-PhaC, as shown in **Figure 4.2a**. The plasmid's replicon is pBBR1, carrying a chloramphenicol resistance gene CmR as selection marker. It originally harbored the *phaC* gene from *P. putida*, with its expression controlled by an arabinose-inducible promoter ParaB. Therefore, it was only necessary to clone the genes encoding the AlkK and PhaG enzymes into this plasmid, generating plasmid pBBR1c-CAG (**Figure 4.2b**).

Subsequent transformation experiments demonstrated that the plasmid could not be used to transform *Rhodococcus* strains as no transformants were obtained. A suitable plasmid pDD56 was used as it was confirmed to function in *R. opacus* PD630 (DeLorenzo et al., 2018). As shown in **Figure 4.2c**, pDD56 carries a pBR322 replicon and a kanamycin resistance gene. The plasmid also contains an enhanced yellow fluorescent protein (EYFP) gene, whose expression is regulated by an arabinose promoter PrhaB. To utilize this plasmid for expressing the enzymes related to the pathway I in *Rhodococcus* strains, the three genes were cloned into pDD56, replacing EYFP, forming plasmid pDD56-CAG (**Figure 4.2d**).

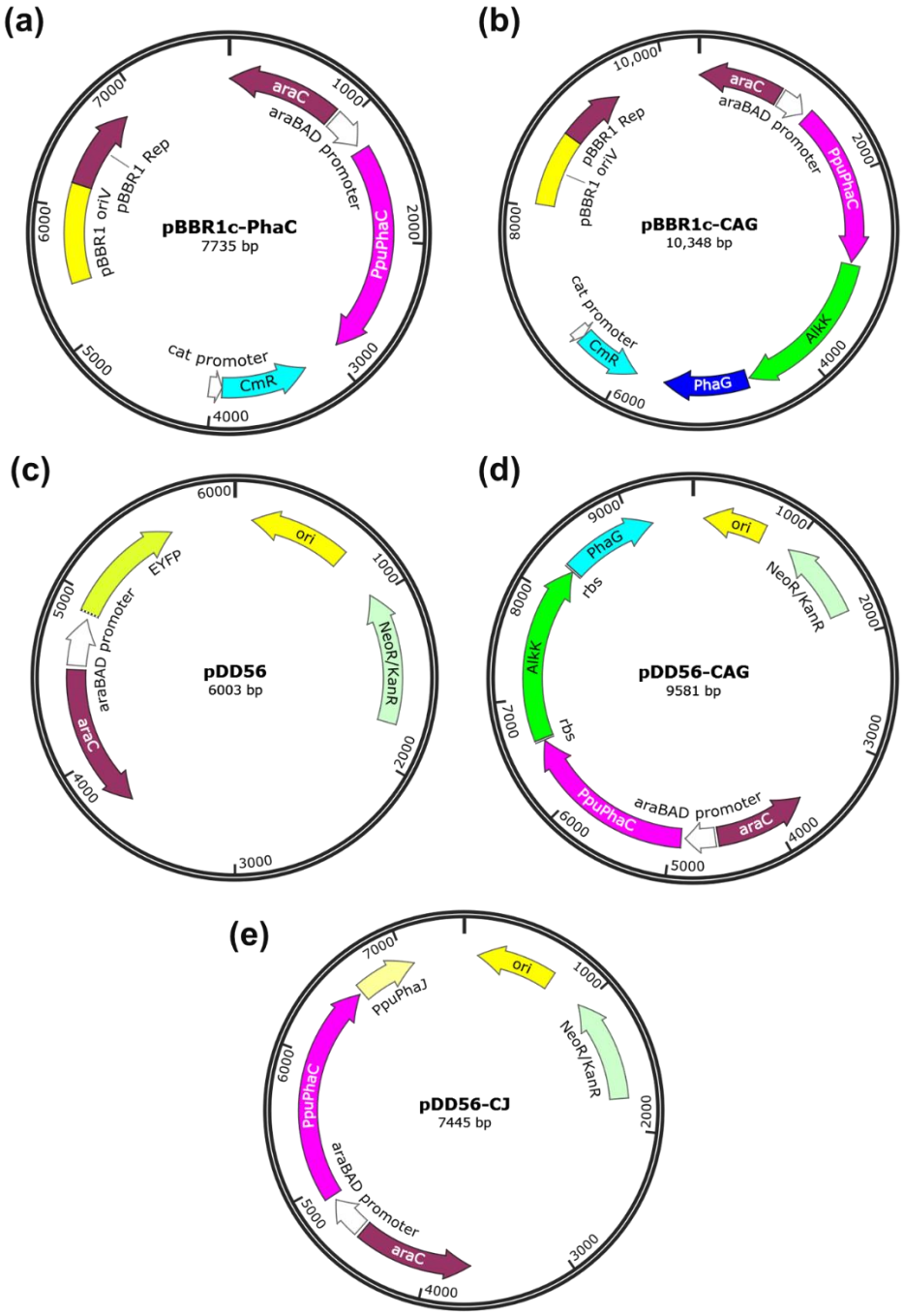

Figure 4.2. Map of plasmids (a) pBBR1c-PhaC, (b) pBBR1c-CAG, (c) pDD56, (d) pDD56-CAG and (e) pDD56-CJ.

The construction of plasmid for pathway II requires the involvement of only two enzymes: PhaC and PhaJ. Based on the existing pDD56-CAG plasmid, a feasible approach is to directly clone the gene encoding PhaJ from the *P. putida* genomic DNA into pDD56-CAG, replacing the *alkK* and *phaG* genes, thereby forming the pDD56-CJ

plasmid (**Figure 4.2e**).

4.2.2 Transformation test of the plasmids in different strains

The original plasmid, pBBR1c-phaC, was derived from the pBBR1c-RFP plasmid and had been successfully employed in studies of promoters in *C. necator* (Johnson et al., 2018). However, when transformation experiments were conducted with these plasmids in three different *Rhodococcus* strains, no transformants were obtained using either pBBR1c-phaC or the modified pBBR1c-CAG plasmid, which contains the inserted *alkK* and *phaG* genes. This result indicates that these plasmids are unsuitable as protein expression vectors for the *Rhodococcus* strains.

As described earlier, the plasmid pDD56, which had been used in *R. opacus* studies, was obtained to serve as a protein expression vector in *Rhodococcus* strains. To confirm its functionality in these strains, transformation experiments were conducted. After incubation on agar plates containing kanamycin, transformants were observed only for *R. jostii* and *R. opacus* (**Figure 4.3**), with no colony growth for *R. ruber*. This result demonstrates that pDD56 can be used to transform *R. jostii* and *R. opacus*, conferring kanamycin resistance, which is critical for selecting transformants. It also suggests the need for a suitable plasmid for *R. ruber*. Plasmid functionality in bacterial strains is often limited by several factors, including incompatibility with the host's replication and gene expression systems. The origin of replication on a plasmid may not align with the host's replication machinery, thereby impeding plasmid propagation (Novick, 1987).

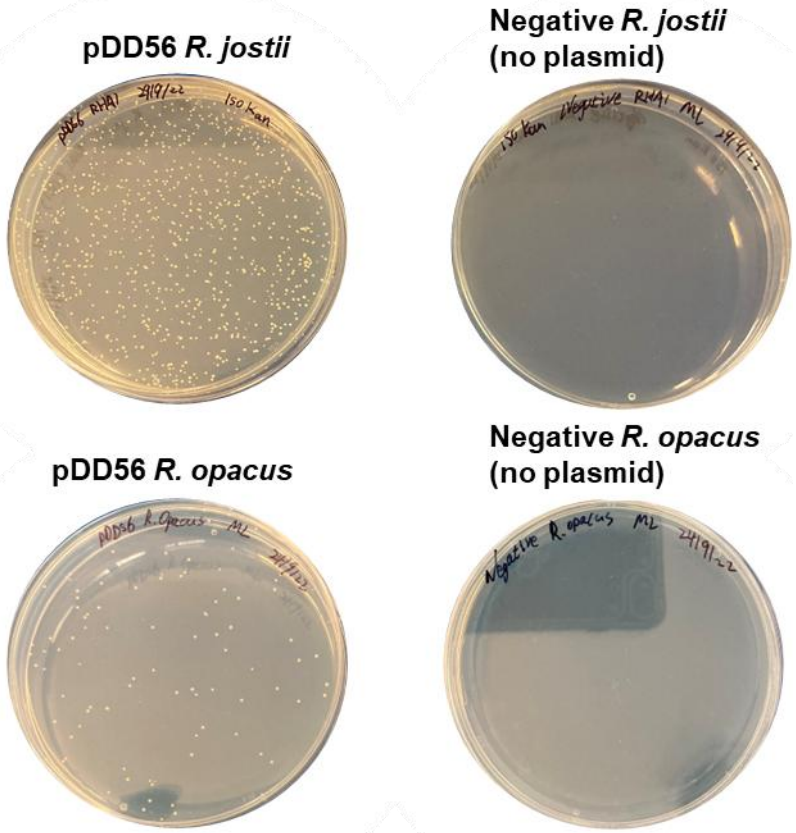

Figure 4.3. Agar plates show transformation results of *R. jostii* and *R. opacus* with plasmid pDD56. Plates contain 50 µg/mL kanamycin for selection. Colonies appear only on transformed strains, confirming successful transformation. Sample identities are labeled above the plates.

4.2.3 Fluorescent protein expression

Subsequently, single colonies of the transformants were cultured in MSM medium for 48 hours and harvested from 1.5 mL culture by centrifugation. Observation of the cell pellets at the bottom of the microcentrifuge tubes (**Figure 4.4**) revealed that, while the wild type cells did not exhibit fluorescence, the transformant cells harboring the plasmid displayed a distinct yellow color. As discussed in **Section 4.2.2.1**, the pDD56 plasmid contains the EYFP gene, with the yellow color arising from the expression of yellow fluorescent protein. These results validate the feasibility of the plasmid pDD56 as a protein expression vector in these two *Rhodococcus* strains.

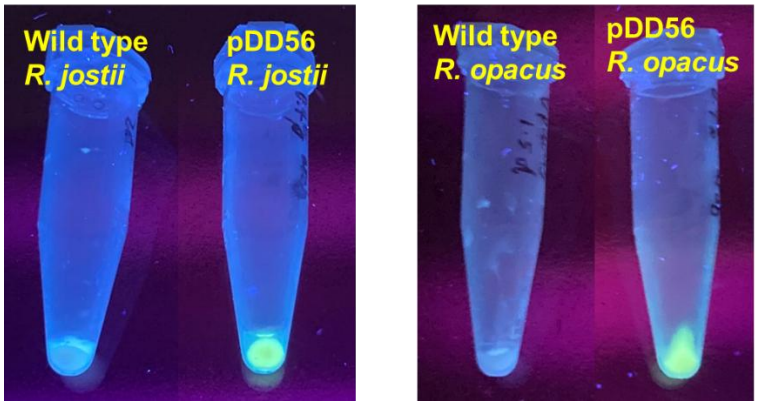

Figure 4.4. Fluorescent cell pellets of *R. jostii* and *R. opacus* transformants. Strains were cultivated in MSM medium with 1% glucose for 48 h. Protein expression was induced with 0.4% (w/w) arabinose. Fluorescence indicates successful expression in pDD56 transformants.

4.2.4 Plasmid verification by restriction endonuclease analysis

The assembled plasmid pBBR1c-CAG is expected to have a length of 10348 base pairs (bp) and contains three restriction enzyme recognition sites. As illustrated in **Figure 4.5a**, these sites are BamHI located between the *phaC* and *alkK* genes, SpeI between the *alkK* and *phaG* genes, and XhoI downstream of the phaG gene. Upon digestion with BamHI and XhoI, two distinct DNA fragments should be generated: one fragment comprising the plasmid backbone along with the *phaC* gene (7726 bp), and the second fragment containing the *alkK* and *phaG* genes, measuring 2622 bp. This is consistent with the results observed in the agarose gel electrophoresis experiment (**Figure 4.5b**), where lane a reveals two clear bands: the upper band corresponds to approximately 8000 bp, while the lower band is located around 2500 bp. When digested with SpeI alone, the plasmid is linearized, retaining its original length, and lane b displays a single band slightly larger than 10000 bp. The accurate fragment sizes obtained from both restriction digests confirm the successful construction of the pBBR1c-CAG plasmids.

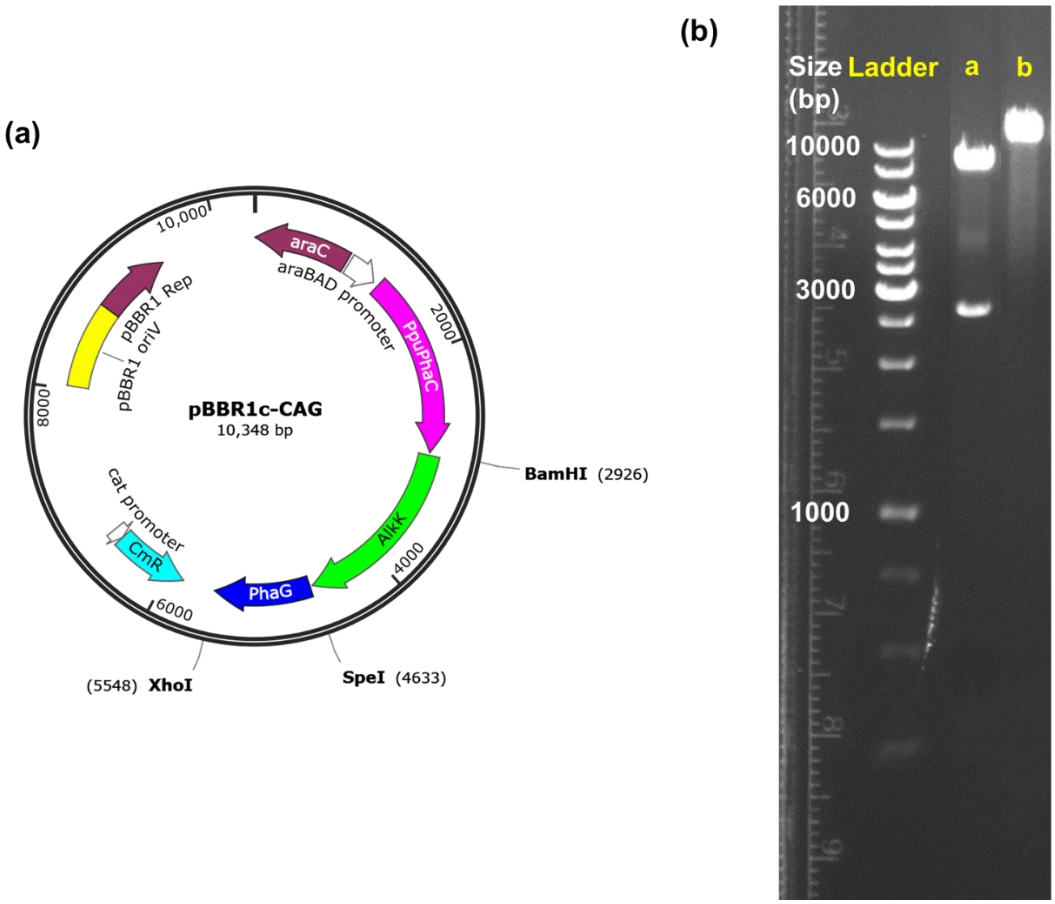

Figure 4.5. Restriction analysis of plasmid pBBR1c-CAG. (a) Plasmid map showing positions of the three restriction sites: BamHI (between phaC and alkK), SpeI (between alkK and phaG), and XhoI (downstream of phaG). (b) Agarose gel electrophoresis of digested plasmid DNA. Lane a: double digestion with BamHI and XhoI, yielding expected fragments of ~7726 bp and ~2622 bp. Lane b: single digestion with SpeI, resulting in a linearized plasmid (~10.3 kb).

The complete pDD56-CAG plasmid is 9581 bp in length and contains three EcoRI restriction sites, as shown in **Figure 4.6a**. When digested with EcoRI, the plasmid was cut into three DNA fragments, with sizes of 834 bp, 2060 bp, and 6687 bp. The agarose gel electrophoresis image confirmed the correct construction of the plasmid. All three bands were clearly visible, and their sizes matched the expected values **Figure 4.6b**.

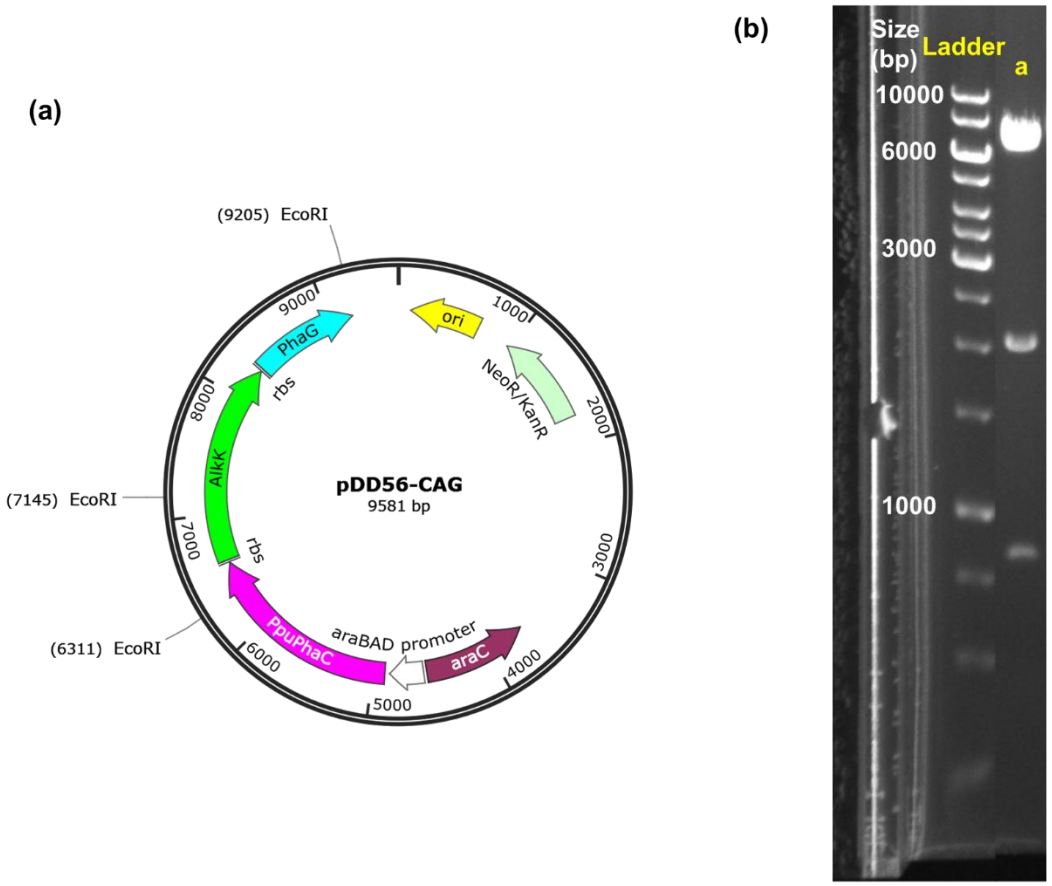

Figure 4.6. Restriction analysis of plasmid pDD56-CAG using EcoRI. (a) Plasmid map showing the three EcoRI restriction sites on pDD56-CAG (total length: 9581 bp). (b) Agarose gel electrophoresis of EcoRI-digested plasmid, producing three expected fragments of 834 bp, 2060 bp, and 6687 bp. The band pattern confirms correct plasmid assembly.

As shown in **Figure 4.7a**, the pDD56-CJ plasmid is 7445 bp in length, which is shorter than the previous plasmids due to the fewer genes required and the shorter length of the *phaJ* gene. To ensure that *phaJ* was correctly inserted into the plasmid, XbaI and HindIII were selected for restriction analysis, as they can specifically excise the DNA fragment containing *phaJ*. When the pDD56-CJ plasmid is digested with these two enzymes, the resulting DNA fragments should be 482 bp and 6963 bp. As shown in **Figure 4.7b**, in the sample lane, the brighter band is located at approximately 7000 bp, while a faint band is seen below 500 bp, as indicated by the yellow arrow. The large size difference between the two DNA fragments led to a significant disparity in band brightness. To ensure the visibility of the smaller fragment, a larger amount of DNA was

loaded than usual, resulting in overloading of the larger fragment, which made the band bigger and brighter. However, the key outcome is that the results confirm the insertion of *phaJ* and the correct construction of the plasmid.

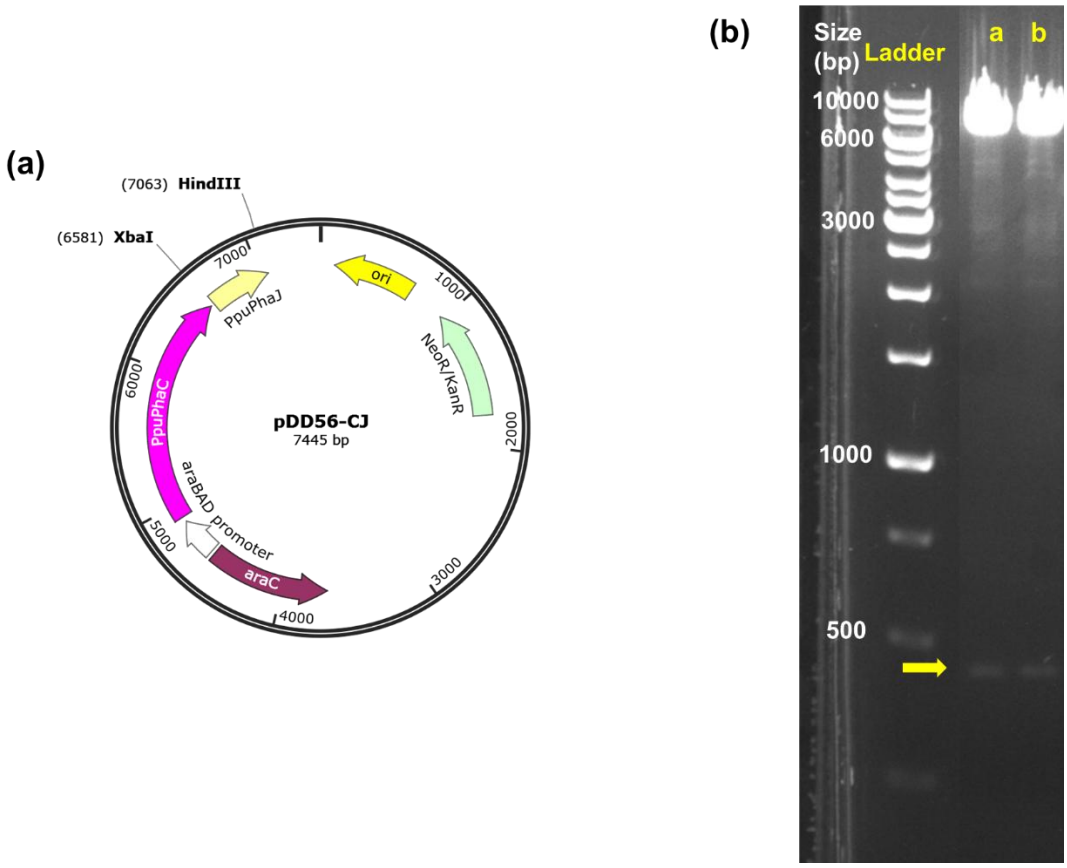

Figure 4.7. Restriction analysis of plasmid pDD56-CJ using XbaI and HindIII. (a) Plasmid map of pDD56-CJ (7445 bp), showing the positions of XbaI and HindIII restriction sites. (b) Agarose gel electrophoresis of the digested plasmid. Both lane a and lane b contain samples digested with XbaI and HindIII, producing fragments of 6963 bp and 482 bp. The smaller fragment appears faint due to size and staining limitations, while the larger fragment is brighter due to increased loading. The results confirm successful insertion of phaJ and correct plasmid construction.

4.2.5 Protein expression analysis in *E. coli* DH5α

While restriction enzyme digestion can confirm the expected size of plasmids, it cannot detect mutations that may occur during the cloning process and potentially affect protein expression. Therefore, the plasmids pDD56-CJ and pDD56-CAG were subjected to protein expression analysis in *E. coli*, and the resulting expression products were evaluated by SDS-PAGE.

To obtain the successful transformants of *E. coli* with recombinant plasmids, cells transformed with pDD56-CJ and pDD56-CAG were plated on agar plates containing kanamycin (50 µg/mL). As shown in **Figure 4.8**, colonies appeared on the selective plates, indicating the transformation was successful. Individual colonies were picked from each plate and cultured for subsequent protein expression analysis and PHA production.

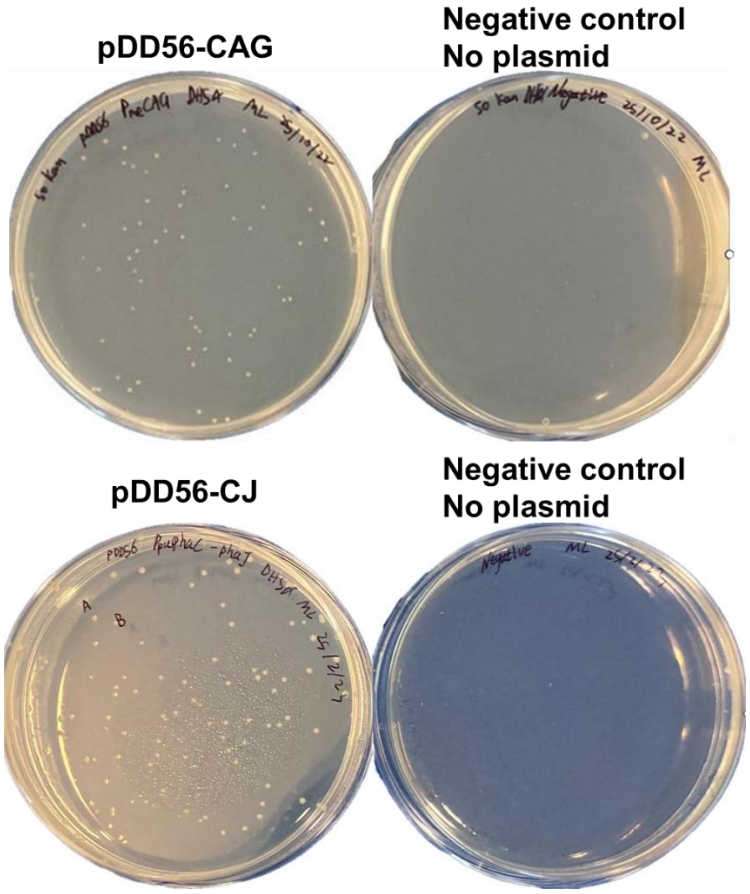

Figure 4.8. Agar plates showing transformation of *E. coli* DH5α with plasmids pDD56-CAG and pDD56-CJ. Colonies observed on selection plates confirm successful transformation. Samples were plated on LB agar containing 50 µg/mL kanamycin. Strain identities are labeled above the plates.

As shown in **Figure 4.9**, SDS-PAGE was used to examine the protein expression profiles of *E. coli* strains carrying different recombinant plasmids. The gel included three samples: a negative control strain without plasmid, and two engineered strains

harboring pDD56-CJ and pDD56-CAG, respectively. The pDD56-CJ plasmid encodes two proteins, PhaC (62.2 kDa) and PhaJ (16.8 kDa), while pDD56-CAG was designed to express PhaC (62.2 kDa), AlkK (65.0 kDa), and PhaG (33.9 kDa).

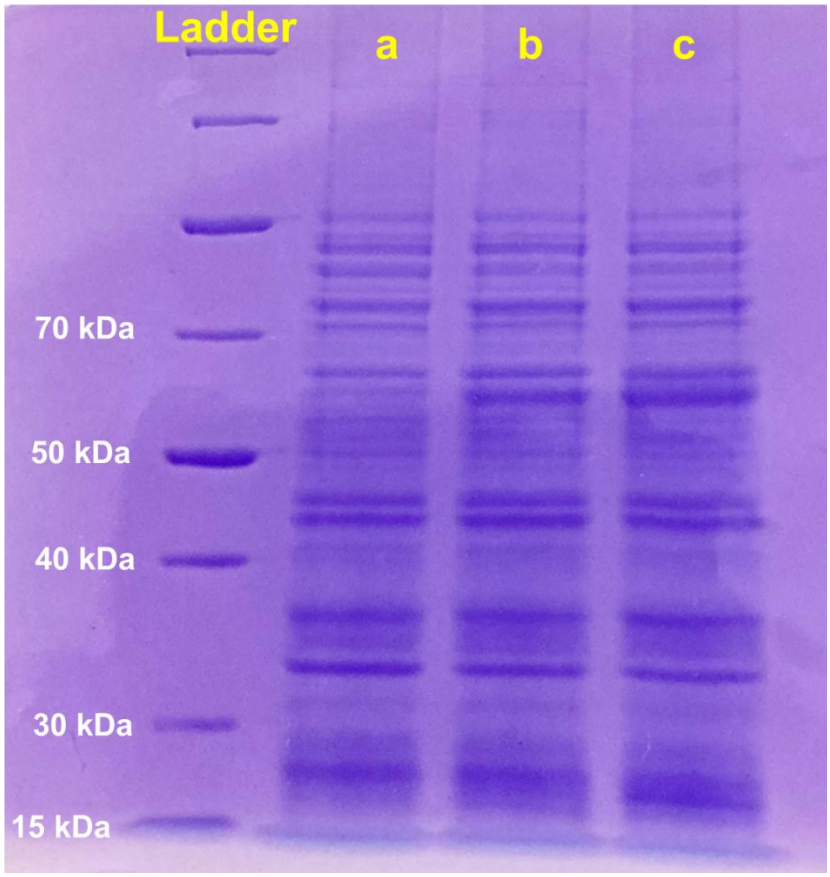

Figure 4.9. SDS-PAGE analysis of recombinant protein expression in *E. coli*. Lane a: Negative control (*E. coli* without plasmid); Lane b: *E. coli* harboring pDD56-CJ, expressing PhaC (62.2 kDa) and PhaJ (16.8 kDa); Lane c: *E. coli* harboring pDD56-CAG, expressing PhaC (62.2 kDa), AlkK (65.0 kDa), and PhaG (33.9 kDa).

In Lane b, a strong band was observed in the 50–70 kDa range, corresponding to the expected molecular weight of PhaC, indicating successful expression. In contrast, no distinct band was detected at ~16.8 kDa, where PhaJ was expected. Only a faint band was observed in this region, close to background staining, suggesting very low expression or instability of PhaJ in *E. coli*. In Lane c, a broader and more intense band was observed in the 50–70 kDa region compared to Lane B, likely due to the co-expression of PhaC and AlkK, whose molecular weights are similar. However, no

distinguishable band was detected at ~33.9 kDa, the expected size of PhaG. Instead, a prominent band was observed between 15–30 kDa, which may correspond to PhaG, potentially due to anomalous migration or partial degradation.

The absence or weak appearance of the PhaJ and PhaG bands could be attributed to multiple factors. First, small proteins such as PhaJ are often difficult to detect by Coomassie staining due to low abundance or weak staining efficiency (Neuhoff et al., 1988). Second, anomalous migration on SDS-PAGE may cause deviations from the expected molecular weights, particularly for small or membrane-associated proteins (Rath et al., 2009). To confirm the expression of these proteins, further analyses such as Western blotting using tagged constructs or specific antibodies will be necessary.

Overall, these results demonstrate that PhaC was successfully expressed from both plasmids, while AlkK was likely co-expressed with PhaC in the pDD56-CAG construct. However, the expression of PhaJ and PhaG remains inconclusive based on SDS-PAGE analysis and warrants further investigation.

4.2.6 PHA production analysis

After obtaining the correct plasmids, they were used to transform the target strains for PHA production. Following cultivation and harvesting, intracellular PHA was quantified by gas chromatography. As shown in **Table 4.1**, PHA accumulation was detected only in wild-type *R. ruber* and *C. necator*, which is consistent with the solvent extraction experiment, where PHA was also recovered exclusively from these two strains. *R. ruber* produced a copolymer of 3-hydroxybutyrate (3HB) and 3-hydroxyvalerate (3HV) (**Figure 4.10a**), while *C. necator* accumulated PHB (**Figure 4.10b**), as expected. These findings align with previous reports, as both strains are well-known native PHA producers (Anderson et al., 1995, Cappelletti et al., 2020, Anjum et al., 2016).

Surprisingly, neither the wild-type nor recombinant *R. jostii* accumulated detectable

PHA, which contradicts a few earlier studies that suggested *R. jostii* RHA1 has the potential for PHA biosynthesis under nitrogen-limited conditions (Hernandez et al., 2008, Tajparast and Frigon, 2018). The discrepancy may stem from strain-specific genomic variation, cultivation conditions, or regulatory differences in PHA gene expression. Notably, reports on PHA accumulation in *R. jostii* are scarce and sometimes inconsistent in terms of polymer titer and composition. In this study, the lack of PHA production under the tested conditions may suggest that *R. jostii* requires specific environmental triggers or carbon sources to activate its PHA biosynthetic pathway.

Table 4.1. PHA production analyzed by GC. All strains were cultivated in MSM medium supplemented with 1% (w/v) glucose for 48 hours. (n.d. = not detected)

Strain	**Plasmid**	**CDW (g/L)**	**PHA content (wt% CDW)**	**PHA composition (mol%)**	
				3HB	**3HV**
R. jostii	None	4.0	n.d.	-	-
	pDD56-CAG	3.5	n.d.	-	-
	pDD56-CJ	3.6	n.d.	-	-
R. opacus	None	4.3	n.d.	-	--
	pDD56-CAG	3.8	n.d.	-	-
	pDD56-CJ	4.0	n.d.	-	-
R. ruber	None	2.3	8.9	44	56
C. necator	None	2.8	67.8	100	-
	pBBR1c-CAG	2.6	66.2	100	n.d.
				3HO (C8)	**3HD (C10)**
E. coli DH5α	pDD56-CAG	1.15	2.97	23.54	76.46
E. coli DH5α	pDD56-CJ	1.43	n.d.	-	-

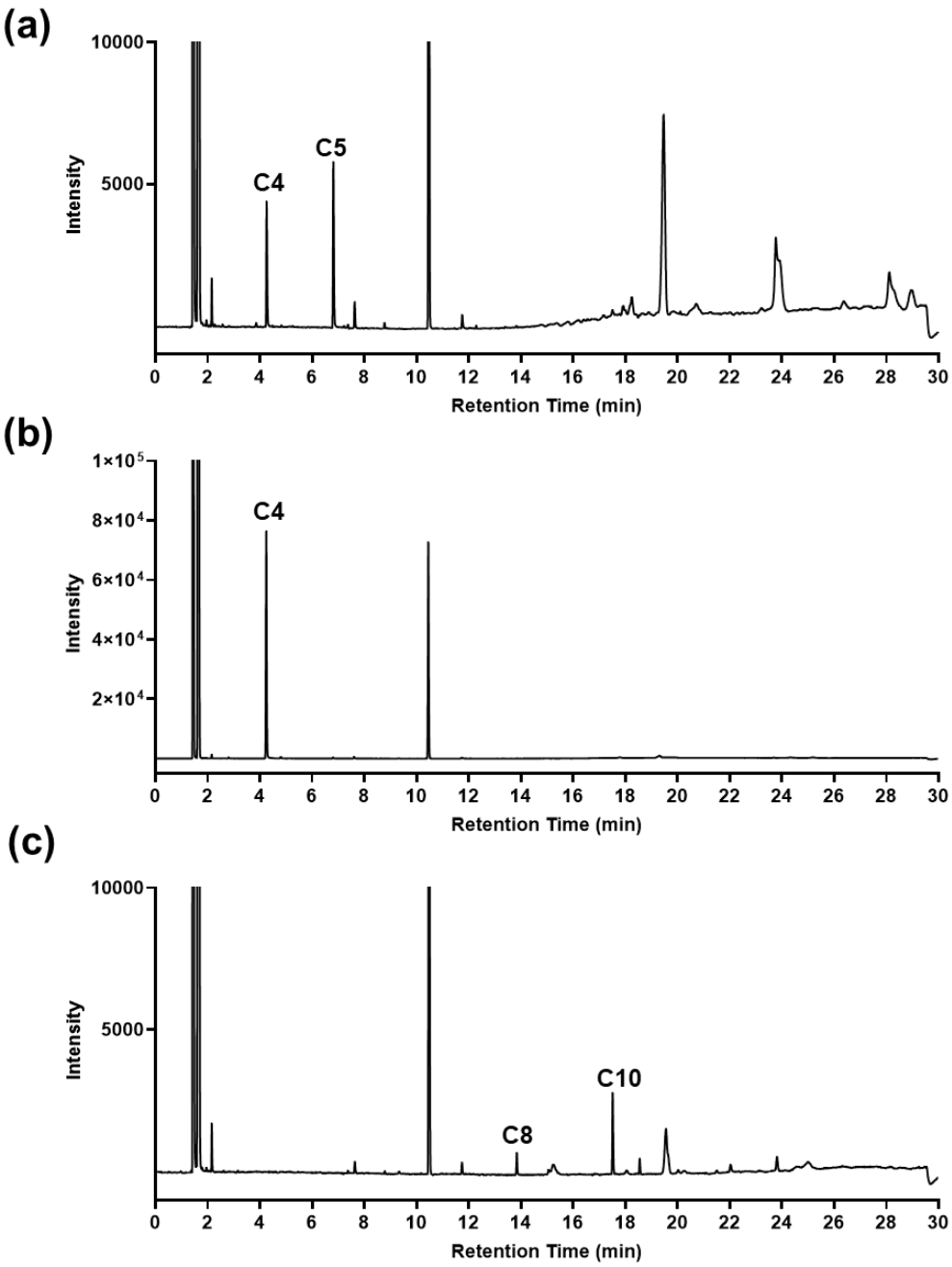

Figure 4.10. GC chromatograms of PHA monomer methyl esters derived from lyophilized cells of three PHA-producing strains. (a) Wild-type *R. ruber*, showing characteristic peaks of 3HB and 3HV; (b) Wild-type *C. necator*, producing PHB with a single dominant 3HB peak; (c) *E. coli* DH5α harboring pDD56-CAG, producing mcl-PHA with dominant C10 monomer signal. All strains were cultivated in MSM medium supplemented with 1% (w/v) glucose for 48 hours. Lyophilized biomass was subjected to methanolysis, and the resulting methyl esters were analyzed by gas chromatography.

Although *E. coli* was not selected as the production chassis in this study, it was used

as a model host to validate the functionality of the constructed plasmids. Two mcl-PHA biosynthetic pathways examined have previously been demonstrated to function in *E. coli* (Wang et al., 2012, Tsuge et al., 2000), making it a suitable system for initial validation. As shown in **Figure 4.10c** and **Table 4.1**, *E. coli* harboring pDD56-CAG accumulated mcl-PHA at 2.97 wt% of cell dry weight, with C10 as the dominant monomer (76.46 mol%). This result is consistent with prior reports and confirms the successful function of the phaC-alkK-phaG pathway encoded by pDD56-CAG. In contrast, no mcl-PHA production was observed in *E. coli* harboring pDD56-CJ, which was expected given the absence of long-chain fatty acids in the medium, which are required as substrates for this pathway (Tsuge et al., 2000, Sato et al., 2011). Due to consideration of avoiding using expensive long chain fatty acid, no further substrate supplementation was performed, leaving the functionality of pDD56-CJ only partially verified.

These results indicate that the introduced production pathways did not lead to mcl-PHA synthesis in *Rhodococcus* and *C. necator* strains. A plausible explanation is that the efficiency of the engineered pathway was insufficient to compete for intracellular carbon flux in the presence of native storage compound biosynthesis pathways. For example, in *Rhodococcus* and *C. necator*, carbon may have been preferentially diverted into the synthesis of triacylglycerols or PHB, both of which are naturally accumulated under nutrient-limited conditions (Cappelletti et al., 2020, Li et al., 2021b, Ahn et al., 2015). This redirection of carbon precursors such as acetyl-CoA or enoyl-CoA may limit the availability of intermediates for heterologous mcl-PHA biosynthesis.

Furthermore, the failure to detect mcl-PHA production in these strains is unlikely to be caused by errors in plasmid construction. The pDD56-CAG plasmid has been independently validated in *E. coli*, demonstrating its complete functionality. The lack of detectable product from pDD56-CJ is likely due to the absence of required substrates, rather than flaws in plasmid design. Overall, these findings underscore the importance of carbon flux optimization, chassis–pathway compatibility, and appropriate substrate

selection in engineering non-model hosts for PHA production. Future efforts may benefit from combining heterologous pathway expressions with strategies such as dynamic regulation, pathway balancing, or knockout of competing native storage routes.

4.3 Summary

In Chapter 4, the metabolic engineering of native scl-PHA producers was undertaken to enable the heterologous synthesis of mcl-PHA. Two model organisms, *Rhodococcus* species and *C. necator*, were selected based on their robust growth characteristics and intrinsic capabilities for polyhydroxyalkanoate accumulation. The engineering strategy focused on the introduction of two distinct mcl-PHA biosynthetic routes—one based on fatty acid de novo synthesis (Pathway I), and the other on β-oxidation (Pathway II).

To implement these pathways, genes encoding the key enzymes (phaG, alkK, phaJ, and phaC) were cloned into broad-host-range expression vectors. The resulting plasmids, pDD56-CAG (for Pathway I) and pDD56-CJ (for Pathway II), were designed for inducible expression and validated through restriction enzyme analysis and protein expression studies. Transformation into *R. jostii* and *R. opacus* confirmed that pDD56-based plasmids were functional in these strains, as evidenced by successful selection and fluorescent protein expression. However, transformation was unsuccessful using the pBBR1c-derived constructs, highlighting the necessity of host–vector compatibility.

Protein expression analysis in *E. coli* DH5α revealed successful expression of PhaC and AlkK from pDD56-CAG, with weaker or undetectable expression of the smaller proteins PhaG and PhaJ, likely due to issues with detection sensitivity or protein instability. Nevertheless, the functionality of the plasmids was partially confirmed by their ability to produce mcl-PHA in *E. coli*. Specifically, pDD56-CAG enabled the synthesis of mcl-PHA at 2.97 wt% of cell dry weight, with 3-hydroxydecanoate (C10)

as the dominant monomer.

In contrast, no detectable mcl-PHA was observed in *Rhodococcus* or *C. necator*, despite successful transformation and, in some cases, expression of pathway components. This result underscores the complexity of pathway–host interactions, particularly in non-model organisms. It is likely that native carbon flux in *Rhodococcus* and *C. necator* was directed toward competing storage molecules such as triacylglycerols or PHB, limiting the availability of precursors for mcl-PHA synthesis.

These findings collectively demonstrate that while synthetic mcl-PHA pathways can be functionally expressed in *E. coli*, achieving production in native scl-PHA producers requires careful optimization of metabolic context, substrate availability, and flux control. Future studies should explore dynamic pathway regulation, precursor supplementation, or genomic integration strategies to enhance pathway stability and carbon utilization efficiency in non-model hosts.

Chapter 5: Engineering of mcl-PHA Producer

Building on the findings of Chapter 4, where attempts to introduce the mcl-PHA biosynthetic pathway into scl-PHA producers did not result in successful mcl-PHA production, the research focus was redirected. Instead, this chapter explores an alternative and potentially more effective strategy: the incorporation of the *phaCAB* operon, responsible for scl-PHA synthesis, into *P. putida*, a natural mcl-PHA producer. This chapter details the experimental approaches undertaken to implement this strategy, including plasmid construction, promoter selection, strain transformation, and polymer characterization. The progress achieved demonstrates the viability of this reversed engineering route for producing PHAs with both scl and mcl monomers.

5.1 Introduce scl-PHA synthesis pathway

PHB, as the most common scl-PHA, has a well-established production pathway that has been extensively studied. The native PHB production pathway in *C. necator* (**Figure 5.1**) is highly efficient, and the associated *phaCAB* operon has been successfully heterologously expressed to produce PHB (Hiroe et al., 2012, Boontip et al., 2021), demonstrating the reliability of this pathway. Therefore, it was chosen as the exogenous pathway for PHB production in *P. putida*.

The key enzymes involved in this production pathway are PhaA, PhaB and PhaC. PhaA utilizes the widely available cellular intermediate acetyl-CoA, which is then converted into 3HB-CoA by PhaB and subsequently polymerized by PhaC to produce PHB. The *phaCAB* operon from *C. necator*, which contains the three genes encoding these enzymes, would be expressed in *P. putida* to enable the enzymes to perform their functions.

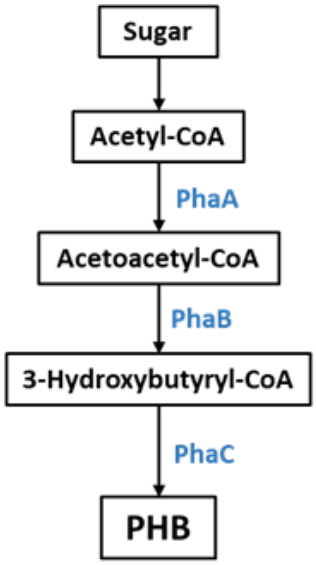

Figure 5.1. Simplified PHB synthesis pathway in *C. necator* (Choi et al., 2020a). PhaA: β-ketothiolase; PhaB: acetoacetyl-CoA reductase; PhaC: PHA polymerase.

5.2 Results and discussion

This section presents the experimental results from the genetic modification of *P. putida*, including the validation of the constructed plasmids, testing of different promoter strengths, measurement of PHA titer and composition and characterization of produced PHA samples.

5.2.1 Promoters and plasmids used

To precisely regulate the expression levels of PHB production-related genes and thereby control the composition of the produced PHA, promoters of varying strengths were employed to modulate the transcription of the *phaCAB* operon. This included four constitutive promoters (PphaC1, PrrsC, Pj5, and Pg25) used in *C. necator* and two inducible promoters (ParaB and PrhaB) that had been tested in *P. putida*.

Different promoters were cloned into separate plasmids, resulting in distinct plasmid constructs, which were used to express fluorescent proteins for measuring promoter strength. The constitutive promoters were cloned into plasmids (**Figure 5.2a-d**) containing the pBBR1 replicon, regulating the expression of the red fluorescent protein.

All these plasmids carried a kanamycin resistance gene, with the only difference being the region of promoters.

The plasmids carrying inducible promoters similarly contained the pBBR1 replicon, a gentamicin resistance gene, and a green fluorescent protein expression gene. The only distinction was in the promoter: plasmid pPS85 carried the arabinose-inducible promoter ParaB, while plasmid pPS87 carried the rhamnose-inducible promoter PrhaB **(Figure 5.2e-f).**

The position of the XhoI restriction site is indicated in each map. These plasmids were used to evaluate promoter strength via fluorescence in *P. putida*. After testing promoter strength, two constitutive promoters and two inducible promoters were selected to control the expression of the *phaCAB* operon. The *phaCAB* operon was cloned into the corresponding plasmids, replacing the fluorescent protein genes, resulting in new plasmids named PphaC1-phaCAB, Pg25-phaCAB, ParaB-phaCAB, and PrhaB-phaCAB, respectively (**Figure 5.3**).

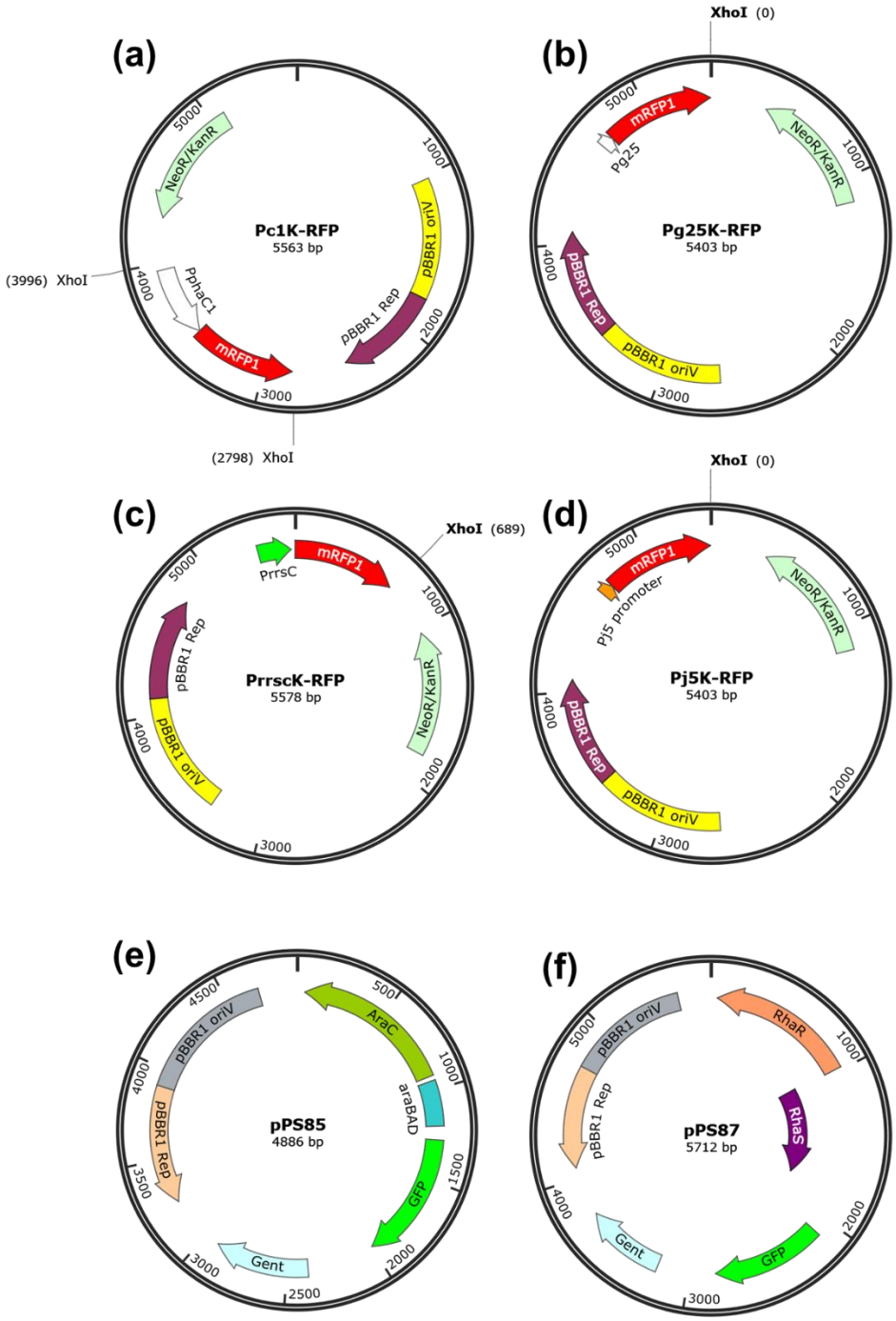

Figure 5.2. Plasmid maps used for promoter activity testing in *P. putida*. (a–d) Constructs carrying constitutive promoters (Pc1, Pg25, Prrsc, and Pj5) driving RFP expression: (a) Pc1K-RFP; (b) Pg25K-RFP; (c) PrrscK-RFP; (d) Pj5K-RFP. (e–f) Constructs carrying inducible promoters controlling GFP expression: (e) pPS85 (Parab-GFP); (f) pPS87 (Prhab-GFP).

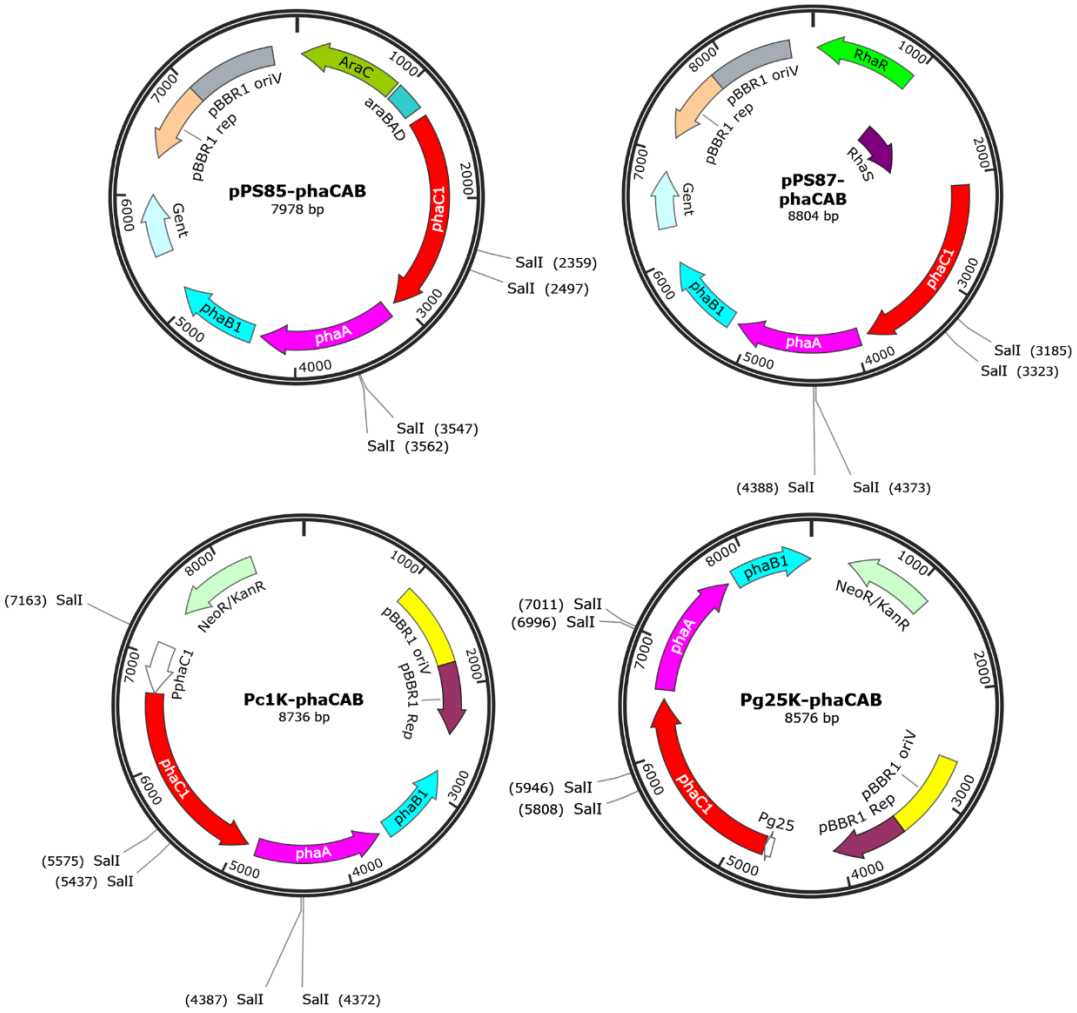

Figure 5.3. Plasmid maps showing *phaCAB* operon under regulation of different promoters and corresponding restriction sites for plasmid analysis. Four constructs were designed to express the *phaCAB* operon under various promoters: ParaB, PrhaB, Pc1K, and Pg25. The locations of key restriction sites are indicated on each map. These plasmids were used for functional expression of PHA biosynthetic genes in *P. putida* to assess promoter-dependent differences in PHA production.

5.2.2 Plasmid verification by restriction endonuclease analysis

A total of six plasmids were used for the promoter testing. Among them, the two plasmids carrying inducible promoters, pPS85 and pPS87, were purchased from Addgene and had been previously tested . The other four plasmids, carrying constitutive promoters, were constructed via molecular cloning, and their sizes were verified through restriction enzyme analysis. As shown in (**Figure 5.3**), the sizes of the four plasmids ranged between 5400 and 5600 bp due to the varying lengths of the promoters, and all of them contained an XhoI restriction site in their sequences.

After digestion with XhoI, the Pc1K-RFP plasmid was expected to be two fragments of approximately 1200 bp and 4400 bp, while the other three plasmids would produce a single linear DNA fragment of the corresponding length. The results of the DNA gel electrophoresis confirmed that the plasmid sizes were correct: in lane a, two bands were observed, with their positions matching the expected fragment sizes, while lanes b, c, and d each showed a single band, all slightly above 5000 bp (**Figure 5.4a**).

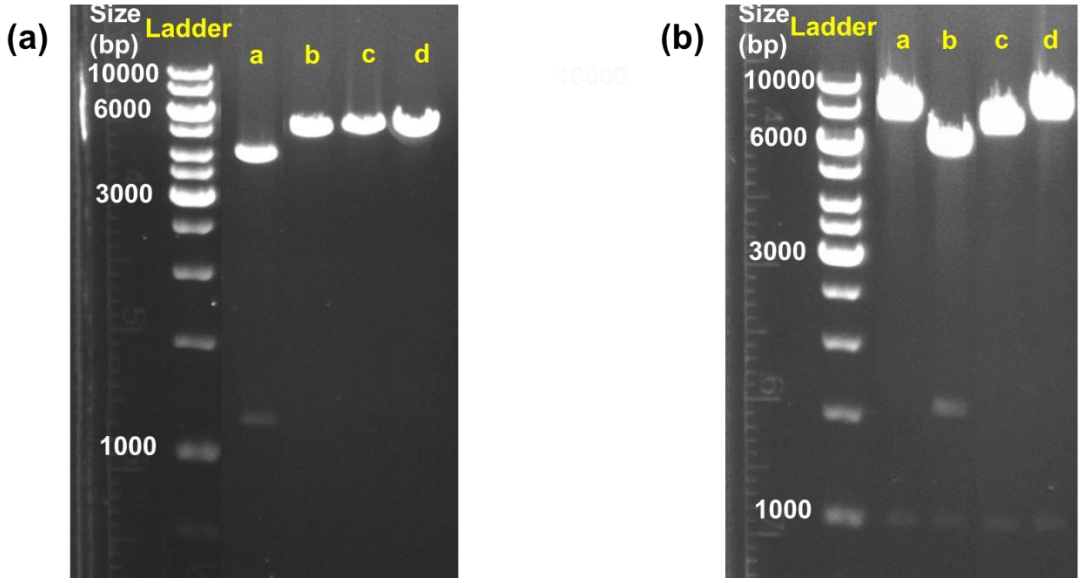

Figure 5.4. (a) Gel electrophoresis image of the digested plasmid Pc1K-RFP (lane a), Pj5K-RFP (lane b), PrrscK-RFP (lane c), Pg25K-RFP (lane d); (b) Gel electrophoresis image of the digested plasmid Pg25-phaCAB (lane a). Pc1K-phaCAB (lane b), pPS85-phaCAB (lane c), pPS87-phaCAB (lane d).

Finally, the *phaCAB* operon was cloned into four different plasmids, each approximately 8000 bp in size and containing multiple SalI restriction sites. Upon digestion with SalI, these plasmids are theoretically expected to produce several DNA fragments of varying sizes, which can be observed on the gel electrophoresis image. However, some fragments are too small to be visible. For instance, two closely spaced SalI sites within the *phaC* gene result in a 138 bp fragment, which is nearly impossible to detect by eye. As an example, the smallest visible band in the DNA ladder is 250 bp, and even that appears faintly.

However, the other bands are large enough to be observed. For example, all plasmids

are digested by SalI to produce a 1050 bp fragment, which is clearly visible in all lanes (**Figure 5.4b**). However, the PphaC1-phaCAB plasmid contains one additional SalI site compared to the other plasmids, resulting in a greater number of fragments, with three distinct bands clearly visible in lane b. In conclusion, all plasmids intended for the expression of *phaCAB* were successfully constructed, and their sizes were verified through restriction enzyme analysis.

5.2.3 *P. putida* transformation test

Although restriction enzyme analysis successfully confirmed the sizes of all constructed plasmid DNA, their functionality has not yet been verified. Transforming *P. putida* with these plasmids not only validates their functionality but also generates transformants carrying the plasmids, providing the foundation for subsequent experiments.

Figure 5.5 shows the transformation of *P. putida* with plasmids designed to express *phaCAB* operon and produce PHA. On each antibiotic-supplemented agar plate, transformants corresponding to the respective plasmids are clearly visible, whereas no colony growth is observed in the negative control group without plasmid addition. The transformation results confirm that the constructed plasmids can be successfully introduced into *P. putida* and are capable of self-replication, demonstrating their usability. Additionally, the antibiotics kanamycin and gentamicin effectively selected the transformants, and their inclusion in subsequent liquid cultures will help maintain the plasmids. Plasmids expressing fluorescent proteins were also successfully transformed into *P. putida* (images not shown).

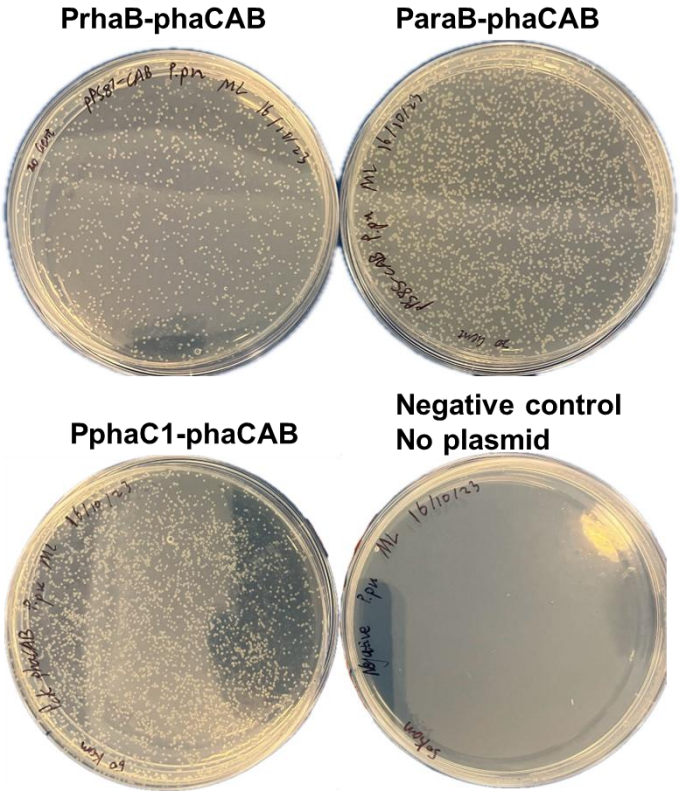

Figure 5.5. Agar plates from transformation experiment with antibiotic selection. No colonies were observed on the two negative control plates containing either Kanamycin (50 μg/mL, for PphaC1-phaCAB) or gentamicin (20 μg/mL, for PrhaB-phaCAB and ParaB-phaCAB). Only one representative blank control plate is shown.

5.2.4 Promoter strength test

The expression level of the fluorescent protein gene is regulated by the promoter, and the promoter's strength can be assessed by measuring fluorescence intensity. The objective of the promoter strength assay is to evaluate whether the selected promoters, particularly the four constitutive promoters, can function effectively in *P. putida*, as they have previously only been tested in *C. necator*. Furthermore, the assay seeks to compare the strengths of these promoters to identify suitable ones for controlling *phaCAB* expression.

The growth of *P. putida* transformants harboring various plasmids was monitored by measuring OD_{600} at certain intervals to generate growth curves (**Figure 5.6**). The results showed that all transformants, regardless of the plasmid and promoter type,

exhibited growth patterns similar to those of wild type *P. putida* throughout the cultivation period.

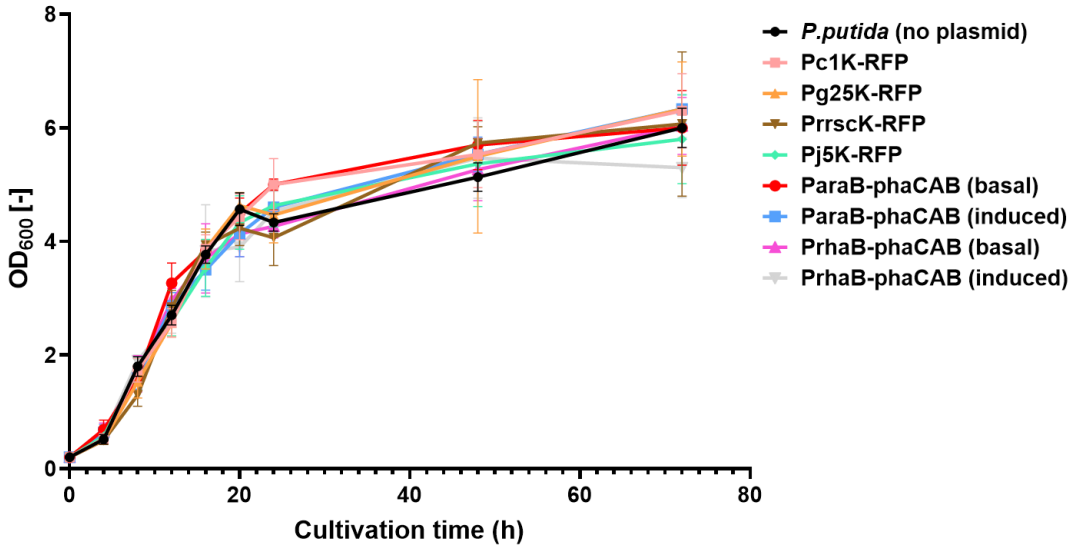

Figure 5.6. Growth curves of wild-type *P. putida* and transformants expressing fluorescent proteins under different promoters. Strains were cultivated with or without inducer to evaluate the impact of plasmid constructs on growth. Black line: wild-type strain; other lines represent plasmid-bearing strains. Basal conditions: no inducer added. Induced conditions: 0.4% (w/v) arabinose (for ParaB) or 10 mM rhamnose (for PrhaB) added when OD_{600}~0.6.

These results indicate that the presence of these plasmids did not affect the growth characteristics of *P. putida* under the specific cultivation conditions. Regardless of the promoter used, the expression of the fluorescent protein did not impose substantial competition for intracellular energy and metabolites, meaning there was no metabolic burden severe enough to impact growth.

The fluorescence intensity curves over time for red fluorescence (**Figure 5.7A**) reveal that *P. putida* cells carrying the Pg25K-RFP plasmid displayed significantly higher red fluorescence intensity compared to other samples. From the early stages of cultivation, the fluorescence level surpassed that of other samples and the gap widened over time. This indicates that the Pg25 promoter has stronger activity compared to other constitutive promoters, with the ability to sustain this over time. The other two

promoters, PphaC1 and Pj5, exhibited much lower and stable expression levels. Under the regulation of the PrrsC promoter, the red fluorescent protein also maintained very low expression levels and gradually decreased after 24 hours, to even the fluorescence levels of wild type *P. putida*.

The intensity curves of green fluorescence indicate that both inducible promoters possess the capacity for rapid and high-level expression of fluorescent proteins, with both reaching their maximum fluorescence intensity in the early stages of cultivation and then beginning to decline. When induced, ParaB displayed higher promoter activities compared to PrhaB, as confirmed by a two-way ANOVA analysis ($\alpha=0.05$, $P<0.01$). Cells without the addition of inducer (basal promoter activity) for both promoters displayed fluorescence levels consistent with those of the wild type, indicating high controllability of expression for both promoters. Inducible promoters, with their high responsiveness and controllability, are well-suited for applications requiring temporary but strong expression.

The data suggests that the Pg25 is the most robust among constitutive promoters, offering strong and persistent expression suitable for applications requiring high and steady protein production. The other promoters might be more applicable in contexts where lower expression levels are sufficient or desirable. Inducible promoters, with their high responsiveness and controllability, are well-suited for applications requiring temporary but strong expression.

Pg25 and PphaC1 exhibit significantly different protein expression intensities, while both inducible promoters demonstrate strong and controllable expression capabilities. They have all been selected to regulate the expression of the *phaCAB* operon, thereby enabling control over PHA production.

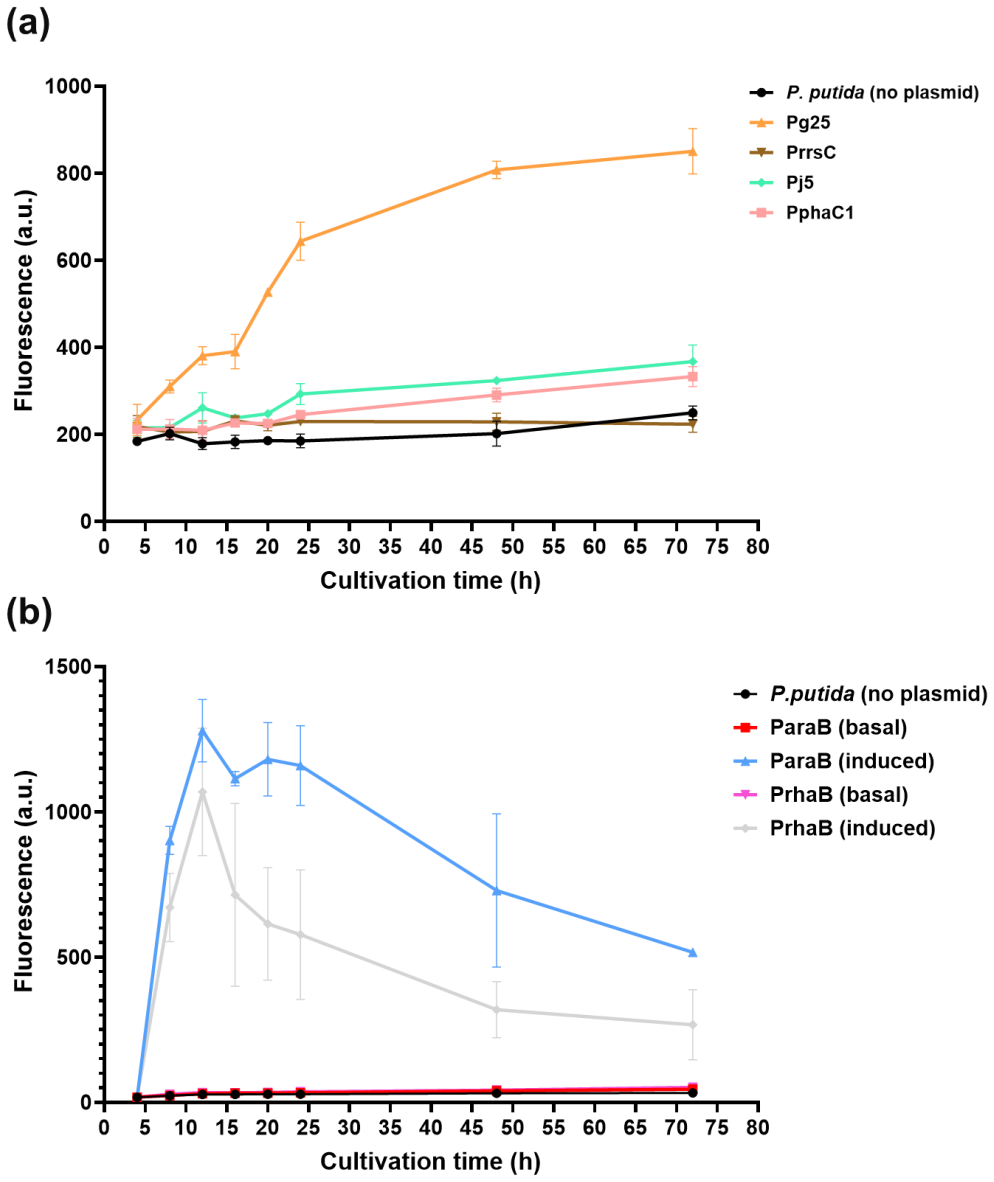

Figure 5.7. Fluorescence intensity curve of cell culture over time. (a) Red fluorescence regulated by different constitutive promoters; (b) Green fluorescence regulated by different inducible promoters. Cells carrying the inducible promoters were induced with either 0.4%(w/v) arabinose or 10 mM rhamnose at OD_{600}~0.6. Basal activities were measured for non-induced cells.

5.2.5 PHA composition modulated by promoter selection

PHA production by wild type *P. putida* and transformants harboring various plasmids was quantified via GC analysis of lyophilized cell (**Figure 5.8**, **table S1-S6**). As expected, native *P. putida* synthesized mcl-PHA with 3-hydroxydecanoate as the major monomer **(Figure 5.8a**), corroborating previous studies (Borrero-de Acuna et al., 2014, Sharma et al., 2012). The introduction of the heterologous *phaCAB* operon enabled

the biosynthesis of P(3HB) in *P. putida*, with the molar fraction of 3HB monomers in the resulting PHA ranging from 17.9 mol% to 99.6 mol% (**Figure 5.8b-f**). Despite no significant differences observed between the ParaB and PrhaB basal activity in regulating fluorescent protein expression (**Figure 5.7b**, 2-way ANOVA analysis with α=0.05), PHA produced by ParaB exhibited up to 41.2 mol% 3HB monomers, which was twice the 3HB content (20.6 mol%) in PHA produced under PrhaB regulation.

The promoter activity comparison based on fluorescent protein expression reflects only protein expression levels, whereas enzyme activity integrates both protein expression and enzyme turnover. The expressed *phaCAB* operon facilitates the repeated conversion of acetyl-CoA into P(3HB), and the continuous occurrence of this process results in sustained PHB production. This effectively amplifies the subtle and difficult-to-distinguish differences in basal protein expression levels between ParaB and PrhaB. Consequently, despite the low basal activities of both ParaB and PrhaB, the composition of 3HB monomers remains relatively high. Upon induction, both promoters lead to the production of PHA consisting almost entirely of 3HB monomers (**Figure 5.8d and 5.8f**).

The PphaC1 promoter was selected from the four constitutive promoters for subsequent PHA production and further characterization. Despite its relatively low promoter activity, it yielded a PHA mixture comprising 89.7 - 93.0 mol% 3HB monomers (**Figure 5.8b**), aligning with the trend observed for the basal activities of ParaB and PrhaB. Although the composition of produced PHA varied across different promoters, the composition remained consistent over time in both the wild type *P. putida* and all engineered strains (**Figure 5.8a-f**).

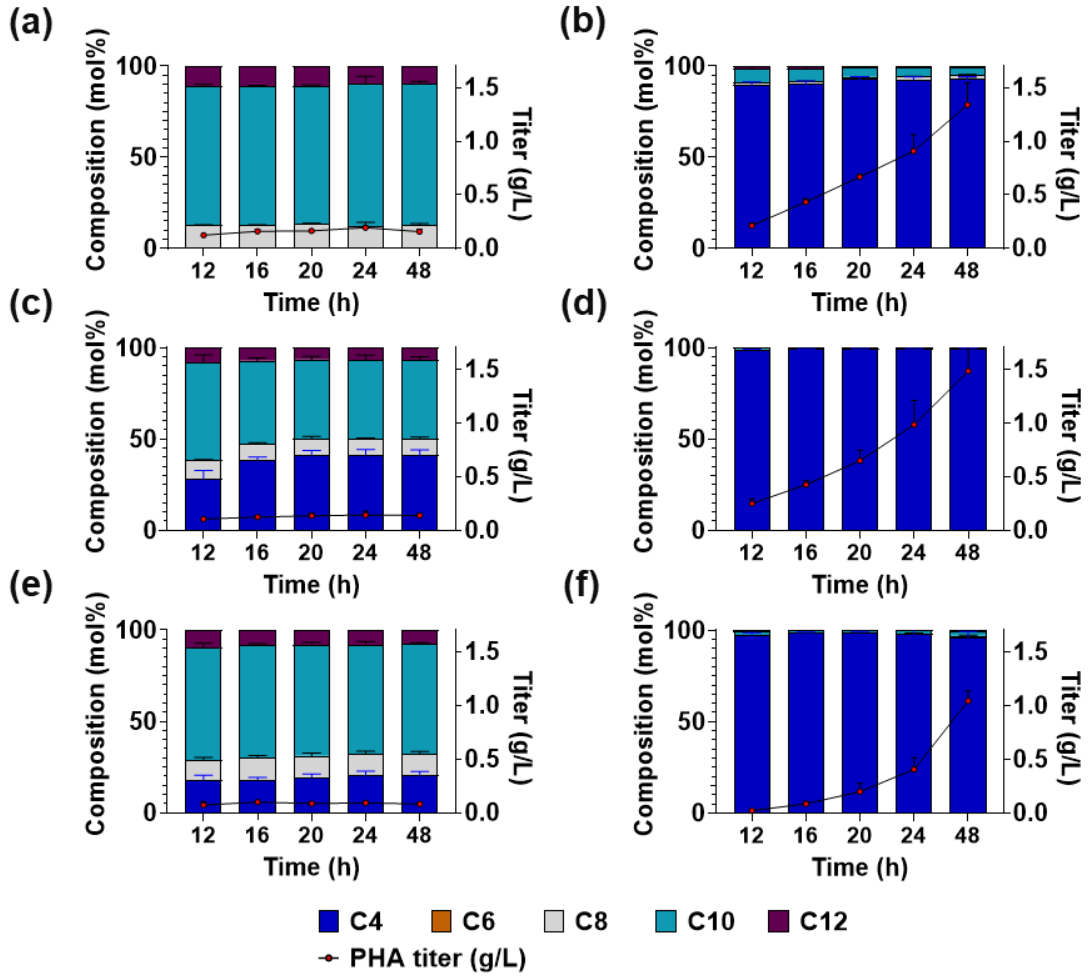

Figure 5.8. Composition and titer of PHA blends produced by *P. putida* harboring plasmids with the *phaCAB* operon controlled by different promoters: (a) No plasmid; (b) PphaC1; (c) ParaB (basal); (d) ParaB (induced); (e) PrhaB (basal); (f) PrhaB (induced). (a–f) The black line indicates the PHA titer (g/L), and the bar chart shows the monomer composition (mol%). PHA was produced in MSM medium with 1%(w/v) glucose. Cells carrying the inducible promoters were induced with either 0.4%(w/v) arabinose or 10 mM rhamnose at OD_{600}~0.6. Data were collected at specific time points post-inoculation and represent PHA detected from lyophilized cells.

Unlike the multi-copy plasmid encoding the P(3HB) pathway, the mcl-PHA components are produced by pathways encoded in the single-copy native genome. Even under conditions of low promoter activity, the presence of the multi-copy phaCAB operon significantly amplifies P(3HB) production. This explains the high P(3HB) content observed with the low-activity PphaC1 promoter, as well as with the basal activities of the ParaB and PrhaB promoters.

5.2.6 PHA titer influenced by promoter strength

At the measured time points, the PHA titer of wild type *P. putida* peaked at 24 hours, similar to the engineered strains where *phaCAB* operon was regulated by the basal activities of the ParaB and PrhaB promoters (**Figures 5.8a, 5.8c and 5.8e**). Among these three strains, native *P. putida* exhibited the highest PHA titer (0.193 g/L, **Table S1**), whereas the strain carrying ParaB (basal) produced the lowest PHA titer (0.100 g/L, **Table S5**). The reduction in PHA production is attributed to the decrease in mcl-PHA, likely caused by the metabolic burden imposed by the heterologous PhaCAB protein expression.

In contrast, the engineered strains harboring the constitutive PphaC1 promoter and the induced ParaB and PrhaB promoters continued to exhibit an increase in cell dry weight over the 48-hour cultivation period, which was also reflected in the sustained increase in OD_{600} for all three strains (**Figure 5.10**). The highest PHA titer was achieved at 48 hours, ranging from 1.04 to 1.48 g/L (**Tables S2, S4, and S6**), which is 7.7 times higher than the PHA titer of native *P. putida*. Interestingly, the strain carrying the induced ParaB plasmid produced the lowest amount of mcl-PHA and the highest P(3HB) titer (**Figures 5.9a** and **5.9b**), indicating a shift of intracellular resources from mcl-PHA to P(3HB) production.

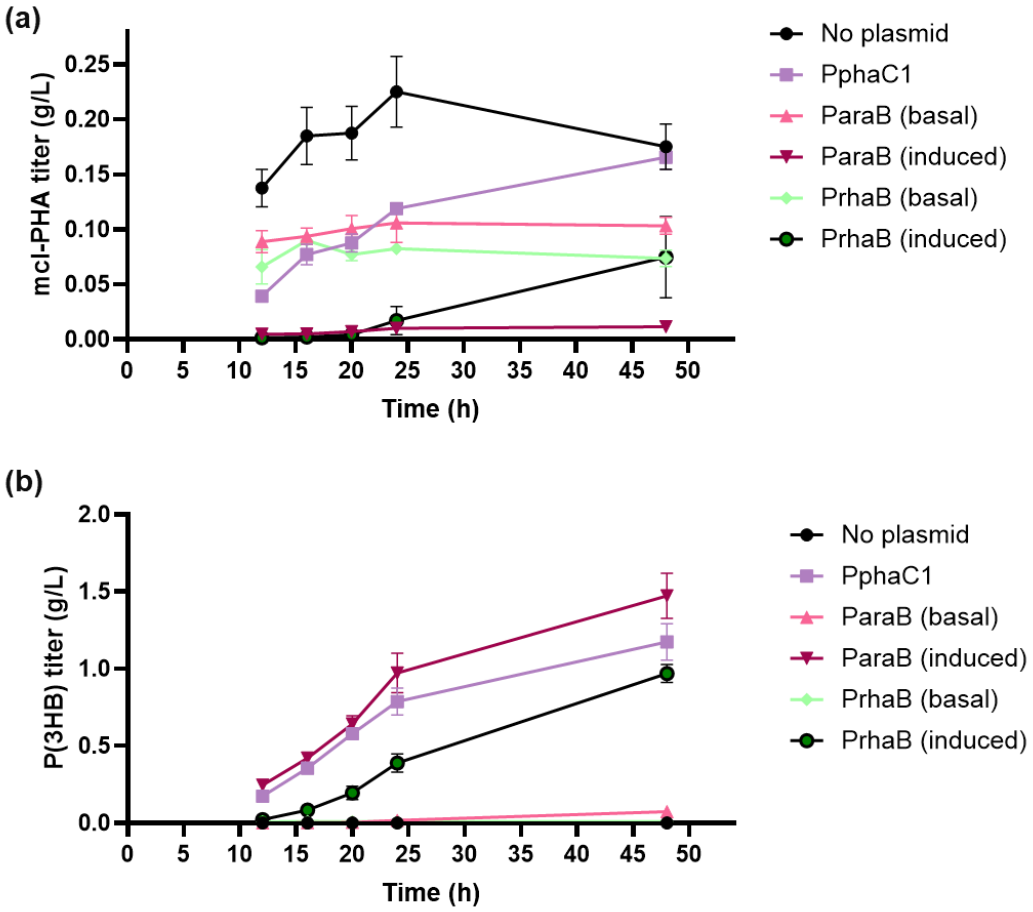

Figure 5.9. Separate quantification of mcl-PHA and PHB produced by engineered *P. putida* strains. This figure provides a breakdown of the total PHA titer presented in **Figure 5.8**, showing the individual titer of (a) mcl-PHA and (b) P(3HB) produced by engineered *P. putida* strains with the *phaCAB* operon controlled by different promoters. PHA was produced in MSM medium with 1%(w/v) glucose. Cells carrying the inducible promoters were induced with either 0.4%(w/v) arabinose or 10 mM rhamnose at OD_{600}~0.6. Data were collected at specific time points post-inoculation and represent PHA detected from lyophilized cells.

The metabolic pathway for mcl-PHA synthesis in *P. putida* is encoded by the chromosome and is regulated by the cellular metabolic state and nutrient limitations (De Eugenio et al., 2010, Mozejko-Ciesielska and Serafim, 2019). Notably, when the cultivation period was extended from 24 to 48 hours, the PHA content in wild type *P. putida* exhibited a gradual decline (**Figure 5.9a**). This phenomenon is likely attributable to the intracellular mobilization of stored mcl-PHA by PHA depolymerase (PhaZ) (Manoli et al., 2022). In *P. putida* KT2440, the phaZ gene is located within a gene cluster between phaC1 and phaC2, and it specifically hydrolyzes the mcl-PHA

accumulated within the cell (de Eugenio et al., 2007). Given that *P. putida* lacks a PHA depolymerase capable of degrading P(3HB), and the P(3HB) synthesis pathway continues to operate throughout the cultivation process, the production of P(3HB) continues to increase, even after mcl-PHA accumulation reaches a plateau **(Figure 5.9**). This pattern is particularly pronounced in cells harboring plasmids with the PphaC1 promoter and induced ParaB and PrhaB promoters.

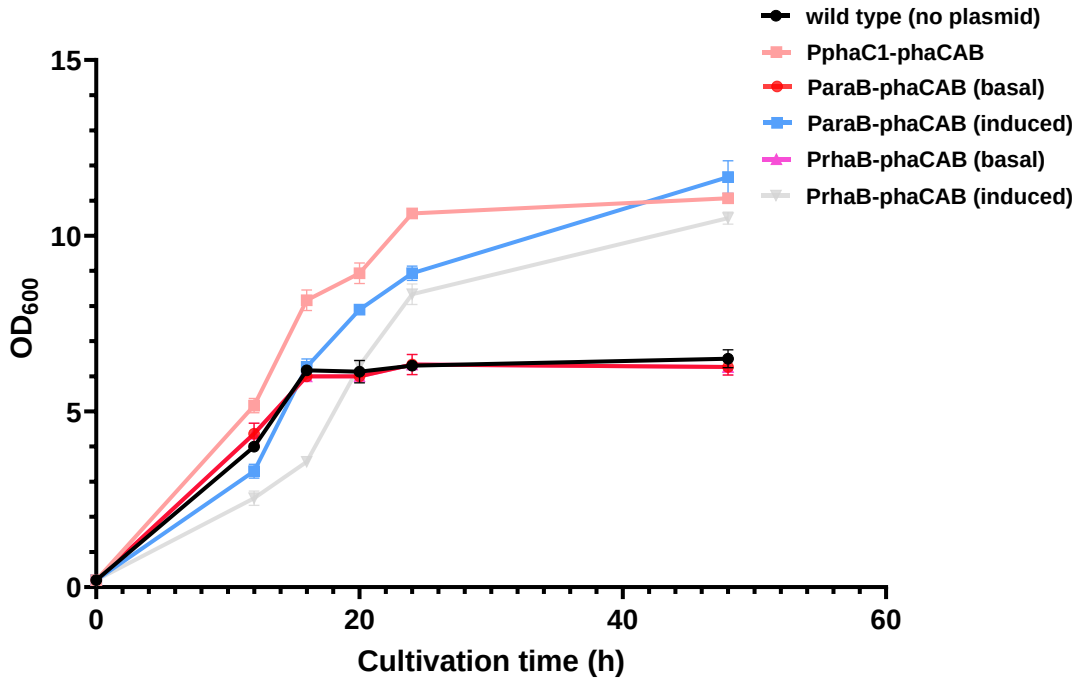

Figure 5.10. Growth curve of wild type *P. putida* and engineered strains with different promoters driving *phaCAB* operon. Cells were cultivated in MSM medium with 1%(w/v) glucose. Cells carrying the inducible promoters were induced with either 0.4%(w/v) arabinose or 10 mM rhamnose at OD_{600}~0.6.

When compared to the industrial benchmark strain *C. necator*, which achieved a PHA titer of approximately 1.90 g/L (2.8 g/L CDW with 67.8 wt% PHA, table 4.1), the engineered *P. putida* strain reached a slightly lower maximum PHA titer of 1.48 g/L. However, the *P. putida* derived polymer was a 3HB-rich PHA blend, with up to 99.6 mol% 3HB content, rather than a homopolymer PHB. While *C. necator* is known for its high-titer PHB production via a native, tightly regulated pathway, it lacks the ability to incorporate mcl-monomers. In contrast, the engineered *P. putida* system offers greater

compositional tunability, enabling the production of PHA blends with variable 3HB:mcl-PHA ratios. This compositional flexibility is advantageous for tailoring polymer properties to specific applications, even if the overall titer is modestly lower.

5.2.7 PHA production influenced by glucose concentration.

PHA is typically produced by microorganisms as a storage compound under nitrogen-limited conditions (Ahn et al., 2015, Cui et al., 2017). Therefore, the glucose concentration in the medium was increased to enhance PHA production. When the glucose concentration was raised from 1% to 6%, the PHA titer increased by more than 10-fold, with the highest intracellular PHA content reaching 42.2 wt% CDW (**Figure 5.11a**). The most significant improvement occurred when the glucose concentration increased from 1% to 2%, which resulted in higher cell mass, PHA content, and 3HB monomer content **(Figure 5.11b)**.

At a glucose concentration of 6% (w/v), the highest PHA titer reached 0.91 ± 0.07 g/L after 48 hours of cultivation. Interestingly, under this condition, the PHA obtained contained 90.4 ± 0.9 mol% of 3HB monomers, a substantial increase compared to the 3HB content observed at 1% glucose concentration (20.6 ± 1.2 mol%) under otherwise identical conditions. In addition, the production of mcl-PHA did not show any increase, once again highlighting the limitations of wild type *P. putida*, which relies on the β-oxidation and de novo fatty acid biosynthesis pathways to supply precursors (**Figure 2.3**) and is subject to stringent regulation within the central carbon metabolism of the cell(Mezzina et al., 2021).

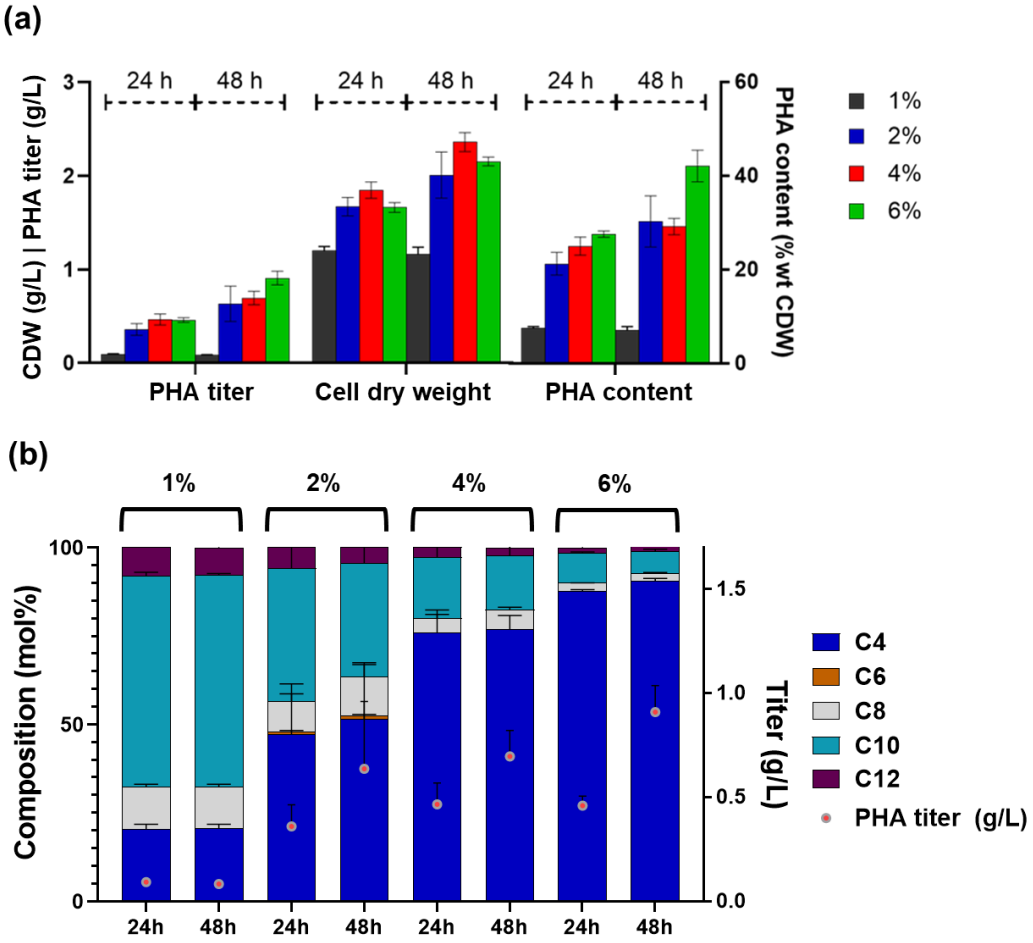

Figure 5.11. Effect of glucose concentration and cultivation time on PHA production and composition in *P. putida* expressing *phaCAB* under basal PrhaB promoter activity. (a) PHA production (titer) measured after 24 h and 48 h of cultivation in MSM medium supplemented with varying glucose concentrations. (b) Corresponding PHA composition (mol%) and titer (g/L) under each condition, showing the influence of both glucose availability and cultivation duration.

5.2.8 PHA extraction and composition detected by GC

To obtain PHA samples and perform subsequent characterization, the cells were cultured with 1% glucose for 24 hours, then lyophilized for PHA extraction using Soxhlet extraction method. The titer and monomer composition of the purified PHA (**Table 5.1**) were similar to the GC analysis results of the freeze-dried cells, confirming the reliability of our method. Low concentrations (0.4–1.6 mol%) of 3-hydroxyhexanoate monomers were detected in some PHA samples but not in the analysis of freeze-dried cells, indicating the lower sensitivity of the direct freeze-dried

cell detection method. The extracted PHA samples are shown in **Figure 5.12a-f**, with differences in monomer composition also reflected in the appearance of the PHA. Visually, mcl-PHA exhibited a transparent and slightly viscous state, while the PHA blend containing 43 mol% PHB appeared as a white paste. As the PHB content increased, the PHA samples remained white and became progressively fluffy.

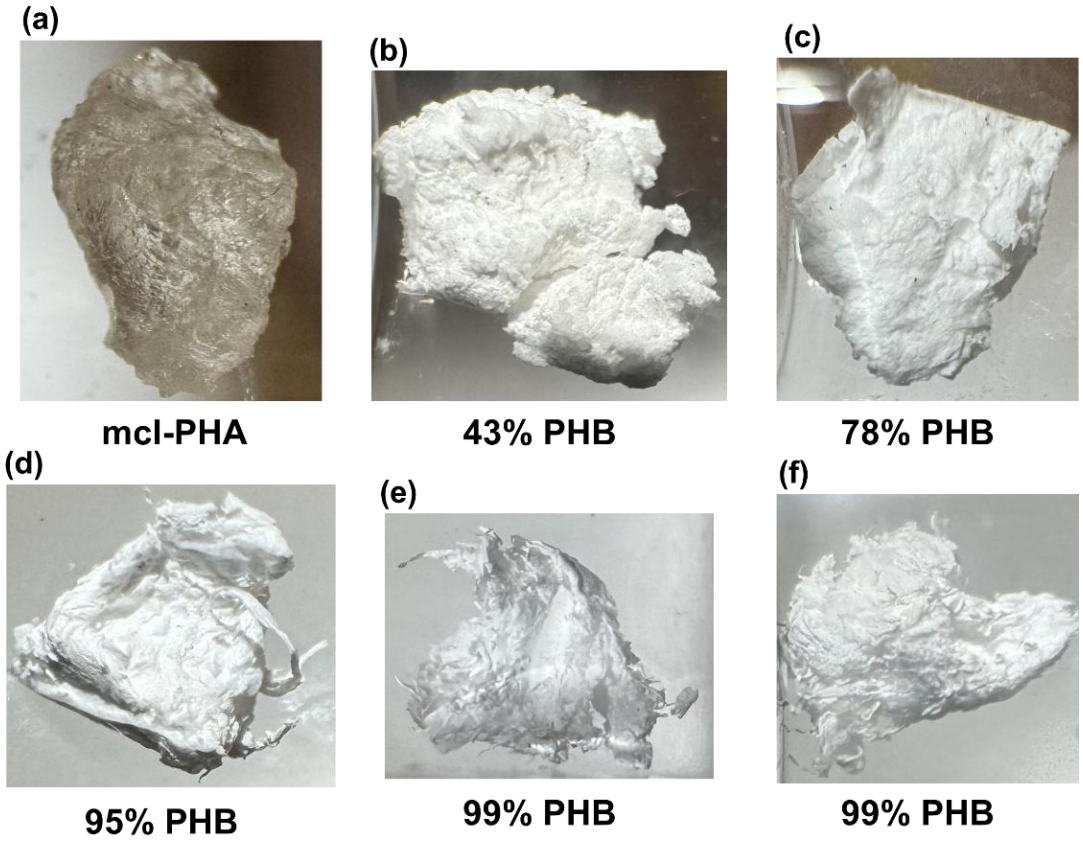

Figure 5.12. Photo of extracted PHA samples from cells of (a) wild type *P. putida* and engineered strain with *phaCAB* driving by (b) PrhaB (basal), (c) ParaB (basal), (d) PphaC1, (e) PrhaB (induced) and (f) ParaB (induced) promoters.

Table 5.1. PHA produced by native and engineered *P. putida* with different plasmids and extracted using the Soxhlet. The plasmids carry the *phaCAB* operon under the control of different promoters. *P. putida* cells were collected from 400 mL of culture after 24 h of cultivation.

	Monomer composition (mol%)					CDW (g/L)	PHA content	PHA titer (g/L)
Promoter	**C4**	**C6**	**C8**	**C10**	**C12**		**(wt% CDW)**	
No plasmid	n.d.	1.6 ± 0.1	13.7 ± 0.5	74.1 ± 0.2	10.1 ± 0.2	1.45 ± 0.07	18.1 ± 2.9	0.263 ± 0.054
ParaB (basal)	81.4 ± 3.1	0.4 ± 0.1	3.4 ± 0.4	12.9 ±2.2	1.9 ± 0.4	1.48 ± 0.06	16.0 ± 2.3	0.238 ± 0.043
PrhaB (basal)	30.4 ± 12.5	1.1 ± 0.2	9.6 ± 2.2	51.3 ± 9.0	7.5 ± 1.0	1.29 ± 0.06	10.5 ± 0.6	0.135 ± 0.013
ParaB (induced)	99.0 ± 0.3	n.d.	0.4 ± 0.0	0.7 ± 0.3	n.d.	1.88 ± 0.05	44.3 ± 2.7	0.829 ± 0.030
PrhaB (induced)	99.2 ± 0.2	n.d.	0.3 ± 0.1	0.5 ± 0.1	n.d.	1.86 ± 0.02	38.5 ± 5.3	0.716 ± 0.104
PphaC1	95.4 ± 0.7	n.d.	1.0 ± 0.1	3.0 ± 0.5	0.6 ± 0.1	2.44 ± 0.04	42.3 ± 3.0	1.031 ± 0.062

n.d. = not detected.

5.2.9 Monomer confirmed by GC-MS

The above analysis of PHA composition was based on GC detection of freeze-dried cells, where the identification of monomers was determined by matching the retention times of the measured substances with those of the corresponding 3-hydroxy methyl ester standards. This is a commonly used method for determining PHA composition; however, for more direct detection, GC is typically combined with mass spectrometry (MS) to analyze the mass spectra of each peak in the chromatogram. By comparing with mass spectral libraries, this method provides a more direct identification of unknown compounds in mixtures.

Figure 5.13 shows the GC-MS analysis of PHA produced by engineered *P. putida* with promoter PrhaB (basal). In the chromatogram, peaks with retention times of 2.87 minutes, 7.99 minutes, 10.70 minutes, and 13.13 minutes were clearly observed. These peaks were confirmed to correspond to the methyl esters of major PHA monomers generated after methanolysis, based on mass spectral comparison with reference spectra from the NIST database (**Figure S4**). For each compound, the characteristic fragment ions (e.g., m/z 103, 87, 74) matched those observed in authentic standard spectra. The identification included 3-hydroxybutyrate (C4), 3-hydroxyhexanoate (C6), 3-hydroxyoctanoate (C8), 3-hydroxydecanoate (C10), and 3-hydroxydodecanoate (C12), each exhibiting diagnostic fragmentation patterns consistent with known methylated 3-hydroxyalkanoates.

Notably, despite its low concentration, the substance corresponding to the peak at a retention time of 15.11 minutes had mass spectrum with a similarity of 51.2% to 3-hydroxytetradecanoic methyl ester, suggesting that PHA produced from *P. putida* likely contains C14 monomer (**Figure S4f**) which is consistent with previous research findings (Huijberts et al., 1992, Davis et al., 2013). However, due to its extremely low concentration and the absence of calibration using relevant standards, C14 was not included in the quantification or verification in this study. For more accurate

identification in future work, it is recommended to analyze a commercially available 3-hydroxytetradecanoate methyl ester standard under identical GC-MS conditions, to obtain a full, unfragmented mass spectrum for comparison.

These results are consistent with the GC data presented in earlier sections, in which the same set of PHA monomers was detected and quantified based on retention time and calibration curves derived from authentic standards. The agreement between GC and GC-MS analyses provides cross-validation for the analytical workflow. These findings collectively demonstrate the reliability and reproducibility of the analytical approach used in this study for characterizing PHA monomer composition.

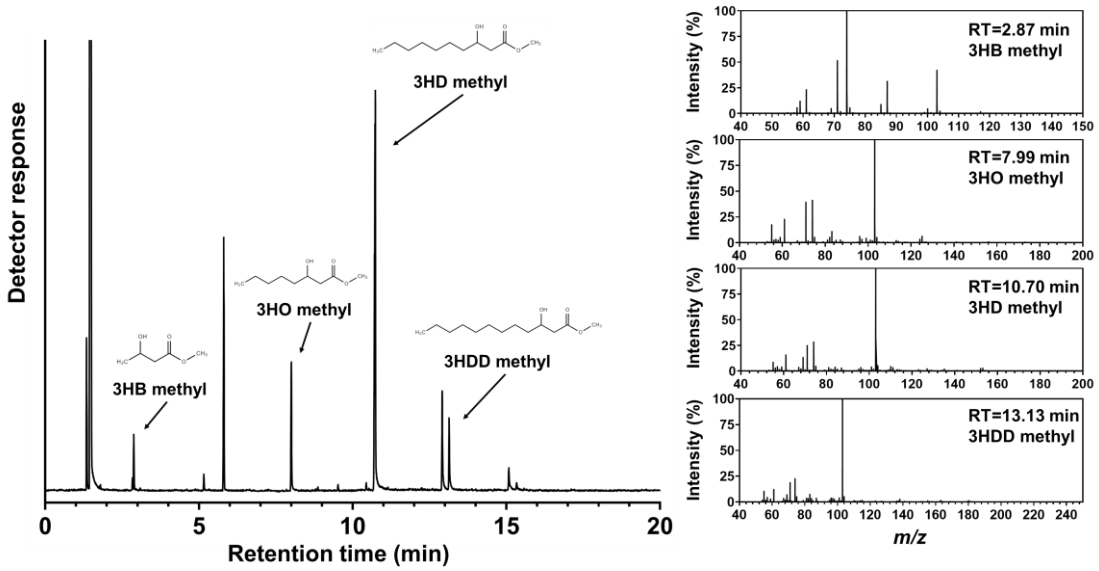

Figure 5.13. GC-MS analysis of PHA blend produced by *P. putida* transformed with PrhaB-CAB (basal, 24-h cultivation). (A) Gas chromatogram of PHA after methanolysis. (B) Mass spectrum of major components detected by GC. GC. Compound identities were confirmed based on fragmentation patterns and comparison with database reference spectra. For detailed MS spectral comparisons of each PHA monomer methyl ester, see Appendix **Figure S4**.

5.2.10 Identification of PHA blend

Following the introduction of PhaCAB enzymes, the engineered *P. putida* possesses two distinct PHA production pathways. The PHA synthases in each pathway polymerize monomers of specific chain lengths, with the PhaC from the PhaCAB (type

I) typically synthesizing scl-PHA, while the native PhaC in *P. putida* (type II) only synthesizes mcl-PHA (Mezzolla et al., 2018). As a result, the PHAs produced by the two pathways are independent and do not interconnect, meaning the engineered *P. putida* produces a blend of mcl-PHA and PHB.

The above conclusion is supported by subsequent characterization results. For instance, PHAs produced from ParaB (basal) and PrhaB (basal) displayed two species with distinctly different molecular weights in Gel permeation chromatography (GPC) analysis (**Figure 5.14a**). To further identify these species, diffusion-ordered spectroscopy (DOSY) was employed. DOSY distinguishes NMR signals by differences in the translational diffusion rates of molecules. Two diffusion coefficients, 1.2×10^{-11} m^2/s and 3.7×10^{-11} m^2/s, were detected, corresponding to the larger, less mobile PHB molecules and the smaller, more mobile mcl-PHA molecules, respectively (**Figure 5.14b**). These results demonstrate that the introduction of PhaCAB enables *P. putida* to produce a PHA blend consisting of PHB and mcl-PHA.

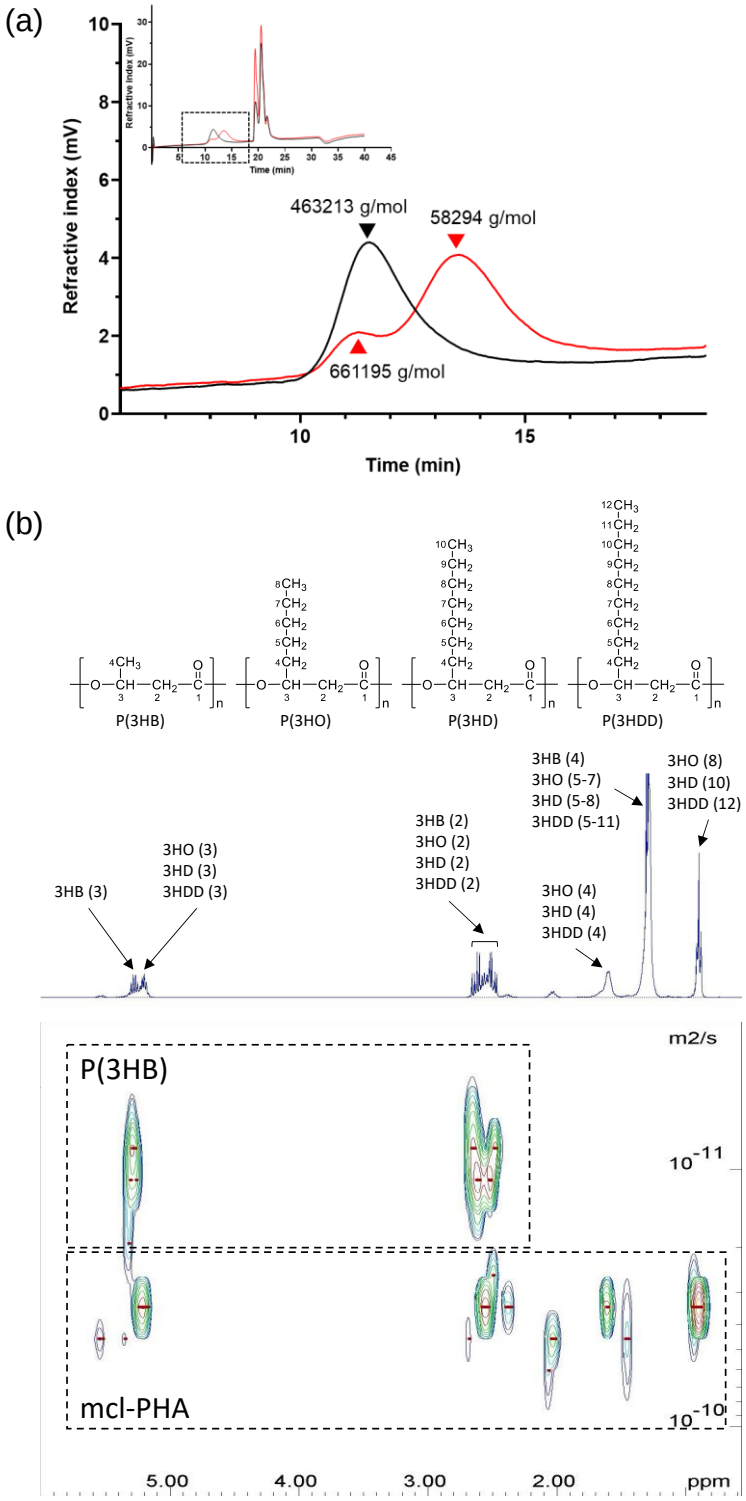

Figure 5.14 Characteristics of PHA produced with *phaCAB* operon controlled by PrhaB (basal) promoter. (a) Gel permeation chromatography of PHA produced under basal (red line) and induced (black line) conditions. The inset shows the complete chromatogram with the magnified region marked in a dotted rectangle. The molecular weights of peaks are indicated in the diagram. (b) DOSY 13C NMR analysis of PHA blends. The diffusion coefficient of P(3HB) and mcl-PHA are distinct.

5.2.11 The P(3HB) and mcl-PHA components had different molecular weights

Gel permeation chromatography analysis showed that the average molecular weight of the PHA produced by *P. putida* was 71.5 ± 4.2 kg/mol (**Table 5.2**). When the *phaCAB* operon was introduced and controlled by PphaC1, ParaB (induced), and PrhaB (induced), the molecular weight of the primary component, P(3HB), ranged from 298.3 ± 44.9 kg/mol to 502.2 ± 50.6 kg/mol, which is 4 to 7 times higher than that of mcl-PHA. Studies have shown that the molecular weight of PHA is related to the amount of PhaC enzyme present in the producing host (Sim et al., 1997). The plasmid used to engineer *P. putida* carried the pBBR1 replicon, which has been reported to have a copy number between 5 and 31 (Buch et al., 2010, Jahn et al., 2016). A higher copy number resulted in elevated levels of PhaC from *C. necator* involved in PHA synthesis, compared to the single-copy PhaC1 and PhaC2 responsible for mcl-PHA synthesis. This also led to a higher molecular weight of PHB in the final PHA blend.

By using the ParaB (basal) and PrhaB (basal) promoters to produce P(3HB) in *P. putida*, the molecular weight of mcl-PHA was reduced from 71.5 ± 4.2 kg/mol to 49.7 ± 4.8 kg/mol and 62.3 ± 4.4 kg/mol, respectively. Along with the reduced mcl-PHA titer (**Figure 5.9a**), these findings further emphasize the complex interplay between nutrient limitation, cellular regulation, the amount and quality of PHA products.

Table 5.2. Molecular weight of PHAs produced by engineered *P. putida* estimated using GPC.

Promoter	PHA	Mn (g/mol)	Mw (g/mol)	PDI
Wild type	mcl-PHA	15005 ± 2828	71486 ± 4196	5.3 ± 0.9
PphaC1	P(3HB)	76212 ± 15984	502207 ± 50598	7.1 ± 0.8
ParaB (induced)	P(3HB)	48217 ± 14669	298312 ± 44875	7.5 ± 1.9
PrhaB (induced)	P(3HB)	80794 ± 24785	374951 ± 41310	5.9 ± 1.3
ParaB (basal)	P(3HB)	220577 ± 99573	466496 ± 71056	6.4 ± 3.4
ParaB (basal)	mcl-PHA	19954 ± 1819	49689 ± 4795	2.0 ± 0.5
PrhaB (basal)	P(3HB)	491112 ± 6856	644222 ± 9522	1.3 ± 0.0

Promoter	PHA	Mn (g/mol)	Mw (g/mol)	PDI
PrhaB (basal)	mcl-PHA	17120 ± 3318	62264 ± 4365	4.7 ± 1.9

5.2.12 Thermal properties of the PHA blends

To better understand the thermal behavior and material characteristics of the synthesized PHA blends, thermogravimetric analysis and differential scanning calorimetry were conducted. These analyses provide insights into thermal stability, crystallization behavior, and melting properties, which are essential for evaluating the processability, storage conditions, and potential applications of the produced PHAs in industrial and biomedical settings.

TGA analysis revealed a single thermal degradation event for all samples, with degradation temperatures (T_d) ranging from 287.0 to 298.3°C (**Table 5.3, Figure 5.15**) with no significant differences in T_d among the PHA samples. The results further demonstrated that all PHA blends remained thermally stable below 263°C (**Table 5.3**). Moreover, the degradation curves of all PHA samples were very smooth, indicating that the extracted PHA had high purity.

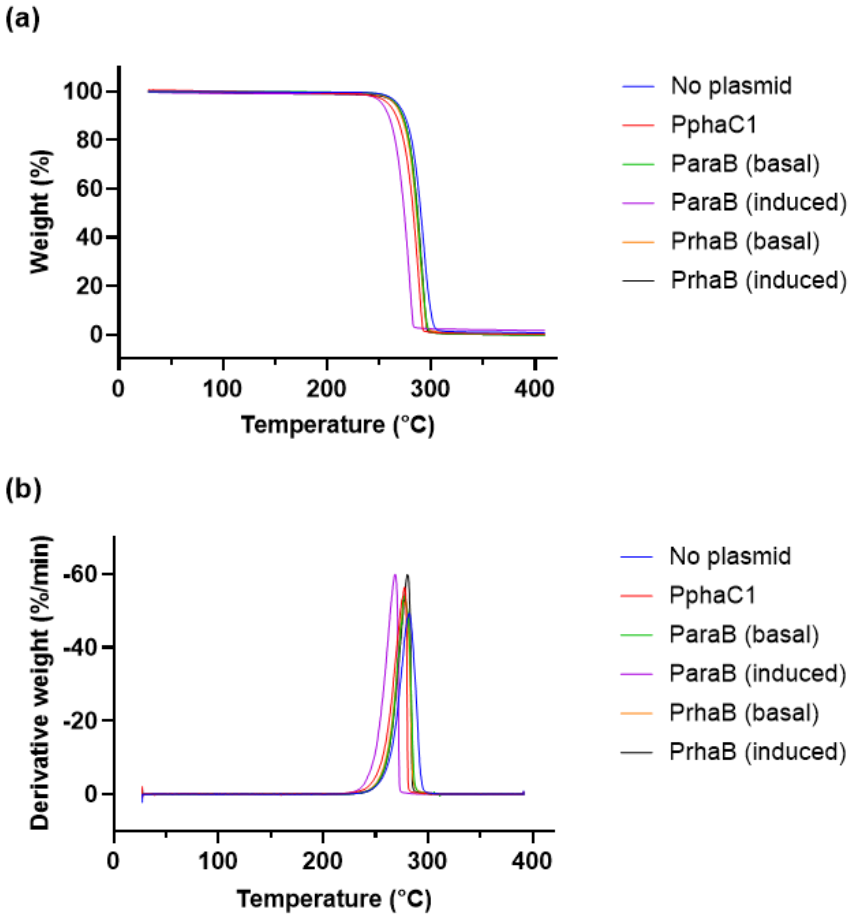

Figure 5.15. Thermogravimetric analysis of mcl-PHA from *P. putida* and PHA blends of engineered strains. Cells were cultivated in MSM with 1% glucose. (a) Weight loss and (b) derivative weight loss when heated at a rate of 10°C/min.

Crystallization peaks were detected between 98°C and 118°C during cooling from the initial melt for all samples, except for the mcl-PHA produced by *P. putida* (**Figure 5.16b**). Mcl-PHA is generally amorphous and does not form a crystalline phase during cooling (Kim et al., 2007, Nigmatullin et al., 2023), accounting for the absence of a distinct crystallization peak. However, a minor peak at 43.7°C was observed during the second heating of mcl-PHA from native *P. putida* (**Figure 5.16c**). For the remaining samples, melting temperatures (Tm) ranged from 163°C to 175°C (**Table 5.3**), with split melting peaks present in the ParaB (induced) and PrhaB (induced) samples. These split peaks were not observed during the first heating (**Figure 5.16a**), likely due to the reorganization of polyester crystals during the melting and cooling cycles, resulting in

double melting peaks. Furthermore, the PHA blend produced from PrhaB (basal) exhibited significantly lower ΔHc and ΔHm values compared to other samples, attributed to the lower proportion of crystalline P(3HB) in the blend.

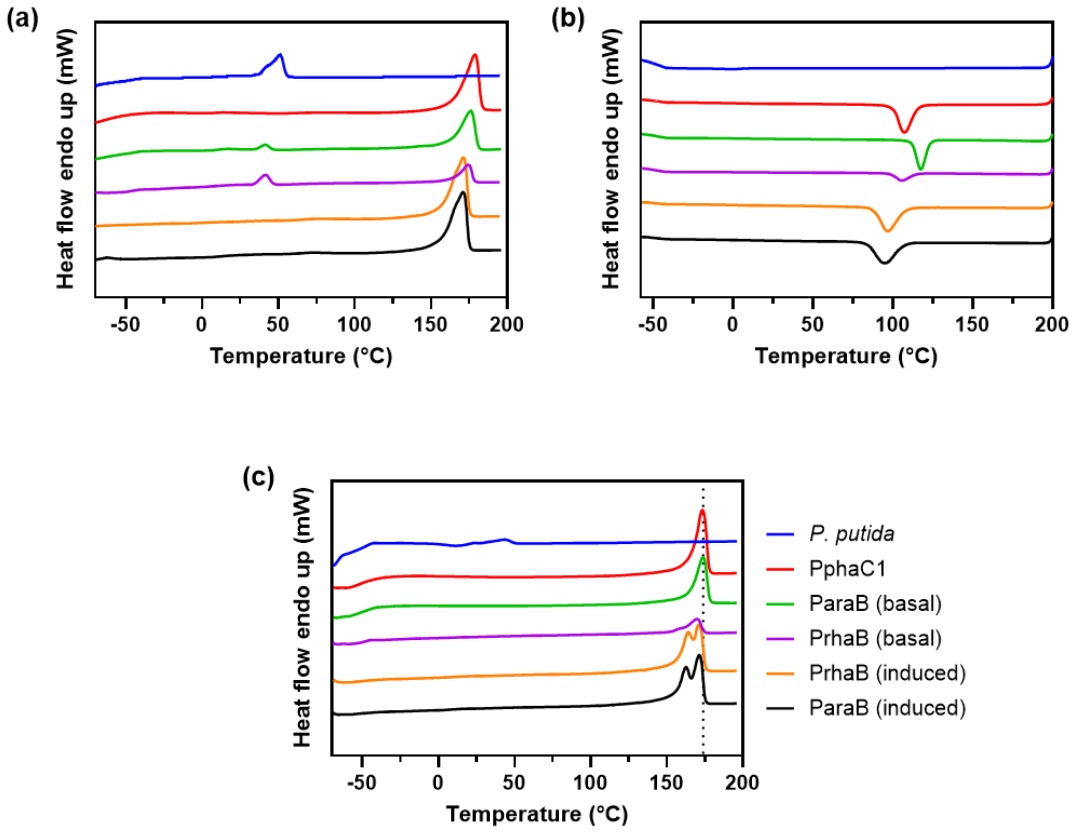

Figure 5.16. DSC thermograms recorded during (a) first heating, (b) cooling and (c) second heating of purified mcl-PHA and PHA blends produced respectively by native and engineered *P. putida*.

Table 5.3. Thermal properties of PHA produced by native *P. putida* and strains harbouring plasmids with the *phaCAB* operon controlled by different promoters. All PHA samples were Soxhlet extracted and purified.

	TGA		DSC			
Promoter	**T_{onset} (°C)**	**T_d (°C)**	**T_c (°C)**	**ΔH_c (J/g)**	**T_m (°C)**	**ΔH_m (J/g)**
No plasmid	281.9 ± 2.3	297.4 ± 3.3	n.d.	n.d.	43.7 ± 0.1	2.6 ± 1.0
ParaB (basal)	276.1 ± 4.7	287.4 ± 2.1	117.6 ± 0.1	-55.0 ± 1.1	174.7 ± 0.8	60.4 ± 0.3
PrhaB (basal)	275.4 ± 12.5	290.4 ± 11.1	107.3 ± 1.6	-20.9 ± 1.7	171.4 ± 1.6	22.7 ± 2.5
ParaB (induced)	274.4 ± 1.5	289.8 ± 0.1	97.8 ± 3.1	-78.6 ± 0.7	163.1 ± 0.3 171.4 ±0.1	79.9 ± 3.2
PrhaB (induced)	273.6 ± 3.0	287.0 ± 5.3	98.3 ± 1.5	-69.9 ± 6.1	164.1 ± 0.2 171.2 ± 0.0	70.1 ± 7.5
PphaC1	280.3 ± 10.9	298.4 ± 8.9	107.6 ± 0.3	-82.4 ± 1.9	173.6 ± 0.1	83.1 ± 1.8

n.d. = not detected.

5.3 Summary

Chapter 5 shifted the engineering strategy by introducing the *phaCAB* operon from *C. necator* into *P. putida*, a native mcl-PHA producer. This "reverse integration" aimed to enable the production of PHA blends containing both scl and mcl monomers within a genetically and metabolically competent host.

To finely control the expression of *phaCAB*, a suite of constitutive and inducible promoters was evaluated for strength in *P. putida* using fluorescent protein reporters. Among the tested promoters, Pg25 demonstrated the strongest constitutive activity, while ParaB and PrhaB offered high inducibility and tight regulation. These promoters were subsequently employed to drive *phaCAB* expression in engineered strains. Expression constructs were validated by restriction analysis and successfully transformed into *P. putida*, confirming plasmid functionality and stable maintenance.

Expression of *phaCAB* in *P. putida* led to a substantial shift in PHA monomer composition. Wild-type *P. putida* predominantly synthesized mcl-PHA, primarily composed of 3-hydroxydecanoate. In contrast, transformants harboring *phaCAB* under various promoters exhibited a broad range of 3-hydroxybutyrate (3HB) content, from as low as 17.9 mol% to as high as 99.6 mol%, depending on promoter strength and induction. These results clearly demonstrate that promoter selection can effectively tune PHA composition, with ParaB and PrhaB enabling dynamic regulation of PHB content. Despite similar basal promoter activities, PHB production under ParaB exceeded that under PrhaB, suggesting that subtle differences in expression may be amplified through enzymatic turnover and precursor flux.

In terms of titer, engineered *P. putida* strains achieved PHA titers of up to 1.48 g/L, with some exceeding the native titer by over 7-fold. Notably, the highest PHA titer corresponded to strains expressing *phaCAB* under strong or induced promoters, while high glucose supplementation (6% w/v) further boosted intracellular PHA content to

over 42 wt% of cell dry weight. Although these titers were slightly lower than those achieved in *C. necator*, the engineered *P. putida* strains offered greater compositional flexibility, producing 3HB-rich copolymers and PHA blends rather than homopolymers.

Comprehensive physicochemical analysis of the extracted PHAs—via GC, GC-MS, GPC, TGA, and NMR—confirmed the formation of distinct PHA blends comprising both scl- and mcl-monomers. Gel permeation chromatography and DOSY NMR identified two separate molecular weight species, attributable to P(3HB) and mcl-PHA, respectively. Moreover, the P(3HB) fractions displayed higher molecular weights than mcl-PHA, consistent with their multi-copy plasmid-based expression and elevated PhaC levels. Thermal analysis revealed that all PHA samples were stable below 263°C, and differences in crystallinity were linked to monomer composition, with PHB-rich samples displaying higher melting points and crystallinity indices.

Collectively, these findings demonstrate the feasibility of engineering *P. putida* as a flexible platform for producing tunable PHA blends. The ability to precisely regulate monomer composition via promoter control opens new avenues for tailoring polymer properties to specific applications, such as packaging or biomedical materials. This work highlights the importance of integrating gene expression regulation with metabolic context to achieve advanced biopolymer design.

Chapter 6: PHA production from sustainable feedstock

This chapter investigates the feasibility of using low-cost, renewable feedstocks for PHA production. Given that substrate cost is a major factor affecting the economic viability of PHA synthesis, agro-industrial by-products such as sugarcane molasses and potato peel hydrolysate were selected for evaluation. These feedstocks are abundant, inexpensive, and rich in carbon sources. The chapter presents experimental results assessing microbial growth, PHA accumulation, and the challenges associated with process scalability. The findings aim to validate the potential of integrating engineered biosynthetic systems with sustainable, real-world substrates.

6.1 Feedstock selection and justification

Among various agro-industrial residues, sugarcane molasses and potato peel hydrolysate (PPH) are abundant byproducts with promising sugar content and fermentability, making them attractive candidates for microbial cultivation.

Sugarcane molasses is a viscous byproduct of sugar refining that typically contains approximately 50% (w/w) of total sugars, primarily composed of sucrose, glucose, and fructose (Vidra et al., 2017, Zhao et al., 2025). Its low cost, availability, and minimal pretreatment requirements make it particularly suitable for industrial-scale fermentation. Numerous studies have demonstrated its effectiveness in supporting PHA production in model microorganisms such as *C. necator* and *P. putida* (Kiselev et al., 2022, Hendrawan et al., 2020). The use of molasses as a substrate for PHA production not only offers a pathway to reduce production costs but also aligns with sustainable bioprocessing by repurposing agro-industrial waste.

By contrast, potato peel is a major solid waste from the food processing industry. The hydrolysis of potato peels can release a large amount of reducing sugars, reaching up

to 72.23% (w/w), predominantly glucose released from starch via enzymatic or acidic hydrolysis (Chohan et al., 2020, Kag et al., 2024). While it requires more extensive processing than molasses, PPH remains a viable substrate due to its global availability, high starch content, and compatibility with microbial metabolism.

In this chapter, the potential of both feedstocks was investigated using distinct microbial systems. Sugarcane molasses was used to evaluate the PHA-producing capabilities of five wild type *Burkholderia* strains, which have received limited attention in the literature but possess significant metabolic flexibility. Potato peel hydrolysate was used to cultivate wild type *C. necator* and engineered *P. putida* harboring a synthetic *phaCAB* operon under the control of the rhaB promoter (see Chapter 5).

6.2 PHA production using sugarcane molasses

This section addresses the research gap by investigating the capacity of five *Burkholderia* strains (**Table 6.1**) to produce PHA when cultivated in molasses-based media. These strains, which have not been previously utilized for PHA production from molasses, are evaluated for their growth, PHA accumulation, and overall production efficiency. The results of this study aim to contribute to the broader understanding of the feasibility of using *Burkholderia* species for sustainable and cost-effective PHA production, thereby expanding the range of viable microbial hosts for industrial PHA biosynthesis.

Table 6.1. List of *Burkholderia* strains used in this study.

No.	TBRC/BCC Code	Name of strain
1	TBRC 1718	*Burkholderia tropica*
2	TBRC 4635	*Burkholderia bannensis*
3	TBRC 4970	*Burkholderia acidipaludis*
4	BCC 81317	*Burkholderia contaminans*
5	BCC 59163	*Burkholderia soli*

6.2.1 Results and discussion

Cultivating the *Burkholderia* strains in a rich medium LB with added 2%(w/v) glucose allows to evaluate their basic growth characteristics. To prevent the produced PHA from potentially being metabolized and consumed by the cells, all five strains were cultivated until the early stationary phase, at which point cultivation was stopped, and the freeze-dried cells were used to assess PHA accumulation. The growth curves (**Figure 6.1**) showed that strain TBRC 1718 achieved the highest cell density in LB medium supplemented with glucose, followed closely by TBRC 4635. Among the five strains, BCC 81317 exhibited the fastest growth rate, reaching the stationary phase within 10 hours. Although BCC 59163 eventually reached a similar cell density to BCC 81317, it displayed the slowest growth, indicating that LB medium may not be the most suitable for its growth. Unexpectedly, TBRC 4970 showed no growth even after nearly 40 hours of cultivation, indicating its poor growth capability.

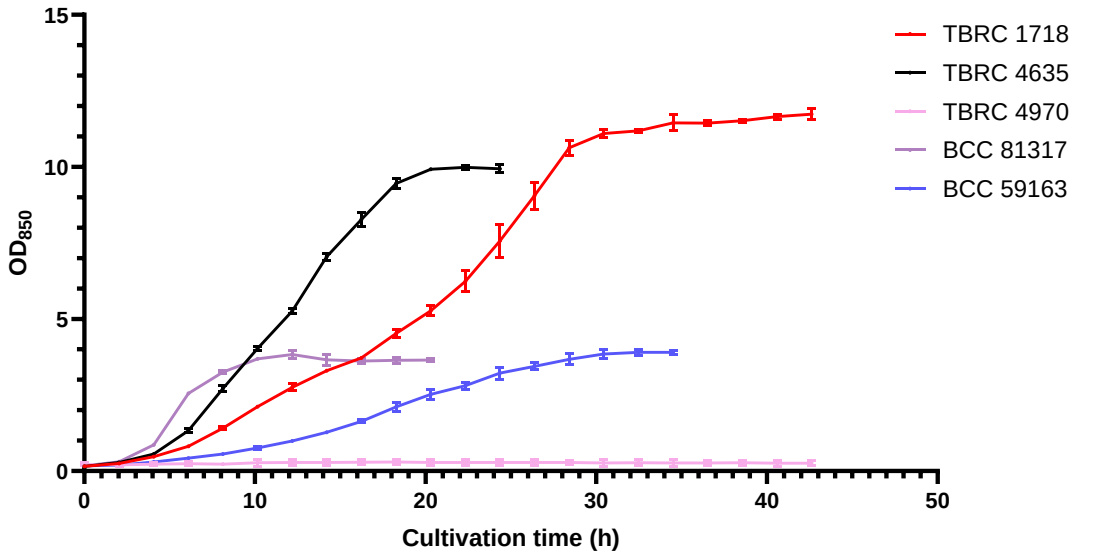

Figure 6.1. Growth curves of five *Burkholderia* strains cultivated in LB medium with 2% (w/v) glucose. Each strain was grown in 10 mL cultures using a tube-based bioreactor system. Optical density at 850 nm (OD_{850}) was automatically recorded every 15 minutes through the tube wall. To improve clarity, only one data point every two hours is shown in the plotted growth curves.

The GC-based PHA analysis revealed that TBRC 1718 had the highest intracellular

PHA content after cultivation, reaching 27.6% of CDW, with the highest PHA titer of 1.65 g/L (**Table 6.2**). This was followed by TBRC 4635, which produced 1.29 g/L of PHA. In contrast, BCC 81317 had the lowest PHA content and titer. Notably, although BCC 59163 did not exhibit high PHA titer, the PHA produced under these cultivation conditions contained not only the monomer 3HB but also a small amount (2.81 mol%) of the monomer 3HV. The PHA produced by the other three strains was exclusively the homopolymer PHB.

Table 6.2. PHA production by *Burkholderia* strains cultivated in 10 mL of LB medium with 2%(w/v) glucose.

Strain	**CDW (g/L)**	**PHA content (wt% of CDW)**	**PHA titer (g/L)**	**PHA Composition (mol%)**	
				C4	**C5**
TBRC 1718	5.98	27.6	1.65	100	0
TBRC 4635	5.78	22.4	1.29	100	0
BCC 81317	1.91	9.2	0.18	100	0
BCC 59163	1.75	16.4	0.29	97.19	2.81

When the different *Burkholderia* strains were cultivated in MSM medium containing 2% molasses, their growth patterns varied significantly (**Figure 6.2**). TBRC 1718 and TBRC 4635 did not reach the high cell densities observed in LB medium, and their final cell densities were similar to that of BCC 81317 (OD_{850}~2), differing only in growth rates. Notably, BCC 59163 adapted much better to these cultivation conditions, achieving a final cell density 5 times higher than the other three strains. Consistently, TBRC 4970 did not show any growth (flat line, not shown), further confirming its weak growth.

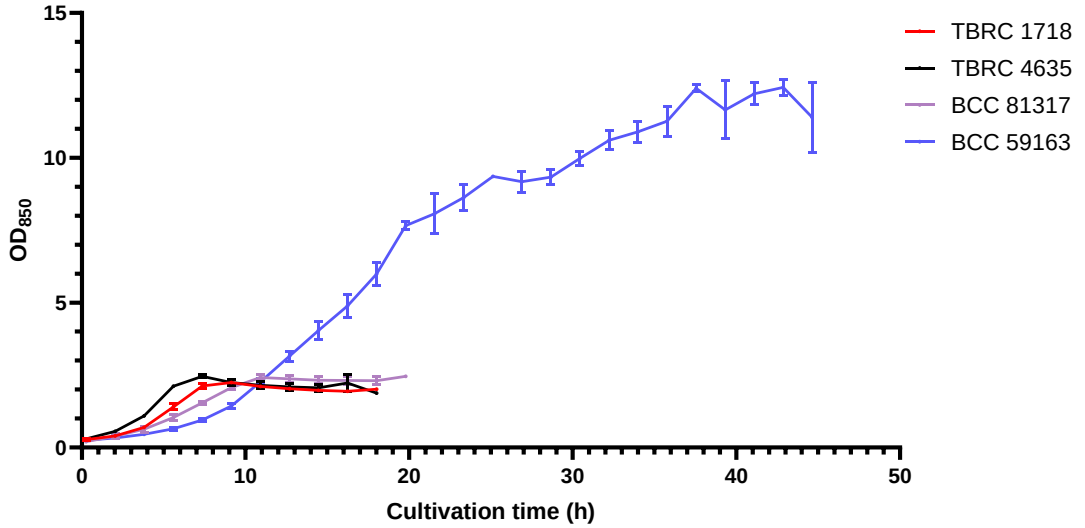

Figure 6.2. Growth curves of four *Burkholderia* strains cultivated in 10 mL MSM medium supplemented with 2% (w/v) molasses. Strains were cultured in bioreactor tubes, and OD_{850} values were recorded at 15-minute intervals. To improve clarity, only one data point every two hours is shown in the plotted growth curves. The BCC 59163 growth curve shows substantial fluctuation in the late phase, which may be attributed to long-term operation of the bioreactor. Similar signal drift has been observed in previous experiments after extended runtime (>7 days), potentially affecting OD_{850} accuracy.

The use of molasses as the sole carbon source also altered PHA production in the *Burkholderia* strains (**Table 6.3**). The PHA content in TBRC 1718 decreased by 155-fold compared to its cultivation in LB, dropping to just 1.78%, while no PHA was detected in the freeze-dried cells of TBRC 4635. Combined with the growth curve data, this indicates that molasses is not suitable for either strain in terms of growth or PHA production. In contrast, the PHA titers of BCC 81317 and BCC 59163 increased, with BCC 59163 achieving an intracellular PHA content of 57.01% of cell dry weight and a PHA titer of 2.3 g/L. This result exceeds that of many studies using other sustainable feedstocks to cultivate *Burkholderia*, indicating that BCC 59163 is a highly promising and efficient PHA producer, and that molasses shows significant potential as a feedstock for PHA production. Furthermore, only the 3HB monomer was detected in all samples, once again confirming the influence of the carbon source on PHA composition.

Table 6.3. PHA (PHB) production by *Burkholderia* strains cultivated in MSM + 2%(w/v) molasses.

Strain	CDW (g/L)	PHA content (wt% of CDW)	PHA titer (g/L)
TBRC 1718	1.24 ± 0.03	1.78 ± 0.43	0.02 ± 0.01
TBRC 4635	1.47 ± 0.18	n.d.	n.d.
BCC 81317	1.54 ± 0.01	13.31 ± 2.03	0.20 ± 0.04
BCC 59163	4.02 ± 0.51	57.01 ± 2.74	2.30 ± 0.40

When attempting to scale up the experiment, a key challenge is the issue of precipitation in the culture medium. The addition of molasses to MSM results in significant precipitation (**Figure 6.3a**). The experimental results presented in the previous section were obtained from small-scale (10 mL) *Burkholderia* cultures conducted in bioreactors, where the culture medium was filtered using syringe filters. However, the presence of precipitates causes frequent clogging of the filters, rendering the filtration of large volumes impractical. Autoclave sterilization of the medium further exacerbates the precipitation, leading to an increased loss of nutrients in the medium. When BCC 59163 was cultured in 500 mL of autoclave-sterilized medium in shake flasks, the cell dry weight decreased to 1.6 g/L, and the intracellular PHA content was significantly reduced to 20%, likely due to the depletion of essential nutrients in the medium.

Additionally, the precipitates formed during autoclave mixed with the cell pellets after centrifugation (**Figure 6.3b**) and cannot be washed away. While this did not interfere with PHA extraction, the presence of precipitates could potentially complicate the accurate quantification of PHA content in the freeze-dried cells. These challenges highlight the need for further research to develop effective solutions, thereby making low-cost large-scale production feasible.

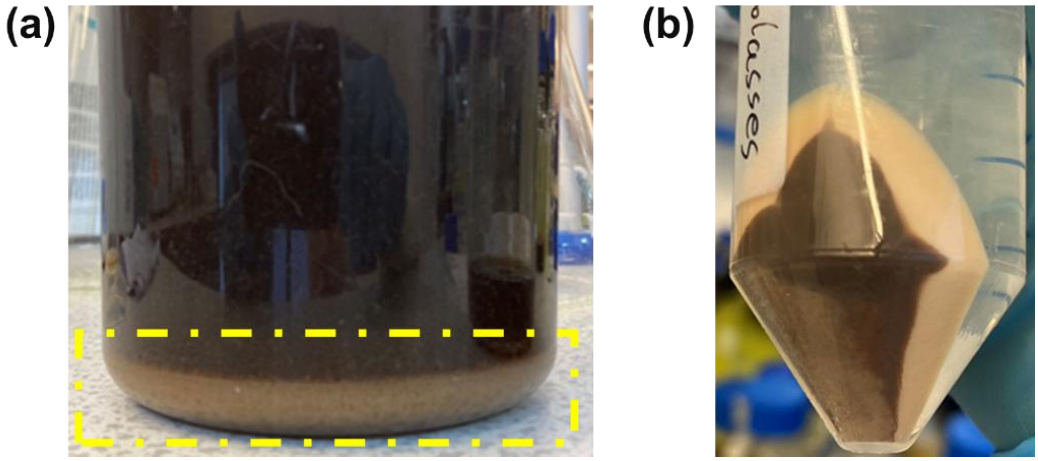

Figure 6.3. Formation of precipitate in MSM medium containing molasses. (a) Yellow box highlights precipitate formed when 2% (w/v) molasses was added to MSM medium prior to sterilization. (b) After cultivation and centrifugation, cell pellets were mixed with dark brown precipitate.

6.3 PHA production using potato peel hydrolysate

This section shifts focus to potato peel hydrolysate (PPH), another low-cost and renewable feedstock with significant potential for microbial PHA production. The feasibility of using PPH as a feedstock for PHA production in *C. necator* and engineered *P. putida* (**Chapter 5**) was investigated. The study evaluates the growth and PHA accumulation of both strains in PPH-based media, aiming to further advance the understanding of PPH as a sustainable feedstock. The findings presented here provide new insights into optimizing PHA production for industrial applications while contributing to the broader goal of using renewable resources in biotechnology.

6.3.1 Results and discussion

C. necator and engineered *P. putida* both demonstrated the ability to grow in a medium derived from potato peel hydrolysate (PPH). Even in the absence of additional nutrients and when diluted with water at a 1:1 ratio, both strains were capable of growth, achieving relatively high cell mass. When the hydrolysate medium was mixed with MSM medium at a 1:1 ratio, the biomass of both strains increased, with the engineered *P. putida* achieving a cell dry weight of 4.45 g/L (**Figure 6.4, table S7**), which is 2.1

times the cell dry weight obtained when cultured in MSM medium with 6% glucose (Section 5.3.6). This enhancement is likely attributable to the MSM medium, which provides most essential elements for microbial growth, except for carbon, thus supplementing the nutrient profile of PPH.

However, the carbon sources present in PPH are not optimal for promoting PHA production in either strain, as indicated by the relatively low PHA content. For instance, *C. necator* cultivated in PPH diluted with water exhibited a PHA content of only 18.45% of cell dry weight, while cells grown in 1% glucose with MSM accumulated PHA at 68% of cell dry weight. Furthermore, the combination of PPH and MSM resulted in a significant reduction in PHA content in both strains. MSM supplies not only additional nutrients but also small amounts of nitrogen (0.5 g/L NH_4Cl), which reduces the C/N ratio in the medium, thereby creating conditions that are less favorable for microbial PHA accumulation.

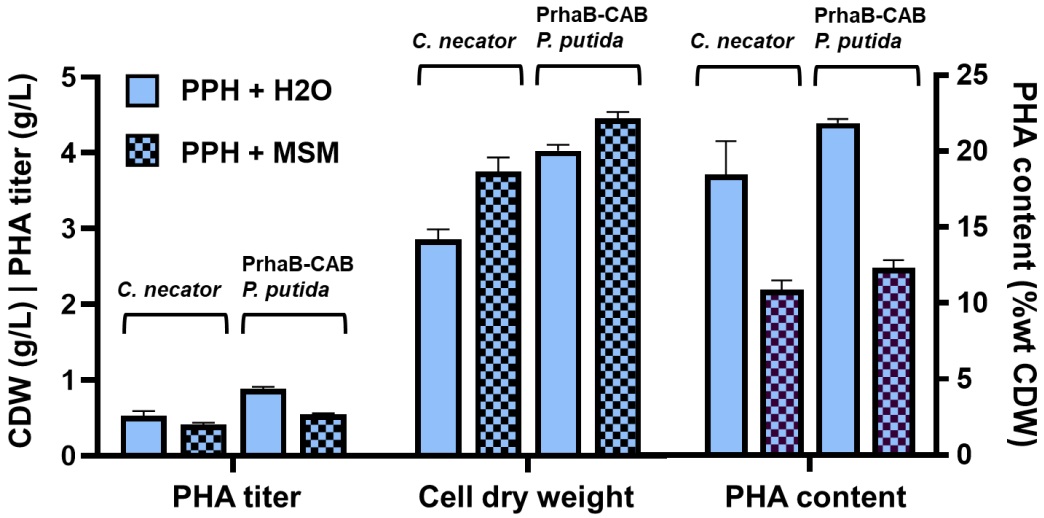

Figure 6.4. PHA produced by *C. necator* and *P. putida* engineered with PrhaB-*phaCAB* plasmid. Strains were cultivated for 72 hours in either PPH + H_2O or PPH + MSM medium (both volume ratio 1:1).

As expected, the composition of the PHA produced by *C. necator* was a homopolymer consisting solely of the 3HB monomer. In contrast, *P. putida* expressing the *phaCAB* operon produced PHA that not only contained 3HB but also monomers of mcl-PHA

with carbon chains ranging from 8 to 12 atoms, which were previously identified as a PHA blend in chapter 5. Nevertheless, even with the basal activity of PrhaB promoter, the 3HB monomer still accounted for 85.8 mol% to 95.68 mol% (**table S7**), further demonstrating the efficiency of the PHB production pathway. This outcome not only confirms the feasibility of using PPH as a sustainable feedstock but also demonstrates the potential to produce different types of PHA depending on the selected microorganism.

6.4 Summary

This chapter evaluated the potential of two agro-industrial residues as sustainable feedstocks for microbial PHA production. The performance of multiple microbial strains was assessed in terms of growth, polymer titer, and monomer composition when cultivated in media derived from these low-cost substrates.

In the case of molasses, five *Burkholderia* strains were screened for their capacity to utilize this carbon source. While TBRC 1718 and TBRC 4635 displayed high PHA production in glucose-based media, their performance declined significantly in molasses-only conditions. By contrast, *Burkholderia* BCC 59163 demonstrated exceptional adaptation, achieving both high cell density and a PHA content of 57.01% of cell dry weight, surpassing production reported in many previous studies using alternative waste-derived substrates. These results highlight strain-specific variability in substrate utilization and identify BCC 59163 as a promising candidate for further development. However, technical barriers such as precipitation during autoclaving, leading to nutrient loss and inaccurate quantification, pose challenges for process scalability. These findings emphasize the need for optimization of both molasses composition and sterilization protocols in future studies.

The investigation of PPH as a carbon source was conducted using *C. necator* and a genetically engineered strain of *P. putida* expressing the *phaCAB* operon. Both strains

were capable of growth and PHA accumulation in PPH-based media, particularly when supplemented with minimal salts. Despite substantial biomass generation, PPH alone did not support high PHA titers compared to glucose, indicating that its carbon profile may be suboptimal for polymer biosynthesis. Interestingly, the engineered *P. putida* synthesized a diverse blend of scl and mcl monomers, while *C. necator* produced a homopolymer of 3HB, demonstrating that the feedstock can influence not only polymer titer but also composition, depending on the microbial host and genetic configuration.

Together, the results confirm the feasibility of using molasses and PPH as sustainable substrates for microbial PHA production, while also revealing key limitations in titer, process consistency, and substrate quality. The work underscores the importance of matching substrate composition with host metabolic capacity and highlights the potential for strain engineering and medium optimization to improve performance. These findings contribute to the growing body of research focused on converting food and agricultural waste into high-value biopolymers, thereby supporting the development of economically and environmentally sustainable bioprocesses.

.

Chapter 7: Conclusion

This final chapter summarizes the key findings and contributions of the research, which aimed to enhance microbial production of PHA through genetic engineering and the use of sustainable substrates. The chapter reflects on how the experimental work addressed the objectives outlined in Chapter 1, particularly in terms of strain development, pathway integration, monomer composition control, and substrate adaptability. In addition, it evaluates the broader implications of the results for industrial biotechnology and sustainable materials research. The chapter concludes with a discussion of future research directions that could further improve the efficiency, scalability, and commercial relevance of PHA biosynthesis.

7.1 Summary of key findings

This thesis presents a comprehensive investigation into the metabolic and process engineering of microbial hosts for the tailored production of PHA. The central aim was to enable the biosynthesis of diverse PHA polymers, particularly blends of scl and mcl monomers using both model and non-model organisms, and to evaluate the viability of sustainable carbon sources for industrial-scale PHA production. Across multiple chapters, the research progressively built and evaluated synthetic biology strategies for improving PHA titer, tunability, and feedstock flexibility.

In Chapter 4, attempts were made to enable mcl-PHA production in native scl-PHA producers, specifically *Rhodococcus* species and *C. necator*. Two biosynthetic pathways were introduced, relying respectively on fatty acid de novo synthesis and β-oxidation, using plasmids pDD56-CAG and pDD56-CJ. While the pathways were successfully expressed in *E. coli* due to detectable levels of mcl-PHA, no polymer production was observed in *Rhodococcus* or *C. necator*. These findings suggest that despite successful transformation and partial expression of the pathway enzymes, the host metabolic context in these organisms is not conducive to mcl-PHA biosynthesis,

likely due to preferential flux toward native storage molecules such as triacylglycerols and PHB. These results highlight the challenges of transferring complex synthetic pathways into metabolically rigid hosts and underscore the importance of native carbon flux balance and competing pathway repression.

Chapter 5 adopted a reverse approach, in which the *phaCAB* operon from *C. necator* was introduced into *P. putida*. A diverse set of constitutive and inducible promoters was characterized in *P. putida*, enabling fine-tuned expression of *phaCAB* and allowing dynamic modulation of polymer composition. This strategy resulted in copolymers containing 3HB in proportions ranging from 17.9% to 99.6%, depending on the promoter used. The highest titer reached 1.48 g/L, with polymer content exceeding 42% of cell dry weight under glucose-rich conditions. Physicochemical analyses, including GC-MS, GPC, and NMR, confirmed the formation of distinct scl- and mcl-PHA blends, each exhibiting unique molecular weight distributions and thermal properties. This study demonstrated the feasibility of regulating PHA composition through promoter engineering, offering a platform for designing polymers with specific material properties.

Chapter 6 investigated the potential of using cost-effective, renewable feedstocks for microbial PHA production. Sugarcane molasses and potato peel hydrolysate were evaluated as alternative carbon sources. Among the tested strains, *Burkholderia* BCC 59163 showed exceptional adaptation to molasses and achieved PHA accumulation exceeding 57% of cell dry weight. However, issues with medium precipitation and sterilization artifacts reduced reproducibility and scalability. potato peel hydrolysate supported biomass generation in both *C. necator* and engineered *P. putida*, although PHA titers were lower than those obtained from glucose. Notably, *P. putida* produced copolymers from potato peel hydrolysate, while *C. necator* generated a homopolymer. These results emphasize the potential of renewable waste streams for sustainable biopolymer production while also highlighting the need for feedstock-specific medium optimization and pretreatment.

Overall, the thesis demonstrates the value of integrating pathway engineering, regulatory control, and feedstock innovation in developing microbial platforms for advanced bioplastic synthesis. It provides both proof-of-concept systems and insight into the practical challenges of scaling microbial PHA production.

7.2 Contributions to the field

The work presented in this thesis makes several substantial contributions to the intersecting fields of synthetic biology, metabolic engineering, and bioprocessing, advancing both the fundamental understanding and practical capabilities of microbial PHA production. Central to this contribution is the deliberate expansion of PHA biosynthesis beyond conventional systems, incorporating novel host organisms, synthetic pathway design, regulatory control, and sustainable carbon sources.

A key theoretical contribution lies in the exploration of mcl-PHA pathway functionality within non-model organisms such as *Rhodococcus* and *C. necator*. This represents one of the few attempts to implement complex synthetic PHA biosynthesis modules in hosts with intrinsically different metabolic architectures. The limited success in these systems not only illustrates the technical challenges of cross-species pathway transfer but also generates valuable insights into host-pathway incompatibility, such as carbon flux competition, regulatory mismatch, and metabolic burden. These findings offer a reference point for future research aiming to unlock the biosynthetic potential of genetically recalcitrant but industrially promising microorganisms.

The study further contributes methodologically by demonstrating a robust and modular framework for controlling polymer composition via promoter strength. Using both constitutive and inducible promoter systems in *P. putida*, this work establishes a clear correlation between gene expression levels and PHA monomer composition. This enables rational design of copolymers with tunable mechanical and thermal properties, offering a new level of precision in biopolymer customization. The successful

deployment of *P. putida* as a chassis for dual-pathway PHA synthesis also highlights its potential as a flexible and high-performance production platform, capable of producing diverse PHA blends that were previously limited to single-monomer outputs in most natural producers.

In addition to genetic and metabolic innovations, the thesis addresses a critical bottleneck in the field economic and environmental sustainability. By evaluating agricultural waste-derived substrates such as sugarcane molasses and potato peel hydrolysate, this research directly engages with global efforts to reduce dependency on refined carbon sources in industrial bioprocesses. Comparative analyses across microbial strains, substrates, and conditions offer a comprehensive dataset that can inform future feedstock selection and process development. The demonstration that certain engineered strains can maintain PHA production efficiency on low-cost feedstocks contributes to the economic feasibility of bioplastic manufacturing and supports a circular bioeconomy model.

Importantly, the outcomes of this research bridge the gap between basic science and translational impact. The integration of pathway engineering, promoter modulation, and feedstock utilization provides a cohesive, scalable strategy for biopolymer production that is adaptable across different hosts and operational settings. The blend materials generated possess application specific potential in fields such as biomedical engineering, sustainable packaging, and environmental remediation. The findings offer not only a scientific basis for polymer property modulation but also an actionable path toward application-oriented bioplastic design.

Overall, this thesis contributes to the advancement of microbial biomanufacturing by demonstrating how systems biology and synthetic biology tools can be systematically combined to address both technological and sustainability challenges in the field. It extends the current paradigm of PHA production beyond conventional hosts and methods, offering new insights, practical tools, and experimental frameworks that can

be leveraged by researchers and industries alike. By laying the groundwork for next-generation bioplastic platforms, this work moves the field closer to realizing environmentally responsible, economically viable, and industrially scalable solutions to plastic pollution.

7.3 Future research directions

Several key areas of future research emerge directly from the findings and limitations identified in this thesis. A primary area requiring further investigation is the optimization of heterologous mcl-PHA pathways in hosts such as *Rhodococcus* and *C. necator*. Although successful transformation and partial expression of the mcl-PHA biosynthetic genes were achieved, the overall polymer titers remained low or undetectable, particularly in *Rhodococcus*. This limitation suggests that native carbon flux is predominantly channeled into competing storage molecules such as PHB or triacylglycerols. To address this, future work should focus on carbon flux redistribution through both genetic and metabolic interventions.

One proposed experimental strategy involves the chromosomal integration of pathway genes using recombineering or transposon-based insertion systems to ensure stable expression without plasmid instability. In parallel, CRISPR interference (CRISPRi) or targeted gene knockouts can be employed to suppress competing native pathways. For instance, repressing key genes in the PHB or triacylglycerol biosynthetic routes, such as phaA, phaB, or atf (acyltransferases), may reroute carbon precursors toward mcl-PHA production. These modifications should be accompanied by 13C-labeled metabolic flux analysis (MFA) to quantify the impact on precursor availability, validate carbon redistribution, and identify bottlenecks in pathway throughput.

Another critical research direction lies in improving the use of sustainable feedstocks such as molasses and potato peel hydrolysate. While both substrates demonstrated feasibility as carbon sources, their complex compositions introduced variability and

limitations in polymer titer. In the case of molasses, future studies should examine the development of defined molasses-based media in which the sugar content and trace nutrients are normalized. Sterilization protocols must also be optimized to prevent the formation of precipitates that impair nutrient availability and quantification accuracy. Potential solutions include filter sterilization of hydrolysates or autoclaving in buffered systems with chelators to prevent inorganic precipitation.

To further exploit the potential of waste-derived feedstocks, enzymatic pretreatment of lignocellulosic material such as cellulase and pectinase hydrolysis of potato peel should be considered to increase fermentable sugar content. These pretreated feedstocks could then be tested under fed-batch fermentation regimes using optimized microbial strains to evaluate productivity and robustness under simulated industrial conditions. Moreover, co-cultivation strategies employing specialized degradation strains (e.g., *Bacillus subtilis*, *Trichoderma reesei*) alongside engineered PHA producers may offer a consolidated bioprocessing approach, improving substrate utilization efficiency.

In parallel, expanding the host repertoire to include additional robust and industrially relevant microbial species could further enhance the scalability and economic feasibility of PHA production. Species such as *Halomonas*, *Bacillus*, or extremophile strains capable of growing under non-sterile conditions may offer advantages in large-scale bioreactors by reducing sterilization and contamination control costs. Screening and engineering of these alternative hosts would require standardization of transformation protocols and pathway modularization using broad-host-range vectors.

Finally, future research should focus on the end-use potential of the synthesized PHAs, particularly in high-value applications such as biomedicine and sustainable packaging. Customization of polymer blends to achieve desired biocompatibility, degradation rates, or mechanical properties will be essential. In this regard, the polymers generated in this thesis should undergo detailed mechanical testing (e.g., tensile strength,

elongation at break), thermal stability analysis (e.g., DSC, TGA), and biodegradability assessment under various environmental conditions (e.g., compost, marine, or soil).

By linking these future directions directly to the challenges encountered and insights gained throughout this work, a coherent research trajectory emerges—one that bridges molecular engineering with bioprocess optimization and material science, moving closer toward the realization of economically viable and environmentally sustainable bioplastic solutions.

7.4 Closing remarks

This research has made significant strides in advancing microbial engineering for PHA production. By integrating strain engineering, promoter optimization, and the exploration of sustainable feedstocks, this thesis contributes to the broader effort to create cost-effective, scalable, and environmentally friendly biopolymers. The experimental outcomes demonstrate not only the technical feasibility of producing PHAs with tunable monomer compositions, but also the potential of using waste-derived substrates to improve process sustainability.

These findings collectively lay the groundwork for future research and industrial implementation, bridging fundamental metabolic engineering with applied bioprocess design. As the demand for biodegradable plastics continues to grow, the strategies developed in this study provide a foundation for next-generation bio-based materials aligned with the goals of a circular bioeconomy.

References

Adam, I., Walker, T. R., Bezerra, J. C. & Clayton, A. 2020. Policies to reduce single-use plastic marine pollution in West Africa. *Marine Policy,* 116**,** 103928.

Adane, L. & Muleta, D. 2011. Survey on the usage of plastic bags, their disposal and adverse impacts on environment: A case study in Jimma City, Southwestern Ethiopia. *Journal of Toxicology and Environmental Health Sciences,* 3**,** 234-248.

Adeleye, A. T., Odoh, C. K., Enudi, O. C., Banjoko, O. O., Osiboye, O. O., Toluwalope Odediran, E. & Louis, H. 2020. Sustainable synthesis and applications of polyhydroxyalkanoates (PHAs) from biomass. *Process Biochemistry,* 96**,** 174-193.

Afrin, S., Uddin, M. K. & Rahman, M. M. 2020. Microplastics contamination in the soil from Urban Landfill site, Dhaka, Bangladesh. *Heliyon,* 6**,** e05572.

Ahmad, H., Chhipi-Shrestha, G., Hewage, K. & Sadiq, R. 2022. A Comprehensive Review on Construction Applications and Life Cycle Sustainability of Natural Fiber Biocomposites. *Sustainability* [Online], 14.

Ahn, J., Jho, E. H. & Nam, K. 2015. - Effect of C/N ratio on polyhydroxyalkanoates (PHA) accumulation by *Cupriavidus necator* and its implication on the use of rice straw hydrolysates. - 20**,** - 253.

Akaraonye, E., Keshavarz, T. & Roy, I. 2010. - Production of polyhydroxyalkanoates: the future green materials of choice. - 85**,** - 743.

Albuquerque, M. G. E., Eiroa, M., Torres, C., Nunes, B. R. & Reis, M. A. M. 2007. - Strategies for the development of a side stream process for polyhydroxyalkanoate (PHA) production from sugar cane molasses. - 130**,** - 421.

Anderson, A. J., Williams, D. R., Dawes, E. A. & Ewing, D. F. 1995. Biosynthesis of poly(3-hydroxybutyrate-co-3-hydroxyvalerate) in *Rhodococcus ruber*. *Canadian Journal of Microbiology,* 41**,** 4-13.

Andrady, A. L. 2015. Persistence of Plastic Litter in the Oceans. *In:* BERGMANN, M., GUTOW, L. & KLAGES, M. (eds.) *Marine Anthropogenic Litter.* Cham: Springer International Publishing.

Anjum, A., Zuber, M., Zia, K. M., Noreen, A., Anjum, M. N. & Tabasum, S. 2016. Microbial production of polyhydroxyalkanoates (PHAs) and its copolymers: A review of recent advancements. *Int J Biol Macromol,* 89**,** 161-74.

Arikawa, H., Sato, S., Fujiki, T. & Matsumoto, K. 2017. Simple and rapid method for isolation and quantitation of polyhydroxyalkanoate by SDS-sonication treatment. *Journal of Bioscience and Bioengineering,* 124**,** 250-254.

Arkin, A. H., Hazer, B. & Borcakli, M. 2000. Chlorination of Poly(3-hydroxy alkanoates) Containing Unsaturated Side Chains. *Macromolecules,* 33**,** 3219-3223.

Ashby, R. D., Solaiman, D. K. Y. & Foglia, T. A. 2002. The synthesis of short- and medium-chain-length poly(hydroxyalkanoate) mixtures from glucose- or alkanoic acid-grown Pseudomonas oleovorans. *Journal of Industrial Microbiology and Biotechnology,* 28**,** 147-153.

Barati, F., Asgarani, E., Gharavi, S. & Soudi, M. R. 2021. Considerable increase in Poly(3-hydroxybutyrate) production via phbC gene overexpression in Ralstonia eutropha PTCC 1615. *BioImpacts,* 11**,** 53-57.

Barboza, L. G. A., Dick Vethaak, A., Lavorante, B. R. B. O., Lundebye, A.-K. & Guilhermino, L. 2018. Marine microplastic debris: An emerging issue for food security, food safety and human health. *Marine Pollution Bulletin,* 133**,** 336-348.

Basak, B., Ince, O., Artan, N., Yagci, N. & Ince, B. K. 2011. - Effect of nitrogen limitation on enrichment of

activated sludge for PHA production. - 34**,** - 1016.

Bear, M.-M., Leboucher-Durand, M.-A., Langlois, V., Lenz, R. W., Goodwin, S. & Guérin, P. 1997. Bacterial poly-3-hydroxyalkenoates with epoxy groups in the side chains. *Reactive and Functional Polymers,* 34**,** 65-77.

Bengtsson, S., Pisco, A. R., Johansson, P., Lemos, P. C. & Reis, M. A. M. 2010. Molecular weight and thermal properties of polyhydroxyalkanoates produced from fermented sugar molasses by open mixed cultures. *Journal of Biotechnology,* 147**,** 172-179.

Bhubalan, K., Chuah, J. A., Shozui, F., Brigham, C. J., Taguchi, S., Sinskey, A. J., Rha, C. & Sudesh, K. 2011. Characterization of the highly active polyhydroxyalkanoate synthase of Chromobacterium sp. strain USM2. *Appl Environ Microbiol,* 77**,** 2926-33.

Bond-Watts, B. B., Bellerose, R. J. & Chang, M. C. Y. 2011. Enzyme mechanism as a kinetic control element for designing synthetic biofuel pathways. *Nature Chemical Biology,* 7**,** 222-227.

Boontip, T., Waditee-Sirisattha, R., Honda, K. & Napathorn, S. C. 2021. Strategies for Poly(3-hydroxybutyrate) Production Using a Cold-Shock Promoter in Escherichia coli. *Frontiers in Bioengineering and Biotechnology,* 9.

Borrero-de Acuna, J. M., Bielecka, A., Haussler, S., Schobert, M., Jahn, M., Wittmann, C., Jahn, D. & Poblete-Castro, I. 2014. Production of medium chain length polyhydroxyalkanoate in metabolic flux optimized *Pseudomonas putida*. *Microbial Cell Factories,* 13.

Brigham, C. J. & Sinskey, A. J. 2012. Applications of polyhydroxyalkanoates in the medical industry. *International Journal of Biotechnology for Wellness Industries,* 1**,** 52.

Buch, A. D., Archana, G. & Naresh Kumar, G. 2010. Broad-host-range plasmid-mediated metabolic perturbations in Pseudomonas fluorescens 13525. *Applied Microbiology and Biotechnology,* 88**,** 209-218.

Bugnicourt, E., Cinelli, P., Lazzeri, A. & Alvarez, V. 2014. Polyhydroxyalkanoate (PHA): Review of synthesis, characteristics, processing and potential applications in packaging. *Express Polymer Letters,* 8**,** 791-808.

Calero, P., Jensen, S. I. & Nielsen, A. T. 2016. Broad-Host-Range ProUSER Vectors Enable Fast Characterization of Inducible Promoters and Optimization of p-Coumaric Acid Production in *Pseudomonas putida* KT2440. *ACS Synthetic Biology,* 5**,** 741-753.

Cappelletti, M., Fedi, S., Zampolli, J., Di Canito, A., D'Ursi, P., Orro, A., Viti, C., Milanesi, L., Zannoni, D. & Di Gennaro, P. 2016. Phenotype microarray analysis may unravel genetic determinants of the stress response by *Rhodococcus* aetherivorans BCP1 and *Rhodococcus opacus* R7. *Res Microbiol,* 167**,** 766-773.

Cappelletti, M., Presentato, A., Piacenza, E., Firrincieli, A., Turner, R. J. & Zannoni, D. 2020. Biotechnology of *Rhodococcus* for the production of valuable compounds. *Appl Microbiol Biotechnol,* 104**,** 8567-8594.

Castilho, L. R., Mitchell, D. A. & Freire, D. M. G. 2009. Production of polyhydroxyalkanoates (PHAs) from waste materials and by-products by submerged and solid-state fermentation. *Bioresource Technology,* 100**,** 5996-6009.

Cavalheiro, J. M. B. T., de Almeida, M. C. M. D., Grandfils, C. & da Fonseca, M. M. R. 2009. - Poly(3-hydroxybutyrate) production by *Cupriavidus necator* using waste glycerol. - 44**,** - 515.

Chanprateep, S., Buasri, K., Muangwong, A. & Utiswannakul, P. 2010. Biosynthesis and biocompatibility of biodegradable poly(3-hydroxybutyrate-co-4-hydroxybutyrate). *Polymer Degradation and Stability,* 95**,** 2003-2012.

Chanprateep, S. & Kulpreecha, S. 2006. Production and characterization of biodegradable terpolymer poly(3-hydroxybutyrate-co-3-hydroxyvalerate-co-4-hydroxybutyrate) by Alcaligenes sp. A-04. *Journal of Bioscience and Bioengineering,* 101**,** 51-56.

Chek, M. F., Hiroe, A., Hakoshima, T., Sudesh, K. & Taguchi, S. 2019. PHA synthase (PhaC): interpreting the functions of bioplastic-producing enzyme from a structural perspective. *Appl Microbiol Biotechnol,* 103**,** 1131-1141.

Chen, C. W., Don, T.-M. & Yen, H.-F. 2006. - Enzymatic extruded starch as a carbon source for the production of poly(3-hydroxybutyrate-co-3-hydroxyvalerate) by Haloferax mediterranei. - 41**,** - 2296.

Chen, G. Q. 2010. Plastics Completely Synthesized by Bacteria: Polyhydroxyalkanoates. *In:* CHEN, G. Q. (ed.) *Plastics from Bacteria: Natural Functions and Applications.*

Cho, J.-H., Kim, E.-K. & So, J.-S. 1995. Improved transformation of *Pseudomonas putida* KT2440 by electroporation. *Biotechnology Techniques,* 9**,** 41-44.

Chohan, N. A., Aruwajoye, G. S., Sewsynker-Sukai, Y. & Gueguim Kana, E. B. 2020. Valorisation of potato peel wastes for bioethanol production using simultaneous saccharification and fermentation: Process optimization and kinetic assessment. *Renewable Energy,* 146**,** 1031-1040.

Choi, S. Y., Rhie, M. N., Kim, H. T., Joo, J. C., Cho, I. J., Son, J., Jo, S. Y., Sohn, Y. J., Baritugo, K.-A., Pyo, J., Lee, Y., Lee, S. Y. & Park, S. J. 2020a. Metabolic engineering for the synthesis of polyesters: A 100-year journey from polyhydroxyalkanoates to non-natural microbial polyesters. *Metabolic Engineering,* 58**,** 47-81.

Choi, S. Y., Rhie, M. N., Kim, H. T., Joo, J. C., Cho, I. J., Son, J., Jo, S. Y., Sohn, Y. J., Baritugo, K. A., Pyo, J., Lee, Y., Lee, S. Y. & Park, S. J. 2020b. Metabolic engineering for the synthesis of polyesters: A 100-year journey from polyhydroxyalkanoates to non-natural microbial polyesters. *Metab Eng,* 58**,** 47-81.

Christian, S. J. & Billington, S. L. 2011. Mechanical response of PHB- and cellulose acetate natural fiber-reinforced composites for construction applications. *Composites Part B: Engineering,* 42**,** 1920-1928.

Chung, A. L., Jin, H. L., Huang, L. J., Ye, H. M., Chen, J. C., Wu, Q. & Chen, G. Q. 2011. Biosynthesis and characterization of poly(3-hydroxydodecanoate) by beta-oxidation inhibited mutant of Pseudomonas entomophila L48. *Biomacromolecules,* 12**,** 3559-66.

Cox, K. D., Covernton, G. A., Davies, H. L., Dower, J. F., Juanes, F. & Dudas, S. E. 2019. Human Consumption of Microplastics. *Environmental Science & Technology,* 53**,** 7068-7074.

Creager, A. N. H. 2020. Recipes for recombining DNA: A history of Molecular Cloning: A Laboratory Manual. *BJHS Themes,* 5**,** 225-243.

Cui, Y.-W., Shi, Y.-P. & Gong, X.-Y. 2017. - Effects of C/N in the substrate on the simultaneous production of polyhydroxyalkanoates and extracellular polymeric substances by Haloferax mediterranei via kinetic model analysis. - 7**,** - 18961.

Dai, Y., Lambert, L., Yuan, Z. & Keller, J. 2008. Characterisation of polyhydroxyalkanoate copolymers with controllable four-monomer composition. *Journal of Biotechnology,* 134**,** 137-145.

Dauvergne, P. 2018. The power of environmental norms: marine plastic pollution and the politics of microbeads. *Environmental Politics,* 27**,** 579-597.

Davis, R., Kataria, R., Cerrone, F., Woods, T., Kenny, S., O'Donovan, A., Guzik, M., Shaikh, H., Duane, G., Gupta, V. K., Tuohy, M. G., Padamatti, R. B., Casey, E. & O'Connor, K. E. 2013. Conversion of grass biomass into fermentable sugars and its utilization for medium chain length

polyhydroxyalkanoate (mcl-PHA) production by Pseudomonas strains. *Bioresource Technology,* 150**,** 202-209.

de Eugenio, L., García, P., Luengo, J., Sanz, J., San Roman, J., García, J. & Prieto, A. 2007. Biochemical Evidence That phaZ Gene Encodes a Specific Intracellular Medium Chain Length Polyhydroxyalkanoate Depolymerase in *Pseudomonas putida* KT2442 CHARACTERIZATION OF A PARADIGMATIC ENZYME. *The Journal of biological chemistry,* 282**,** 4951-62.

De Eugenio, L. I., Galán, B., Escapa, I. F., Maestro, B., Sanz, J. M., García, J. L. & Prieto, M. A. 2010. The PhaD regulator controls the simultaneous expression of the pha genes involved in polyhydroxyalkanoate metabolism and turnover in *Pseudomonas putida* KT2442. *Environmental Microbiology,* 12**,** 1591-1603.

de las Heras, A. M., Portugal-Nunes, D. J., Rizza, N., Sandström, A. G. & Gorwa-Grauslund, M. F. 2016. Anaerobic poly-3-d-hydroxybutyrate production from xylose in recombinant Saccharomyces cerevisiae using a NADH-dependent acetoacetyl-CoA reductase. *Microbial Cell Factories,* 15**,** 197.

DeLorenzo, D. M., Rottinghaus, A. G., Henson, W. R. & Moon, T. S. 2018. Molecular Toolkit for Gene Expression Control and Genome Modification in *Rhodococcus opacus* PD630. *ACS Synthetic Biology,* 7**,** 727-738.

Divyashree, M. S., Shamala, T. R. & Rastogi, N. K. 2009. - Isolation of Polyhydroxyalkanoate from Hydrolyzed Cells of Bacillus flexus using Aqueous Two-phase System Containing Polyethylene Glycol and Phosphate. - 14**,** - 489.

Dong, Z. L. & Sun, X. N. 2000. - A new method of recovering polyhydroxyalkanoate from Azotobacter chroococcum. - 45**,** - 256.

Durre, P. & Eikmanns, B. J. 2015. C1-carbon sources for chemical and fuel production by microbial gas fermentation. *Current Opinion in Biotechnology,* 35**,** 63-72.

El-Shafee, E., Saad, G. R. & Fahmy, S. M. 2001. Miscibility, crystallization and phase structure of poly(3-hydroxybutyrate)/cellulose acetate butyrate blends. *European Polymer Journal,* 37**,** 2091-2104.

Elhadi, D., Lv, L., Jiang, X.-R., Wu, H. & Chen, G.-Q. 2016. CRISPRi engineering E. coli for morphology diversification. *Metabolic Engineering,* 38**,** 358-369.

Flores-Sanchez, A., Rathinasabapathy, P. D. A., López-Cuellar, M. D. R., Vergara Porras, B. & Fermín, P.-G. 2020. Biosynthesis of polyhydroxyalkanoates from vegetable oil under the co-expression of fadE and phaJ genes in *Cupriavidus necator*. *International Journal of Biological Macromolecules,* 164.

Fu, X. Z., Tan, D., Aibaidula, G., Wu, Q., Chen, J. C. & Chen, G. Q. 2014. Development of Halomonas TD01 as a host for open production of chemicals. *Metabolic Engineering,* 23**,** 78-91.

Furrer, P., Panke, S. & Zinn, M. 2007. - Efficient recovery of low endotoxin medium-chain-length poly(R -3-hydroxyalkanoate) from bacterial biomass. - 69**,** - 213.

Gallagher, S. R. 2012. SDS-Polyacrylamide Gel Electrophoresis (SDS-PAGE). *Current Protocols Essential Laboratory Techniques,* 6**,** 7.3.1-7.3.28.

Gao, X., Chen, J.-C., Wu, Q. & Chen, G.-Q. 2011. Polyhydroxyalkanoates as a source of chemicals, polymers, and biofuels. *Current Opinion in Biotechnology,* 22**,** 768-774.

Geyer, R., Jambeck, J. R. & Law, K. L. 2017. Production, use, and fate of all plastics ever made. *SCIENCE ADVANCES,* 3.

Gonzalez-Villanueva, M., Galaiya, H., Staniland, P., Staniland, J., Savill, I., Wong, T. S. & Tee, K. L. 2019. Adaptive Laboratory Evolution of *Cupriavidus necator* H16 for Carbon Co-Utilization with

Glycerol. *Int J Mol Sci,* 20.

Green, P. R., Kemper, J., Schechtman, L., Guo, L., Satkowski, M., Fiedler, S., Steinbuchel, A. & Rehm, B. H. A. 2002. Formation of short chain length/medium chain length polyhydroxyalkanoate copolymers by fatty acid beta-oxidation inhibited Ralstonia eutropha. *Biomacromolecules,* 3**,** 208-213.

Gregory, D. A., Taylor, C. S., Fricker, A. T. R., Asare, E., Tetali, S. S. V., Haycock, J. W. & Roy, I. 2022. Polyhydroxyalkanoates and their advances for biomedical applications. *Trends in Molecular Medicine,* 28**,** 331-342.

Haas, R., Jin, B. & Zepf, F. T. 2008. - Production of poly(3-hydroxybutyrate) from waste potato starch. - 72**,** - 256.

Haba, E., Vidal-Mas, J., Bassas, M., Espuny, M. J., Llorens, J. & Manresa, A. 2007. - Poly 3-(hydroxyalkanoates) produced from oily substrates by Pseudomonas aeruginosa 47T2 (NCBIM 40044): Effect of nutrients and incubation temperature on polymer composition. - 35**,** - 106.

Hames, B. D. 1998. *Gel electrophoresis of proteins: a practical approach*, OUP Oxford.

Hampson, J. W. & Ashby, R. D. 1999. - Extraction of lipid-grown bacterial cells by supercritical fluid and organic solvent to obtain pure medium chain-length polyhydroxyalkanoates. - 76**,** - 1374.

Harmaen, A. S., Khalina, A., Ali, H. M. & Azowa, I. N. 2016. Thermal, Morphological, and Biodegradability Properties of Bioplastic Fertilizer Composites Made of Oil Palm Biomass, Fertilizer, and Poly(hydroxybutyrate-co-valerate). *International Journal of Polymer Science,* 2016**,** 3230109.

Heinrich, D., Raberg, M. & Steinbüchel, A. 2015. Synthesis of poly(3-hydroxybutyrate-co-3-hydroxyvalerate) from unrelated carbon sources in engineered Rhodospirillum rubrum. *FEMS Microbiology Letters,* 362.

Hejazi, P., Vasheghani-Farahani, E. & Yamini, Y. 2003. - Supercritical fluid disruption of Ralstonia eutropha for poly(beta-hydroxybutyrate) recovery. - 19**,** - 1523.

Hendrawan, Y., Alvianto, D., Sumarlan, S. & Wibisono, Y. 2020. Characterization of Pseudomonas fluorescens polyhydroxyalkanoate produced from molasses as a carbon source. *Advances in Food Science, Sustainable Agriculture and Agroindustrial Engineering,* 3**,** 1-10.

Hermida, É. B., Mega, V. I., Yashchuk, O., Fernández, V., Eisenberg, P. & Miyazaki, S. S. 2008. Gamma Irradiation Effects on Mechanical and Thermal Properties and Biodegradation of Poly(3-hydroxybutyrate) Based Films. *Macromolecular Symposia,* 263**,** 102-113.

Hernandez, M. A., Mohn, W. W., Martinez, E., Rost, E., Alvarez, A. F. & Alvarez, H. M. 2008. Biosynthesis of storage compounds by *Rhodococcus jostii* RHA1 and global identification of genes involved in their metabolism. *Bmc Genomics,* 9.

Hiroe, A., Tsuge, K., Nomura Christopher, T., Itaya, M. & Tsuge, T. 2012. Rearrangement of Gene Order in the phaCAB Operon Leads to Effective Production of Ultrahigh-Molecular-Weight Poly[(R)-3-Hydroxybutyrate] in Genetically Engineered Escherichia coli. *Applied and Environmental Microbiology,* 78**,** 3177-3184.

Huang, T.-Y., Duan, K.-J., Huang, S.-Y. & Chen, C. W. 2006. - Production of polyhydroxyalkanoates from inexpensive extruded rice bran and starch by Haloferax mediterranei. - 33**,** - 706.

Huijberts, G. N., Eggink, G., de Waard, P., Huisman, G. W. & Witholt, B. 1992. *Pseudomonas putida* KT2442 cultivated on glucose accumulates poly(3-hydroxyalkanoates) consisting of saturated and unsaturated monomers. *Applied and Environmental Microbiology,* 58**,** 536-544.

Huisman, G. W., Deleeuw, O., Eggink, G. & Witholt, B. 1989. SYNTHESIS OF POLY-3-HYDROXYALKANOATES IS A COMMON FEATURE OF FLUORESCENT PSEUDOMONADS. *APPLIED*

AND ENVIRONMENTAL MICROBIOLOGY, 55**,** 1949-1954.

Ibrahim, M. H. A. & Steinbuechel, A. 2009. - Poly(3-Hydroxybutyrate) Production from Glycerol by Zobellella denitrificans MW1 via High-Cell-Density Fed-Batch Fermentation and Simplified Solvent Extraction. - 75**,** - 6231.

Indest, K. J., Eberly, J. O., Hancock, D. E., Jung, C. M., Carr, M. R. & Blakeney, G. A. 2016. *Rhodococcus jostii* RHA1 TadA-homolog deletion mutants accumulate less polyhydroxyalkanoates (PHAs) than the parental strain. *J Gen Appl Microbiol,* 62**,** 213-6.

Ivanov, V., Stabnikov, V., Ahmed, Z., Dobrenko, S. & Saliuk, A. 2015. Production and applications of crude polyhydroxyalkanoate-containing bioplastic from the organic fraction of municipal solid waste. *International Journal of Environmental Science and Technology,* 12**,** 725-738.

Iwata, T. 2005. Strong Fibers and Films of Microbial Polyesters. *Macromolecular Bioscience,* 5**,** 689-701.

Jacquel, N., Lo, C. W., Wei, Y. H., Wu, H. S. & Wang, S. S. 2008. Isolation and purification of bacterial poly (3-hydroxyalkanoates). *Biochemical Engineering Journal,* 39**,** 15-27.

Jacques, O. & Prosser, R. S. 2021. A probabilistic risk assessment of microplastics in soil ecosystems. *Science of The Total Environment,* 757**,** 143987.

Jahn, M., Vorpahl, C., Hübschmann, T., Harms, H. & Müller, S. 2016. Copy number variability of expression plasmids determined by cell sorting and Droplet Digital PCR. *Microbial Cell Factories,* 15.

Jawed, K., Irorere, V. U., Bommareddy, R. R., Minton, N. P. & Kovács, K. 2022. Establishing Mixotrophic Growth of *Cupriavidus necator* H16 on CO2 and Volatile Fatty Acids. *Fermentation* [Online], 8.

Jiang, X. J., Sun, Z. Y., Ramsay, J. A. & Ramsay, B. A. 2013. Fed-batch production of MCL-PHA with elevated 3-hydroxynonanoate content. *Amb Express,* 3.

Jiang, X. R. & Chen, G. Q. 2016. Morphology engineering of bacteria for bio-production. *Biotechnology Advances,* 34**,** 435-440.

Jiang, X. R., Wang, H., Shen, R. & Chen, G. Q. 2015. Engineering the bacterial shapes for enhanced inclusion bodies accumulation. *Metabolic Engineering,* 29**,** 227-237.

Jiang, X. R., Yao, Z. H. & Chen, G. Q. 2017. Controlling cell volume for efficient PHB production by Halomonas. *Metabolic Engineering,* 44**,** 30-37.

Jiang, Y., Chen, Y. & Zheng, X. 2009. Efficient Polyhydroxyalkanoates Production from a Waste-Activated Sludge Alkaline Fermentation Liquid by Activated Sludge Submitted to the Aerobic Feeding and Discharge Process. *Environmental Science & Technology,* 43**,** 7734-7741.

Jiang, Y., Song, X., Gong, L., Li, P., Dai, C. & Shao, W. 2008. - High poly(beta-hydroxybutyrate) production by Pseudomonas fluorescens A2a5 from inexpensive substrates. - 42**,** - 172.

Johnson, A. O., Gonzalez-Villanueva, M., Tee, K. L. & Wong, T. S. 2018. An Engineered Constitutive Promoter Set with Broad Activity Range for *Cupriavidus necator* H16. *ACS Synthetic Biology,* 7**,** 1918-1928.

Johnson, K., Jiang, Y., Kleerebezem, R., Muyzer, G. & van Loosdrecht, M. C. M. 2009. Enrichment of a Mixed Bacterial Culture with a High Polyhydroxyalkanoate Storage Capacity. *Biomacromolecules,* 10**,** 670-676.

Kabir, E., Kaur, R., Lee, J., Kim, K.-H. & Kwon, E. E. 2020. Prospects of biopolymer technology as an alternative option for non-degradable plastics and sustainable management of plastic wastes. *Journal of Cleaner Production,* 258**,** 120536.

Kag, S., Kumar, P. & Kataria, R. 2024. Potato Peel Waste as an Economic Feedstock for PHA Production by Bacillus circulans. *Applied Biochemistry and Biotechnology,* 196**,** 2451-2465.

Kai, D. & Loh, X. J. 2014. Polyhydroxyalkanoates: Chemical Modifications Toward Biomedical Applications. *ACS Sustainable Chemistry & Engineering,* 2**,** 106-119.

Kang, S. & Yu, J. 2014. One-pot production of hydrocarbon oil from poly(3-hydroxybutyrate). *RSC Advances,* 4**,** 14320.

Karasik, R., Vegh, T., Diana, Z., Bering, J., Caldas, J., Pickle, A., Rittschof, D. & Virdin, J. 2020. Years of government responses to the global plastic pollution problem: The plastics policy inventory. *NI X,* 20.

Kepka, C., Collet, E., Persson, J., Stahl, A., Lagerstedt, T., Tjerneld, F. & Veide, A. 2003. - Pilot-scale extraction of an intracellular recombinant cutinase from E-coli cell homogenate using a thermoseparating aqueous two-phase system. - 103**,** - 181.

Keskin, G., Kızıl, G., Bechelany, M., Pochat-Bohatier, C. & Öner, M. 2017. Potential of polyhydroxyalkanoate (PHA) polymers family as substitutes of petroleum based polymers for packaging applications and solutions brought by their composites to form barrier materials. 89**,** 1841-1848.

Khosravi-Darani, K., Vasheghani-Farahani, E., Yamini, Y. & Bahramifar, N. 2003. - Solubility of poly(beta-hydroxybutyrate) in supercritical carbon dioxide. - 48**,** - 863.

Kim, B. S. 2000. - Production of poly(3-hydroxybutyrate) from inexpensive substrates. - 27**,** - 777.

Kim, D. Y., Kim, H. W., Chung, M. G. & Rhee, Y. H. 2007. - Biosynthesis, modification, and biodegradation of bacterial medium-chain-length polyhydroxyalkanoates. - 45**,** - 97.

Kim, D. Y., Kim, Y. B. & Rhee, Y. H. 2000. - Evaluation of various carbon substrates for the biosynthesis of polyhydroxyalkanoates bearing functional groups by *Pseudomonas putida*. - 28**,** - 29.

Kim, J., Kim, Y.-J., Choi, S. Y., Lee, S. Y. & Kim, K.-J. 2017. Crystal structure of Ralstonia eutropha polyhydroxyalkanoate synthase C-terminal domain and reaction mechanisms. *Biotechnology Journal,* 12**,** 1600648.

Kiselev, E. G., Demidenko, A. V., Zhila, N. O., Shishatskaya, E. I. & Volova, T. G. 2022. Sugar Beet Molasses as a Potential C-Substrate for PHA Production by *Cupriavidus necator*. *Bioengineering* [Online], 9.

Klinke, S., Ren, Q., Witholt, B. & Kessler, B. 1999. Production of Medium-Chain-Length Poly(3-Hydroxyalkanoates) from Gluconate by Recombinant Escherichia coli. *Appl Environ Microbiol,* 65**,** 540-548.

Kobayashi, J. & Kondo, A. 2019. Disruption of poly (3-hydroxyalkanoate) depolymerase gene and overexpression of three poly (3-hydroxybutyrate) biosynthetic genes improve poly (3-hydroxybutyrate) production from nitrogen rich medium by Rhodobacter sphaeroides. *Microbial Cell Factories,* 18**,** 40.

Koller, M. 2016. Characterization of polyhydroxyalkanoates. *Microbial Biopolyester, Recent Advances in Biotechnology,* 2.

Koller, M. 2018. Biodegradable and Biocompatible Polyhydroxy-alkanoates (PHA): Auspicious Microbial Macromolecules for Pharmaceutical and Therapeutic Applications. *Molecules,* 23.

Koller, M. 2019. Chemical and Biochemical Engineering Approaches in Manufacturing Polyhydroxyalkanoate (PHA) Biopolyesters of Tailored Structure with Focus on the Diversity of Building Blocks. *Chemical and Biochemical Engineering Quarterly,* 32**,** 413-438.

Koller, M., Niebelschutz, H. & Braunegg, G. 2013a. Strategies for recovery and purification of poly (R)-3-hydroxyalkanoates (PHA) biopolyesters from surrounding biomass. *Engineering in Life Sciences,* 13**,** 549-562.

Koller, M., Sandholzer, D., Salerno, A., Braunegg, G. & Narodoslawsky, M. 2013b. - Biopolymer from industrial residues: Life cycle assessment of poly(hydroxyalkanoates) from whey. - 73**,** - 71.

Kovach, M. E., Elzer, P. H., Steven Hill, D., Robertson, G. T., Farris, M. A., Roop, R. M. & Peterson, K. M. 1995. Four new derivatives of the broad-host-range cloning vector pBBR1MCS, carrying different antibiotic-resistance cassettes. *Gene,* 166**,** 175-176.

Krivoruchko, A., Kuyukina, M. & Ivshina, I. 2019. Advanced *Rhodococcus* Biocatalysts for Environmental Biotechnologies. *Catalysts,* 9.

Kumar, P., Jun, H. B. & Kim, B. S. 2018. Co-production of polyhydroxyalkanoates and carotenoids through bioconversion of glycerol by Paracoccus sp strain LL1. *International Journal of Biological Macromolecules,* 107**,** 2552-2558.

Kumar, P., Patel, S. K. S., Lee, J.-K. & Kalia, V. C. 2013. Extending the limits of Bacillus for novel biotechnological applications. *Biotechnology Advances,* 31**,** 1543-1561.

Kumar, P., Ray, S., Patel, S. K. S., Lee, J.-K. & Kalia, V. C. 2015. Bioconversion of crude glycerol to polyhydroxyalkanoate by Bacillus thuringiensis under non-limiting nitrogen conditions. *International Journal of Biological Macromolecules,* 78**,** 9-16.

Kunasundari, B. & Sudesh, K. 2011. - Isolation and recovery of microbial polyhydroxyalkanoates. - 5**,** - 634.

Laemmli, U. K. 1970. Cleavage of Structural Proteins during the Assembly of the Head of Bacteriophage T4. *Nature,* 227**,** 680-685.

Lee, H.-J., Kim, S.-G., Cho, D.-H., Bhatia, S. K., Gurav, R., Yang, S.-Y., Yang, J., Jeon, J.-M., Yoon, J.-J., Choi, K.-Y. & Yang, Y.-H. 2022. Finding of novel lactate utilizing Bacillus sp. YHY22 and its evaluation for polyhydroxybutyrate (PHB) production. *International Journal of Biological Macromolecules,* 201**,** 653-661.

Lee, J., Park, H. J., Moon, M., Lee, J.-S. & Min, K. 2021. Recent progress and challenges in microbial polyhydroxybutyrate (PHB) production from CO2 as a sustainable feedstock: A state-of-the-art review. *Bioresource Technology,* 339**,** 125616.

Lemoigne, M. 1926. Produits de deshydration et de polymerisation de l'acide β= oxybutyrique. *Bull. Soc. Chim. Biol.,* 8**,** 770-782.

Li, H.-L., Deng, R.-X., Wang, W., Liu, K.-Q., Hu, H.-B., Huang, X.-Q. & Zhang, X.-H. 2021a. Biosynthesis and Characterization of Medium-Chain-Length Polyhydroxyalkanoate with an Enriched 3-Hydroxydodecanoate Monomer from a Pseudomonas chlororaphis Cell Factory. *Journal of Agricultural and Food Chemistry,* 69**,** 3895-3903.

Li, X., Xu, Z., Cort, J. R., Qian, W.-J. & Yang, B. 2021b. Lipid production from non-sugar compounds in pretreated lignocellulose hydrolysates by *Rhodococcus jostii* RHA1. *Biomass and Bioenergy,* 145.

Li, Z., Yang, J. & Loh, X. J. 2016. Polyhydroxyalkanoates: opening doors for a sustainable future. *NPG Asia Materials,* 8**,** e265-e265.

Ling, C., Qiao, G. Q., Shuai, B. W., Olavarria, K., Yin, J., Xiang, R. J., Song, K. N., Shen, Y. H., Guo, Y. Y. & Chen, G. Q. 2018. Engineering NADH/NAD(+) ratio in Halomonas bluephagenesis for enhanced production of polyhydroxyalkanoates (PHA). *Metabolic Engineering,* 49**,** 275-286.

Liu, H., Chen, Y., Wang, S., Liu, Y., Zhao, W., Huo, K., Guo, H., Xiong, W., Wang, S., Yang, C. & Liu, R. 2023. Metabolic engineering of genome-streamlined strain *Pseudomonas putida* KTU-U27 for medium-chain-length polyhydroxyalkanoate production from xylose and cellobiose. *International Journal of Biological Macromolecules,* 253**,** 126732.

Liu, H., Chen, Y., Zhang, Y., Zhao, W., Guo, H., Wang, S., Xia, W., Wang, S., Liu, R. & Yang, C. 2022. Enhanced production of polyhydroxyalkanoates in *Pseudomonas putida* KT2440 by a combination of genome streamlining and promoter engineering. *International Journal of Biological Macromolecules,* 209**,** 117-124.

Liu, Q., Luo, G., Zhou, X. R. & Chen, G. Q. 2011. Biosynthesis of poly(3-hydroxydecanoate) and 3-hydroxydodecanoate dominating polyhydroxyalkanoates by beta-oxidation pathway inhibited *Pseudomonas putida*. *Metab Eng,* 13**,** 11-7.

Loeschcke, A. & Thies, S. 2015. *Pseudomonas putida*—a versatile host for the production of natural products. *Applied Microbiology and Biotechnology,* 99**,** 6197-6214.

Loeschcke, A. & Thies, S. 2020. Engineering of natural product biosynthesis in *Pseudomonas putida*. *Current Opinion in Biotechnology,* 65**,** 213-224.

Lusher, A. L., Hernandez-Milian, G., Berrow, S., Rogan, E. & O'Connor, I. 2018. Incidence of marine debris in cetaceans stranded and bycaught in Ireland: Recent findings and a review of historical knowledge. *Environmental Pollution,* 232**,** 467-476.

Lütke-Eversloh, T. & Steinbüchel, A. 1999. Biochemical and molecular characterization of a succinate semialdehyde dehydrogenase involved in the catabolism of 4-hydroxybutyric acid in Ralstonia eutropha. *FEMS Microbiology Letters,* 181**,** 63-71.

Macrae, R. M. & Wilkinson, J. F. 1958. Poly-{beta}-hyroxybutyrate Metabolism in Washed Suspensions of Bacillus cereus and Bacillus megaterium. *Journal of general microbiology,* 19**,** 210-222.

Manoli, M.-T., Nogales, J. & Prieto, A. 2022. Synthetic Control of Metabolic States in *Pseudomonas putida* by Tuning Polyhydroxyalkanoate Cycle. *mBio,* 13**,** e01794-21.

Marsudi, S., Unno, H. & Hori, K. 2008. - Palm oil utilization for the simultaneous production of polyhydroxyalkanoates and rhamnolipids by Pseudomonas aeruginosa. - 78**,** - 961.

Martinkova, L., Uhnakova, B., Patek, M., Nesvera, J. & Kren, V. 2009. Biodegradation potential of the genus *Rhodococcus*. *Environ Int,* 35**,** 162-77.

McChalicher, C. W. J. & Srienc, F. 2007. Investigating the structure-property relationship of bacterial PHA block copolymers. *Journal of Biotechnology,* 132**,** 296-302.

Mendonça, T. T., Gomez, J. G. C., Buffoni, E., Sánchez Rodriguez, R. J., Schripsema, J., Lopes, M. S. G. & Silva, L. F. 2014. Exploring the potential of *Burkholderia sacchari* to produce polyhydroxyalkanoates. *Journal of Applied Microbiology,* 116**,** 815-829.

Meng, D. C., Shen, R., Yao, H., Chen, J. C., Wu, Q. & Chen, G. Q. 2014. Engineering the diversity of polyesters. *Current Opinion in Biotechnology,* 29**,** 24-33.

Mezzina, M. P., Manoli, M. T., Prieto, M. A. & Nikel, P. I. 2021. Engineering Native and Synthetic Pathways in *Pseudomonas putida* for the Production of Tailored Polyhydroxyalkanoates. *Biotechnology Journal,* 16**,** 2000165.

Mezzolla, V., D'Urso, O. F. & Poltronieri, P. 2018. Role of PhaC Type I and Type II Enzymes during PHA Biosynthesis. *Polymers (Basel),* 10.

Mohanrasu, K., Guru Raj Rao, R., Dinesh, G. H., Zhang, K., Sudhakar, M., Pugazhendhi, A., Jeyakanthan, J., Ponnuchamy, K., Govarthanan, M. & Arun, A. 2021. Production and characterization of biodegradable polyhydroxybutyrate by Micrococcus luteus isolated from marine environment. *International Journal of Biological Macromolecules,* 186**,** 125-134.

Moharir, R. V. & Kumar, S. 2019. Challenges associated with plastic waste disposal and allied microbial routes for its effective degradation: A comprehensive review. *Journal of Cleaner Production,* 208**,** 65-76.

Morlino, M. S., Serna García, R., Savio, F., Zampieri, G., Morosinotto, T., Treu, L. & Campanaro, S. 2023. *Cupriavidus necator* as a platform for polyhydroxyalkanoate production: An overview of strains, metabolism, and modeling approaches. *Biotechnology Advances,* 69**,** 108264.

Moshood, T. D., Nawanir, G., Mahmud, F., Mohamad, F., Ahmad, M. H. & AbdulGhani, A. 2022. Biodegradable plastic applications towards sustainability: A recent innovations in the green product. *Cleaner Engineering and Technology,* 6**,** 100404.

Mousavioun, P., George, G. A. & Doherty, W. O. S. 2012. Environmental degradation of lignin/poly(hydroxybutyrate) blends. *Polymer Degradation and Stability,* 97**,** 1114-1122.

Mozejko-Ciesielska, J. & Serafim, L. 2019. Proteomic Response of *Pseudomonas putida* KT2440 to Dual Carbon-Phosphorus Limitation during mcl-PHAs Synthesis.

Muhammadi, Shabina, Afzal, M. & Hameed, S. 2015. Bacterial polyhydroxyalkanoates-eco-friendly next generation plastic: Production, biocompatibility, biodegradation, physical properties and applications. *Green Chemistry Letters and Reviews,* 8**,** 56-77.

Muizniece-Brasava, S. & Dukalska, L. 2006. Impact of biodegradable PHB packaging composite materials on dairy product quality. *Proceedings of the Latvia University of Agriculture,* 16**,** 79-87.

Murueva, A. V., Shershneva, A. M., Shishatskaya, E. I. & Volova, T. G. 2014. The Use of Polymeric Microcarriers Loaded with Anti-Inflammatory Substances in the Therapy of Experimental Skin Wounds. *Bulletin of Experimental Biology and Medicine,* 157**,** 597-602.

Murugan, P., Han, L. Z., Gan, C. Y., Maurer, F. H. J. & Sudesh, K. 2016. A new biological recovery approach for PHA using mealworm, Tenebrio molitor. *Journal of Biotechnology,* 239**,** 98-105.

Myshkina, V. L., Nikolaeva, D. A., Makhina, T. K., Bonartsev, A. P. & Bonartseva, G. A. 2008. Effect of growth conditions on the molecular weight of poly-3-hydroxybutyrate produced by Azotobacter chroococcum 7B. *Applied Biochemistry and Microbiology,* 44**,** 482-486.

Neuhoff, V., Arold, N., Taube, D. & Ehrhardt, W. 1988. Improved staining of proteins in polyacrylamide gels including isoelectric focusing gels with clear background at nanogram sensitivity using Coomassie Brilliant Blue G-250 and R-250. *ELECTROPHORESIS,* 9**,** 255-262.

Nigmatullin, R., Taylor, C., Basnett, P., Lukasiewicz, B., Paxinou, A., Lizarraga Valderrama, L. R., Haycock, J. & Roy, I. 2023. Medium chain length Polyhydroxyalkanoates as potential matrix materials for peripheral nerve regeneration. *Regenerative Biomaterials,* 10.

Novick, R. P. 1987. Plasmid incompatibility. *Microbiological Reviews,* 51**,** 381-395.

Obruca, S., Marova, I., Melusova, S. & Mravcova, L. 2011. Production of polyhydroxyalkanoates from cheese whey employing Bacillus megaterium CCM 2037. *Annals of Microbiology,* 61**,** 947-953.

Obruca, S., Petrik, S., Benesova, P., Svoboda, Z., Eremka, L. & Marova, I. 2014. - Utilization of oil extracted from spent coffee grounds for sustainable production of polyhydroxyalkanoates. - 98**,** - 5890.

Ochi, A., Matsumoto, K., Ooba, T., Sakai, K., Tsuge, T. & Taguchi, S. 2013. Engineering of class I lactate-polymerizing polyhydroxyalkanoate synthases from Ralstonia eutropha that synthesize lactate-based polyester with a block nature. *Appl Microbiol Biotechnol,* 97**,** 3441-7.

Ong, S. Y., Zainab-L, I., Pyary, S. & Sudesh, K. 2018. A novel biological recovery approach for PHA employing selective digestion of bacterial biomass in animals. *Applied Microbiology and Biotechnology,* 102**,** 2117-2127.

Pan, P. & Inoue, Y. 2009. Polymorphism and isomorphism in biodegradable polyesters. *Progress in Polymer Science,* 34**,** 605-640.

Patel, M., Gapes, D. J., Newman, R. H. & Dare, P. H. 2009. Physico-chemical properties of polyhydroxyalkanoate produced by mixed-culture nitrogen-fixing bacteria. *Applied*

Microbiology and Biotechnology, 82**,** 545-555.

Patel, S. K. S., Lee, J.-K. & Kalia, V. C. 2016. Integrative Approach for Producing Hydrogen and Polyhydroxyalkanoate from Mixed Wastes of Biological Origin. *Indian Journal of Microbiology,* 56**,** 293-300.

Poli, A., Di Donato, P., Abbamondi, G. R. & Nicolaus, B. 2011. - Synthesis, Production, and Biotechnological Applications of Exopolysaccharides and Polyhydroxyalkanoates by Archaea. - 2011.

Preusting, H., van Houten, R., Hoefs, A., van Langenberghe, E. K., Favre-Bulle, O. & Witholt, B. 1993. High cell density cultivation of Pseudomonas oleovorans: Growth and production of poly (3-hydroxyalkanoates) in two-liquid phase batch and fed-batch systems. *Biotechnology and Bioengineering,* 41**,** 550-556.

Rajdeep, S. & Naithani, S. 2013. Scope of natural and synthetic biodegradable materials in development of ecofriendly substitutes for nursery polybags—A review. eJournal Appl. *For. Ecol,* 1**,** 35-44.

Ramesh, B. N., Anitha, N. & Rani, H. 2010. Recent trends in biodegradable products from biopolymers. *Adv Biotechnol,* 9**,** 30-34.

Rath, A., Glibowicka, M., Nadeau, V. G., Chen, G. & Deber, C. M. 2009. Detergent binding explains anomalous SDS-PAGE migration of membrane proteins. *Proceedings of the National Academy of Sciences,* 106**,** 1760-1765.

Raza, Z. A., Abid, S. & Banat, I. M. 2018. Polyhydroxyalkanoates: Characteristics, production, recent developments and applications. *International Biodeterioration & Biodegradation,* 126**,** 45-56.

Raza, Z. A., Khan, M. S. & Khalid, Z. M. 2007. - Physicochemical and surface-active properties of biosurfactant produced using molasses by a Pseudomonas aeruginosa mutant. - 42**,** - 80.

Reinecke, F. & Steinbüchel, A. 2008. Ralstonia eutropha Strain H16 as Model Organism for PHA Metabolism and for Biotechnological Production of Technically Interesting Biopolymers. *Journal of Molecular Microbiology and Biotechnology,* 16**,** 91-108.

Rigouin, C., Lajus, S., Ocando, C., Borsenberger, V., Nicaud, J. M., Marty, A., Averous, L. & Bordes, F. 2019. Production and characterization of two medium-chain-length polydroxyalkanoates by engineered strains of Yarrowia lipolytica. *Microb Cell Fact,* 18**,** 99.

Ryu, H. W., Cho, K. S., Goodrich, P. R. & Park, C.-H. 2008. - Production of Polyhydroxyalkanoates by Azotobacter vinelandii UWD Using Swine Wastewater: Effect of Supplementing Glucose, Yeast Extract, and Inorganic Salts. - 13**,** - 658.

Salvachua, D., Rydzak, T., Auwae, R., De Capite, A., Black, B. A., Bouvier, J. T., Cleveland, N. S., Elmore, J. R., Huenemann, J. D., Katahira, R., Michener, W. E., Peterson, D. J., Rohrer, H., Vardon, D. R., Beckham, G. T. & Guss, A. M. 2020. Metabolic engineering of *Pseudomonas putida* for increased polyhydroxyalkanoate production from lignin. *Microb Biotechnol,* 13**,** 290-298.

Sandberg, T. E., Salazar, M. J., Weng, L. L., Palsson, B. O. & Feist, A. M. 2019. The emergence of adaptive laboratory evolution as an efficient tool for biological discovery and industrial biotechnology. *Metabolic Engineering,* 56**,** 1-16.

Sato, S., Kanazawa, H. & Tsuge, T. 2011. Expression and characterization of (R)-specific enoyl coenzyme A hydratases making a channeling route to polyhydroxyalkanoate biosynthesis in *Pseudomonas putida*. *Applied Microbiology and Biotechnology,* 90**,** 951-959.

Sayyed, R. Z., Gangurde, N. S. & Chincholkar, S. B. 2009. - Hypochlorite digestion method for efficient recovery of PHB from Alcaligenes faecalis. - 49**,** - 232.

Schlegel, H. G., Kaltwasser, H. & Gottschalk, G. 1961. Ein Submersverfahren zur Kultur

wasserstoffoxydierender Bakterien: Wachstumsphysiologische Untersuchungen. *Archiv für Mikrobiologie,* 38**,** 209-222.

Schmaltz, E., Melvin, E. C., Diana, Z., Gunady, E. F., Rittschof, D., Somarelli, J. A., Virdin, J. & Dunphy-Daly, M. M. 2020. Plastic pollution solutions: emerging technologies to prevent and collectmarineplastic pollution. *Environ Int,* 144**,** 106067.

Schnurr, R. E. J., Alboiu, V., Chaudhary, M., Corbett, R. A., Quanz, M. E., Sankar, K., Srain, H. S., Thavarajah, V., Xanthos, D. & Walker, T. R. 2018. Reducing marine pollution from single-use plastics (SUPs): A review. *Marine Pollution Bulletin,* 137**,** 157-171.

Sharma, P. K., Fu, J., Cicek, N., Sparling, R. & Levin, D. B. 2012. Kinetics of medium-chain-length polyhydroxyalkanoate production by a novel isolate of *Pseudomonas putida* LS46. *Canadian Journal of Microbiology,* 58**,** 982-989.

Sharma, V., Sehgal, R. & Gupta, R. 2021. Polyhydroxyalkanoate (PHA): Properties and Modifications. *Polymer,* 212**,** 123161.

Shasaltaneh, M. D., Moosavi-Nejad, Z., Gharavi, S. & Fooladi, J. 2013. - Cane molasses as a source of precursors in the bioproduction of tryptophan by Bacillus subtilis. - 5**,** - 292.

Shen, R., Ning, Z. Y., Lan, Y. X., Chen, J. C. & Chen, G. Q. 2019. Manipulation of polyhydroxyalkanoate granular sizes in Halomonas bluephagenesis. *Metabolic Engineering,* 54**,** 117-126.

Shen, X. W., Shi, Z. Y., Song, G., Li, Z. J. & Chen, G. Q. 2011. Engineering of polyhydroxyalkanoate (PHA) synthase PhaC2Ps of Pseudomonas stutzeri via site-specific mutation for efficient production of PHA copolymers. *Appl Microbiol Biotechnol,* 91**,** 655-65.

Shishatskaya, E. I., Nikolaeva, E. D., Vinogradova, O. N. & Volova, T. G. 2016. - Experimental wound dressings of degradable PHA for skin defect repair. - 27.

Sid, S., Mor, R. S., Kishore, A. & Sharanagat, V. S. 2021. Bio-sourced polymers as alternatives to conventional food packaging materials: A review. *Trends in Food Science & Technology,* 115**,** 87-104.

Sim, S. J., Snell, K. D., Hogan, S. A., Stubbe, J., Rha, C. K. & Sinskey, A. J. 1997. PHA synthase activity controls the molecular weight and polydispersity of polyhydroxybutyrate in vivo. *Nature Biotechnology,* 15**,** 63-67.

Sindhu, R., Madhavan, A., Arun, K. B., Pugazhendhi, A., Reshmy, R., Awasthi, M. K., Sirohi, R., Tarafdar, A., Pandey, A. & Binod, P. 2021. Metabolic circuits and gene regulators in polyhydroxyalkanoate producing organisms: Intervention strategies for enhanced production. *Bioresource Technology,* 327**,** 124791.

Singh, A. K. & Mallick, N. 2009. Exploitation of inexpensive substrates for production of a novel SCL–LCL-PHA co-polymer by Pseudomonas aeruginosa MTCC 7925. *Journal of Industrial Microbiology and Biotechnology,* 36**,** 347-354.

Singh, M., Kumar, P., Ray, S. & Kalia, V. C. 2015. Challenges and Opportunities for Customizing Polyhydroxyalkanoates. *Indian Journal of Microbiology,* 55**,** 235-249.

Song, J. H., Jeon, C. O., Choi, M. H., Yoon, S. C. & Park, W. 2008. Polyhydroxyalkanoate (PHA) production using waste vegetable oil by Pseudomonas sp strain DR2. *Journal of Microbiology and Biotechnology,* 18**,** 1408-1415.

Sudesh, K., Abe, H. & Doi, Y. 2000. Synthesis, structure and properties of polyhydroxyalkanoates: biological polyesters. *Progress in Polymer Science,* 25**,** 1503-1555.

Sudo, M., Hori, C., Ooi, T., Mizuno, S., Tsuge, T. & Matsumoto, K. i. 2020. Synergy of valine and threonine supplementation on poly(2-hydroxybutyrate-block-3-hydroxybutyrate) synthesis in engineered

Escherichia coli expressing chimeric polyhydroxyalkanoate synthase. *Journal of Bioscience and Bioengineering,* 129**,** 302-306.

Tajima, K., Igari, T., Nishimura, D., Nakamura, M., Satoh, Y. & Munekata, M. 2003. Isolation and characterization of Bacillus sp INT005 accumulating polyhydroxyalkanoate (PHA) from gas field soil. *JOURNAL OF BIOSCIENCE AND BIOENGINEERING,* 95**,** 77-81.

Tajparast, M. & Frigon, D. 2018. Predicting the accumulation of storage compounds by *Rhodococcus* jostii RHA1 in the feast-famine growth cycles using genome-scale flux balance analysis. *PLoS One,* 13**,** e0191835.

Takagi, Y., Yasuda, R., Yamaoka, M. & Yamane, T. 2004. Morphologies and mechanical properties of polylactide blends with medium chain length poly(3-hydroxyalkanoate) and chemically modified poly(3-hydroxyalkanoate). *Journal of Applied Polymer Science,* 93**,** 2363-2369.

Takase, K., Matsumoto, K., Taguchi, S. & Doi, Y. 2004. Alteration of substrate chain-length specificity of type II synthase for polyhydroxyalkanoate biosynthesis by in vitro evolution: in vivo and in vitro enzyme assays. *Biomacromolecules,* 5**,** 480-485.

Tan, G.-Y. A., Chen, C.-L., Li, L., Ge, L., Wang, L., Razaad, I. M., Li, Y., Zhao, L., Mo, Y. & Wang, J.-Y. 2014. Start a Research on Biopolymer Polyhydroxyalkanoate (PHA): A Review. *Polymers* [Online], 6.

Tao, W., Lv, L. & Chen, G.-Q. 2017. Engineering Halomonas species TD01 for enhanced polyhydroxyalkanoates synthesis via CRISPRi. *Microbial Cell Factories,* 16**,** 48.

Tee, K. L., Grinham, J., Othusitse, A. M., González-Villanueva, M., Johnson, A. O. & Wong, T. S. 2017. An Efficient Transformation Method for the Bioplastic-Producing "Knallgas" Bacterium Ralstonia eutropha H16. *Biotechnology Journal,* 12**,** 1700081.

Teresa Cesario, M., Raposo, R. S., de Almeida, M. C. M. D., van Keulen, F., Ferreira, B. S. & da Fonseca, M. M. R. 2014. - Enhanced bioproduction of poly-3-hydroxybutyrate from wheat straw lignocellulosic hydrolysates. - 31**,** - 113.

Tsuge, T., Fukui, T., Matsusaki, H., Taguchi, S., Kobayashi, G., Ishizaki, A. & Doi, Y. 2000. Molecular cloning of two (R)-specific enoyl-CoA hydratase genes from Pseudomonas aeruginosa and their use for polyhydroxyalkanoate synthesis. *FEMS Microbiology Letters,* 184**,** 193-198.

Tsuge, T., Saito, Y., Narike, M., Muneta, K., Normi, Y. M., Kikkawa, Y., Hiraishi, T. & Doi, Y. 2004. Mutation effects of a conserved alanine (Ala510) in type I polyhydroxyalkanoate synthase from Ralstonia eutropha on polyester biosynthesis. *Macromol Biosci,* 4**,** 963-70.

Tsuge, T., Yamamoto, T., Yano, K., Abe, H., Doi, Y. & Taguchi, S. 2009. Evaluating the Ability of Polyhydroxyalkanoate Synthase Mutants to Produce P(3HB-co-3HA) from Soybean Oil. *Macromolecular Bioscience,* 9**,** 71-78.

Van-Thuoc, D., Quillaguaman, J., Mamo, G. & Mattiasson, B. 2008. - Utilization of agricultural residues for poly(3-hydroxybutyrate) production by Halomonas boliviensis LC1. - 104**,** - 428.

Vicente, D., Proença, D. & Morais, P. 2023. The Role of Bacterial Polyhydroalkanoate (PHA) in a Sustainable Future: A Review on the Biological Diversity. *International Journal of Environmental Research and Public Health,* 20**,** 2959.

Vidra, A., Toth, A. J. & Nemeth, A. 2017. Lactic acid production from cane molasses. *Liquid Waste Recovery,* 2**,** 13-16.

Volova, T., Shishatskaya, E., Sevastianov, V., Efremov, S. & Mogilnaya, O. 2003. - Results of biomedical investigations of PHB and PHB/PHV fibers. - 16**,** - 133.

Wallen, L. L. 1973. POLY-BETA-HYDROXYALKANOATE FROM ACTIVATED-SLUDGE. *Abstracts of Papers of the American Chemical Society***,** 5-5.

Wang, H. H., Li, X. T. & Chen, G. Q. 2009. Production and characterization of homopolymer polyhydroxyheptanoate (P3HHp) by a fadBA knockout mutant *Pseudomonas putida* KTOY06 derived from *P. putida* KT2442. *Process Biochemistry,* 44**,** 106-111.

Wang, H. H., Zhou, X. R., Liu, Q. A. & Chen, G. Q. 2011. Biosynthesis of polyhydroxyalkanoate homopolymers by *Pseudomonas putida*. *Applied Microbiology and Biotechnology,* 89**,** 1497-1507.

Wang, J., Liu, S., Huang, J., Cui, R., Xu, Y. & Song, Z. 2023. Genetic engineering strategies for sustainable polyhydroxyalkanoate (PHA) production from carbon-rich wastes. *Environmental Technology & Innovation,* 30**,** 103069.

Wang, Q. & Nomura, C. T. 2010. Monitoring differences in gene expression levels and polyhydroxyalkanoate (PHA) production in *Pseudomonas putida* KT2440 grown on different carbon sources. *Journal of Bioscience and Bioengineering,* 110**,** 653-659.

Wang, Q., Tappel, R. C., Zhu, C. & Nomura, C. T. 2012. Development of a new strategy for production of medium-chain-length polyhydroxyalkanoates by recombinant Escherichia coli via inexpensive non-fatty acid feedstocks. *Appl Environ Microbiol,* 78**,** 519-27.

Wang, X., Lin, L., Dong, J., Ling, J., Wang, W., Wang, H., Zhang, Z. & Yu, X. 2018. Simultaneous improvements of Pseudomonas cell growth and polyhydroxyalkanoate production from a lignin derivative for lignin-consolidated bioprocessing. *Appl Environ Microbiol,* 84.

Wang, Y., Wu, H., Jiang, X. R. & Chen, G. Q. 2014. Engineering Escherichia coli for enhanced production of poly(3-hydroxybutyrate-co-4-hydroxybutyrate) in larger cellular space. *Metabolic Engineering,* 25**,** 183-193.

Ward, P. G. & O'Connor, K. E. 2005. Bacterial synthesis of polyhydroxyalkanoates containing aromatic and aliphatic monomers by *Pseudomonas putida* CA-3. *Int J Biol Macromol,* 35**,** 127-33.

Weimer, A., Kohlstedt, M., Volke, D. C., Nikel, P. I. & Wittmann, C. 2020. Industrial biotechnology of *Pseudomonas putida*: advances and prospects. *Applied Microbiology and Biotechnology,* 104**,** 7745-7766.

Williams, S. F. & Martin, D. P. 2005. Applications of Polyhydroxyalkanoates (PHA) in Medicine and Pharmacy. *Biopolymers Online*.

Wu, C.-S. 2008. Controlled release evaluation of bacterial fertilizer using polymer composites as matrix. *Journal of Controlled Release,* 132**,** 42-48.

Xu, N., Wei, L. & Liu, J. 2019. Recent advances in the applications of promoter engineering for the optimization of metabolite biosynthesis. *World Journal of Microbiology and Biotechnology,* 35**,** 33.

Yan, S., Tyagi, R. D. & Surampalli, R. Y. 2006. - Polyhydroxyalkanoates (PHA) production using wastewater as carbon source and activated sludge as microorganisms. - 53**,** - 180.

Yang, T. H., Kim, T. W., Kang, H. O., Lee, S.-H., Lee, E. J., Lim, S.-C., Oh, S. O., Song, A.-J., Park, S. J. & Lee, S. Y. 2010. Biosynthesis of Polylactic Acid and Its Copolymers Using Evolved Propionate CoA Transferase and PHA Synthase. *BIOTECHNOLOGY AND BIOENGINEERING,* 105**,** 150-160.

Yao, J., Zhang, G., Wu, Q., Chen, G. Q. & Zhang, R. Q. 1999. - Production of polyhydroxyalkanoates by Pseudomonas nitroreducens. - 75**,** - 349.

Zhang, H.-F., Ma, L., Wang, Z.-H. & Chen, G.-Q. 2009. Biosynthesis and Characterization of 3-Hydroxyalkanoate Terpolyesters With Adjustable Properties by Aeromonas hydrophila. *BIOTECHNOLOGY AND BIOENGINEERING,* 104**,** 582-589.

Zhang, J., Jin, B., Fu, J., Wang, Z. & Chen, T. 2022. Adaptive Laboratory Evolution of Halomonas

bluephagenesis Enhances Acetate Tolerance and Utilization to Produce Poly(3-hydroxybutyrate). *Molecules* [Online], 27.

Zhang, L., Deng, X. & Huang, Z. 1997. Miscibility, thermal behaviour and morphological structure of poly(3-hydroxybutyrate) and ethyl cellulose binary blends. *Polymer,* 38**,** 5379-5387.

Zhang, Y., Liu, H., Liu, Y., Huo, K., Wang, S., Liu, R. & Yang, C. 2021. A promoter engineering-based strategy enhances polyhydroxyalkanoate production in *Pseudomonas putida* KT2440. *International Journal of Biological Macromolecules,* 191**,** 608-617.

Zhao, F., Gong, T., Liu, X., Fan, X., Huang, R., Ma, T., Wang, S., Gao, W. & Yang, C. 2019a. Morphology engineering for enhanced production of medium-chain-length polyhydroxyalkanoates in Pseudomonas mendocina NK-01. *Applied Microbiology and Biotechnology,* 103**,** 1713-1724.

Zhao, F., Liu, X., Kong, A., Zhao, Y., Fan, X., Ma, T., Gao, W., Wang, S. & Yang, C. 2019b. Screening of endogenous strong promoters for enhanced production of medium-chain-length polyhydroxyalkanoates in Pseudomonas mendocina NK-01. *Scientific Reports,* 9**,** 1798.

Zhao, L., Sun, G., Zhai, M., Zhao, S., Ye, B. & Qu, J. 2025. Biorefinery of sugarcane molasses for poly(3-hydroxybutyrate) fermentation and genomic elucidation of metabolic mechanism using Paracoccus sp. P2. *International Journal of Biological Macromolecules,* 303**,** 140684.

Zhao, W. & Chen, G.-Q. 2007. Production and characterization of terpolyester poly (3-hydroxybutyrate-co-3-hydroxyvalerate-co-3-hydroxyhexanoate) by recombinant Aeromonas hydrophila 4AK4 harboring genes phaAB. *PROCESS BIOCHEMISTRY,* 42**,** 1342-1347.

Zheng, Y., Yuan, Q., Yang, X. & Ma, H. 2017. Engineering Escherichia coli for poly-(3-hydroxybutyrate) production guided by genome-scale metabolic network analysis. *Enzyme and Microbial Technology,* 106**,** 60-66.

Zher Neoh, S., Fey Chek, M., Tiang Tan, H., Linares-Pastén, J. A., Nandakumar, A., Hakoshima, T. & Sudesh, K. 2022. Polyhydroxyalkanoate synthase (PhaC): The key enzyme for biopolyester synthesis. *Current Research in Biotechnology,* 4**,** 87-101.

Zhou, J., Peng, S.-W., Wang, Y.-Y., Zheng, S.-B., Wang, Y. & Chen, G.-Q. 2010. The use of poly(3-hydroxybutyrate-co-3-hydroxyhexanoate) scaffolds for tarsal repair in eyelid reconstruction in the rat. *Biomaterials,* 31**,** 7512-7518.

Appendix

Table S1: Titer and composition of PHA from *P. putida*. Analysis was performed using lyophilised cells. [n.d. = not detected]

Time (h)	Monomer composition (mol%)					CDW (g/L)	PHA content (wt% CDW)	PHA titer (g/L)	mcl PHA titer (g/L)
	C4	C6	C8	C10	C12				
12	n.d.	n.d.	12.6 ± 0.2	76.4 ± 0.6	11.0 ± 0.7	1.33 ± 0.1	9.2 ± 0.46	0.123 ± 0.013	0.123 ± 0.013
16	n.d.	n.d.	12.5 ± 0.2	76.2 ± 0.3	11.2 ± 0.2	1.32 ± 0.1	12.0 ± 0.54	0.160 ± 0.010	0.160 ± 0.010
20	n.d.	n.d.	13.2 ± 0.4	75.8 ± 0.4	11.0 ± 0.8	1.28 ± 0.1	12.8 ± 0.23	0.163 ± 0.003	0.163 ± 0.003
24	n.d.	n.d.	11.8 ± 1.4	78.6 ± 2.3	9.6 ± 1.2	1.28 ± 0.1	15.2 ± 1.33	0.193 ± 0.009	0.193 ± 0.009
48	n.d.	n.d.	13.0 ± 0.4	77.2 ± 0.9	9.9 ± 0.9	1.26 ± 0.0	12.3 ± 0.88	0.157 ± 0.013	0.157 ± 0.013

Table S2: Titer and composition of PHA from *P. putida* with plasmid PphaC1k-phaCAB. Analysis was performed using lyophilised cells. [n.d. = not detected]

Time (h)	Monomer composition (mol%)					CDW (g/L)	PHA content (wt% CDW)	PHA titer (g/L)	mcl PHA titer (g/L)
	C4	C6	C8	C10	C12				
12	89.7 ± 0.9	n.d.	1.2 ± 0.1	7.6 ± 0.7	1.5 ± 0.1	1.40 ± 0.03	15.3 ± 0.9	0.213 ± 0.015	0.039 ± 0.003
16	90.1 ± 1.0	n.d.	1.4 ± 0.1	7.1 ± 0.8	1.4 ± 0.1	1.82 ± 0.02	24.0 ± 0.9	0.433 ± 0.018	0.077 ± 0.009
20	92.8 ± 0.9	n.d.	1.3 ± 0.1	5.0 ± 0.7	0.9 ± 0.1	2.13 ± 0.04	31.1 ± 0.8	0.667 ± 0.015	0.088 ± 0.008
24	92.6 ± 0.9	n.d.	1.5 ± 0.2	5.0 ± 0.6	0.9 ± 0.1	2.38 ± 0.05	38.0 ± 3.0	0.907 ± 0.088	0.119 ± 0.005
48	93.0 ± 0.8	0.1 ± 0.1	2.2 ± 0.2	4.0 ± 0.5	0.7 ± 0.0	2.77 ± 0.14	48.2 ± 2.2	1.340 ± 0.118	0.165 ± 0.011

Table S3: Titer and composition of PHA for *P. putida* with plasmid pPS85-phaCAB and no inducer. Analysis was performed using lyophilised cells. [n.d. = not detected]

Time (h)	Monomer composition (mol%)					CDW (g/L)	PHA content (wt% CDW)	PHA titer (g/L)	mcl PHA titer (g/L)
	C4	C6	C8	C10	C12				
12	28.3 ± 2.6	n.d.	10.2 ± 0.2	53.1 ± 2.7	8.5 ± 0.1	1.21 ± 0.08	8.5 ± 0.8	0.107 ± 0.012	0.089 ± 0.010
16	38.6 ± 0.9	n.d.	8.6 ± 0.5	45.7 ± 1.0	7.1 ± 0.1	1.27 ± 0.08	9.8 ± 0.4	0.123 ± 0.009	0.094 ± 0.008
20	41.4 ± 1.4	n.d.	8.8 ± 0.7	43.3 ± 1.1	6.5 ± 0.2	1.26 ± 0.09	10.8 ± 0.4	0.137 ± 0.015	0.101 ± 0.012
24	41.5 ± 1.7	n.d.	8.5 ± 0.5	43.5 ± 1.5	6.5 ± 0.5	1.23 ± 0.10	11.4 ± 0.9	0.143 ± 0.022	0.106 ± 0.018
48	41.2 ± 1.7	n.d.	8.9 ± 0.6	43.2 ± 1.1	6.7 ± 0.3	1.19 ± 0.04	11.7 ± 0.5	0.140 ± 0.010	0.103 ± 0.008

Table S4: Titer and composition of PHA for *P. putida* with plasmid pPS85-phaCAB induced with 0.4%(w/v) arabinose. Analysis was performed using lyophilised cells. [n.d. = not detected]

Time (h)	Monomer composition (mol%)					CDW (g/L)	PHA content (wt% CDW)	PHA titer (g/L)	mcl-PHA titer (g/L)
	C4	C6	C8	C10	C12				
12	99.1 ± 0.1	n.d.	n.d.	0.7 ± 0.0	0.2 ± 0.1	1.21 ± 0.03	20.4 ± 1.6	0.250 ± 0.025	0.005 ± 0.001
16	99.4 ± 0.0	n.d.	n.d.	0.5 ± 0.0	0.1 ± 0.1	1.59 ± 0.02	26.7 ± 1.0	0.427 ± 0.020	0.006 ± 0.001
20	99.5 ± 0.1	n.d.	n.d.	0.5 ± 0.0	0.1 ± 0.1	1.89 ± 0.04	34.3 ± 2.5	0.650 ± 0.056	0.007 ± 0.002
24	99.5 ± 0.1	n.d.	0.1 ± 0.1	0.4 ± 0.0	0.1 ± 0.1	2.21 ± 0.09	44.1 ± 4.3	0.983 ± 0.131	0.010 ± 0.002
48	99.6 ± 0.1	n.d.	0.2 ± 0.1	0.2 ± 0.0	0.0 ± 0.0	2.83 ± 0.10	52.2 ± 4.3	1.483 ± 0.152	0.012 ± 0.004

Table S5: Titer and composition of PHA for *P. putida* with plasmid pPS87-phaCAB and no inducer. Analysis was performed using lyophilised cells. [n.d. = not detected]

Time (h)	Monomer composition (mol%)					CDW (g/L)	PHA content (wt% CDW)	PHA titer (g/L)	mcl-PHA titer (g/L)
	C4	C6	C8	C10	C12				
12	17.9 ± 1.5	n.d.	11.0 ± 0.9	61.4 ± 1.5	9.7 ± 0.4	1.16 ± 0.09	6.0 ± 1.1	0.073 ± 0.018	0.066 ± 0.016
16	18.1 ± 0.8	n.d.	12.3 ± 0.6	61.1 ± 0.6	8.5 ± 0.5	1.25 ± 0.03	8.0 ± 0.3	0.100 ± 0.006	0.090 ± 0.005
20	19.4 ± 1.1	n.d.	11.7 ± 0.9	60.7 ± 0.8	8.2 ± 0.3	1.20 ± 0.05	7.4 ± 0.1	0.087 ± 0.007	0.077 ± 0.006
24	20.5 ± 1.4	n.d.	11.8 ± 0.8	59.7 ± 1.0	8.1 ± 0.4	1.20 ± 0.04	7.6 ± 0.3	0.093 ± 0.007	0.082 ± 0.005
48	20.6 ± 1.2	n.d.	11.8 ± 0.7	59.8 ± 0.5	7.8 ± 0.0	1.17 ± 0.07	7.2 ± 0.7	0.083 ± 0.009	0.074 ± 0.008

Table S6: Titer and composition of PHA for *P. putida* with plasmid pPS87-phaCAB induced with 10 mM rhamnose. Analysis was performed using lyophilised cells. [n.d. = not detected]

Time (h)	Monomer composition (mol%)					CDW (g/L)	PHA content (wt% CDW)	PHA titer (g/L)	mcl-PHA titer (g/L)
	C4	C6	C8	C10	C12				
12	97.0 ± 1.0	n.d.	n.d.	2.5 ± 0.7	0.5 ± 0.5	0.35 ± 0.06	6.7 ± 1.2	0.023 ± 0.003	0.001 ± 0.001
16	98.8 ± 0.1	n.d.	n.d.	1.2 ± 0.1	n.d.	0.70 ± 0.11	12.4 ± 0.1	0.087 ± 0.013	0.002 ± 0.001
20	99.0 ± 0.3	n.d.	n.d.	0.9 ± 0.2	0.1 ± 0.1	1.06 ± 0.22	18.7 ± 1.0	0.200 ± 0.045	0.004 ± 0.002
24	98.0 ± 1.5	n.d.	0.2 ± 0.2	1.7 ± 1.1	0.1 ± 0.1	1.50 ± 0.16	26.8 ± 1.4	0.407 ± 0.064	0.017 ± 0.013
48	96.1 ± 1.9	n.d.	0.8 ± 0.3	2.8 ± 1.3	0.3 ± 0.3	2.31 ± 0.04	45.3 ± 2.7	1.043 ± 0.054	0.075 ± 0.037

Table S7: Titer and composition of PHA from *C. necator* and *P. putida* engineered with PrhaB-phaCAB plasmid. Strains were cultivated 72 hours in either PPH + H2O or PPH + MSM medium. [n.d. = not detected]

Strains	**Medium**	**CDW (g/L)**	**PHA content (wt% CDW)**	**PHA titer (g/L)**	**Monomer composition (mol%)**			
					C4	**C8**	**C10**	**C12**
C. necator	PPH+H_2O	2.86 ± 0.13	18.45 ± 2.21	0.53 ± 0.06	100	n.d.	n.d.	n.d.
C. necator	PPH+MSM	3.75 ± 0.19	10.88 ± 0.61	0.41 ± 0.03	100	n.d.	n.d.	n.d.
PrhaB-phaCAB *P. putida*	PPH+H_2O	4.03 ± 0.08	21.83 ± 0.28	0.88 ± 0.03	85.80 ± 0.42	1.91 ± 0.03	10.15 ± 0.35	2.14 ± 0.13
PrhaB-phaCAB *P. putida*	PPH+MSM	4.46 ± 0.08	12.32 ± 0.51	0.55 ± 0.01	95.68 ± 0.25	n.d.	3.83 ± 0.12	0.49 ± 0.27

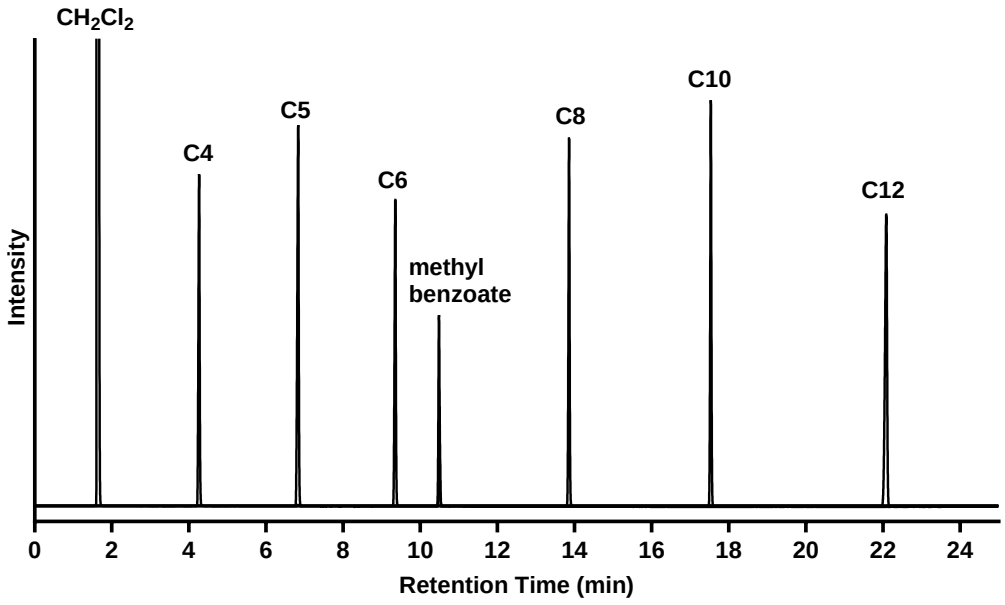

Figure S1. GC chromatograms of 3-hydroxyalkanoate methyl ester standards. Individual chromatograms of 3-hydroxyalkanoate methyl esters used for peak identification in PHA analysis. Standards include 3-hydroxybutyrate (C4), 3-hydroxyvalerate (C5), 3-hydroxyhexanoate (C6), 3-hydroxyoctanoate (C8), 3-hydroxydecanoate (C10), and 3-hydroxydodecanoate (C12). The resulting chromatograms were overlaid for comparison. Peak labels indicate the corresponding monomer identities. Typical retention times under the described GC conditions were approximately: C4 = 4.2 min, C5 = 6.8 min, C6 = 9.3 min, C8 = 13.8 min, C10 = 17.5 min, and C12 = 22.0 min.

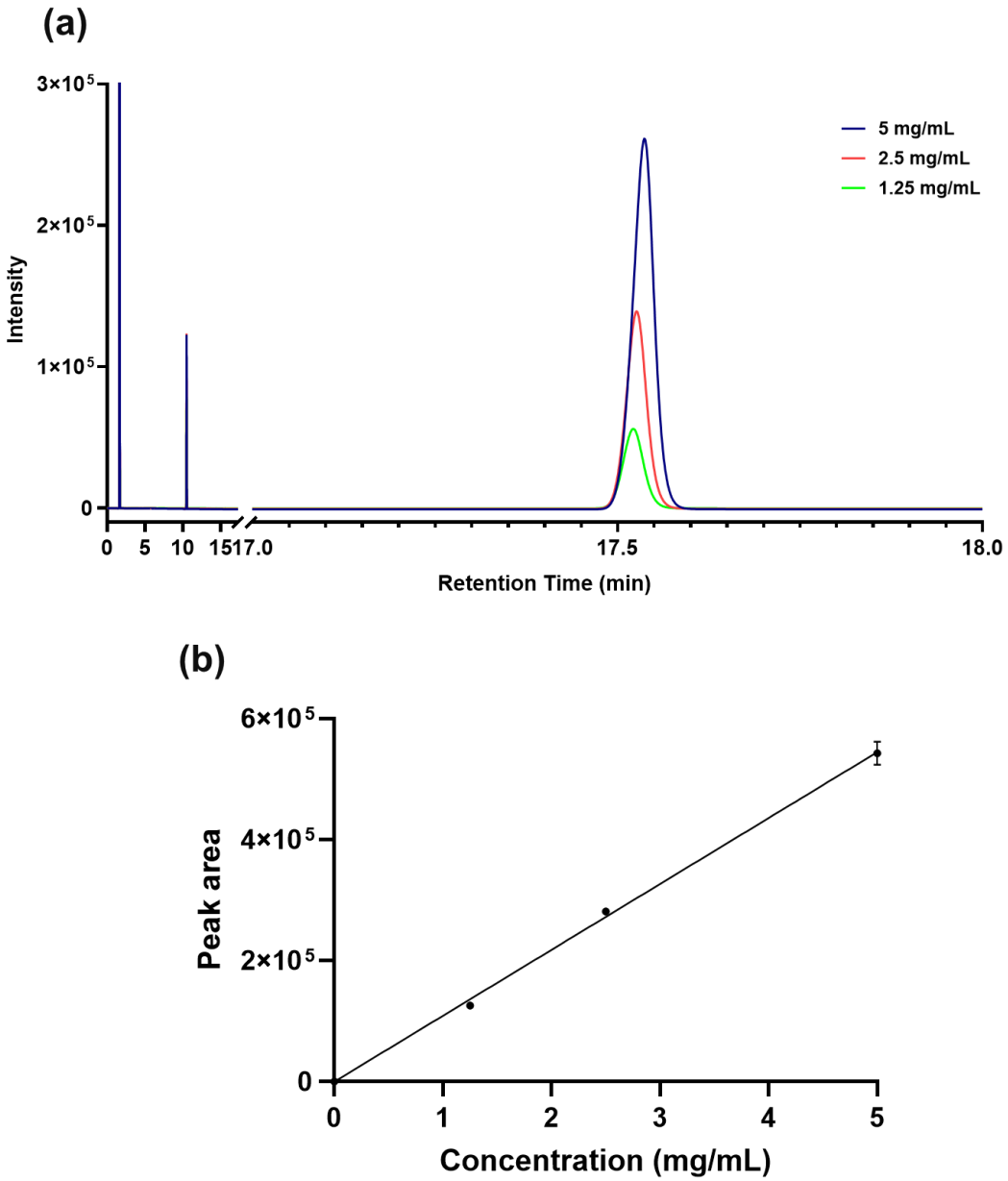

Figure S2. GC-based calibration of 3-hydroxydecanoate (C10) and summary of monomer calibration equations. (a) GC chromatograms of 3-hydroxydecanoate (C10) methyl ester at three concentrations (1.25, 2.5, and 5.0 mg/mL), showing increased peak areas with increasing concentration. (b) Calibration curve generated by plotting peak area versus concentration, fitted by linear regression. The resulting equation was Y = 108940X (R^2 = 0.998), where Y is peak area and X is concentration in mg/mL.

Calibration equations for other monomers (C4–C12) are listed below:
C4 (3HB): Y = 98187X (R^2 = 0.999)

C5 (3HV): Y = 132083X (R^2 = 0.995)
C6 (3HHx): Y = 14475X (R^2 = 0.998)
C8 (3HO): Y = 101730X (R^2 = 0.999)
C10 (3HD): Y = 108940X (R^2 = 0.998)
C12 (3HDD): Y = 145171X (R^2 = 0.999)

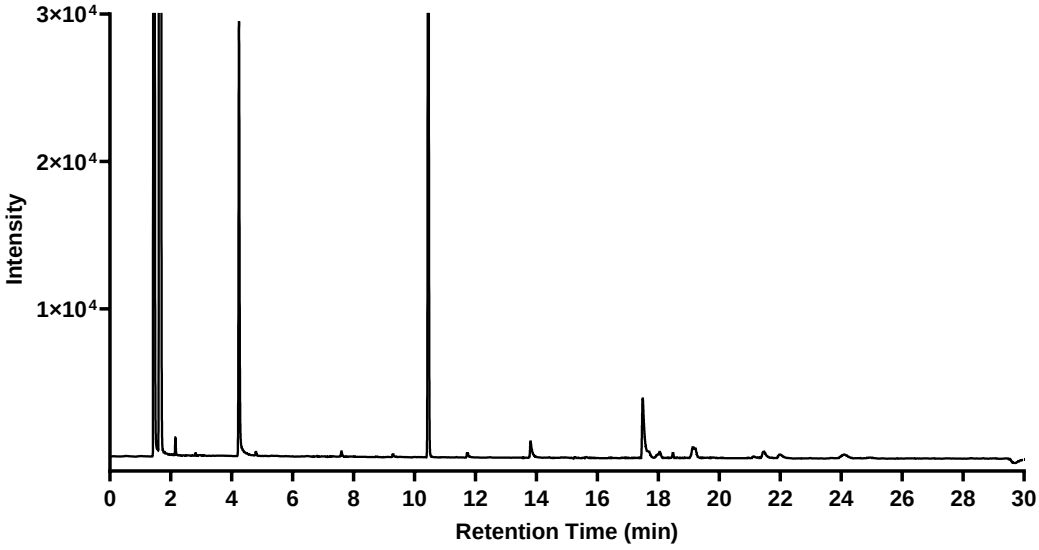

Figure S3. Representative GC chromatogram of a PHA blend sample derived from lyophilized *P. putida* cells harboring plasmid Pc1K-CAB after 24 hours of cultivation. The sample was subjected to methanolysis prior to analysis. Monomer peaks were identified based on retention time comparison with authentic standards, and their relative amounts were calculated from peak areas using the established calibration curves above. The resulting composition reflects the distribution of 3-hydroxyalkanoate monomers present in the PHA synthesized by the engineered strain.

(a)

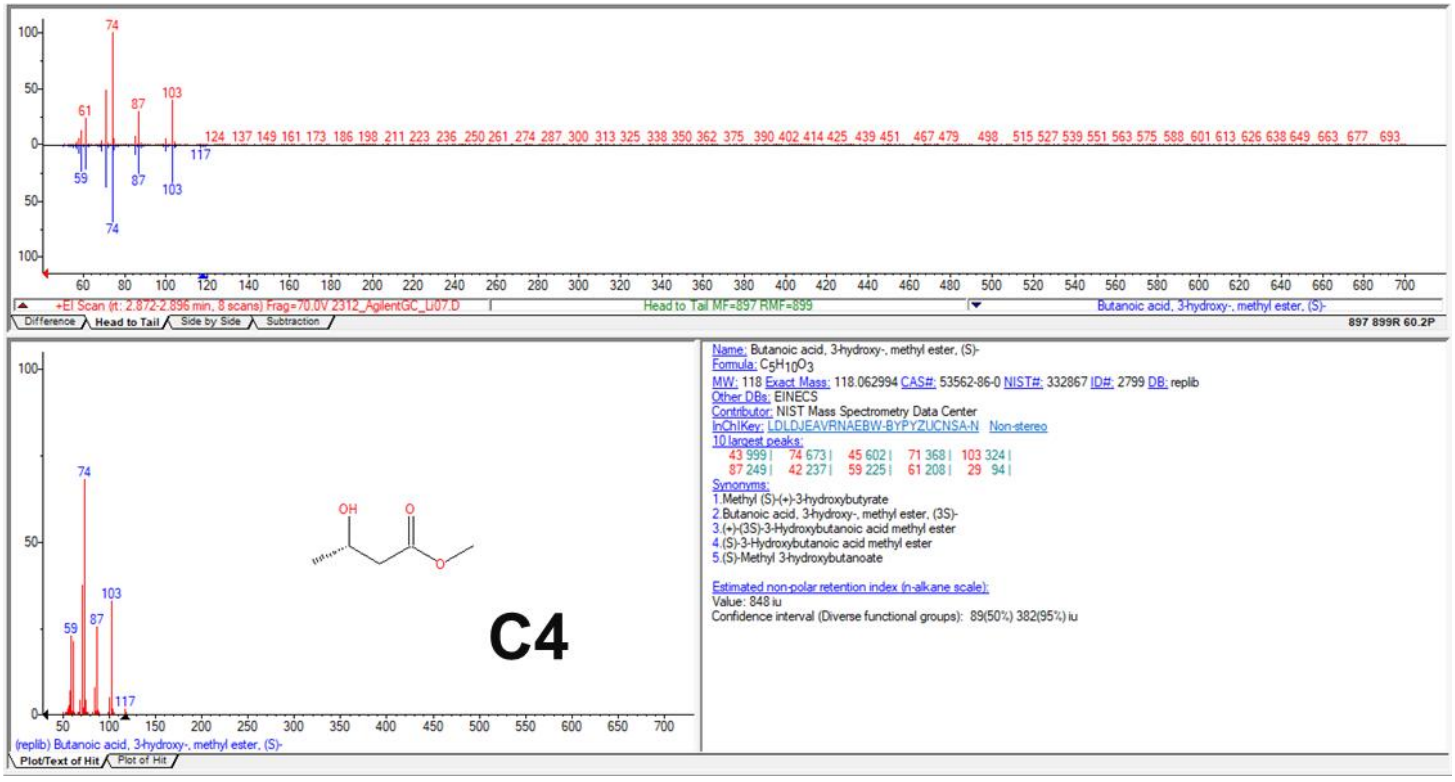
+EI Scan (rt: 2.872-2.896 min, 8 scans) Frag=70.0V 2312_AgilentGC_Li07.D
Head to Tail MF=897 RMF=899
Butanoic acid, 3-hydroxy-, methyl ester, (S)-
Difference
Head to Tail
Side by Side
Subtraction
897 899R 60.2P
C4
(replib) Butanoic acid, 3-hydroxy-, methyl ester, (S)-
Plot/Text of Hit
Plot of Hit
Name: Butanoic acid, 3-hydroxy-, methyl ester, (S)-
Formula: C5H10O3
MW: 118 Exact Mass: 118.062994 CAS#: 53562-86-0 NIST#: 332867 ID#: 2799 DB: replib
Other DBs: EINECS
Contributor: NIST Mass Spectrometry Data Center
InChIKey: LDLDJEAVRNAEBW-BYPYZUCNSA-N Non-stereo
10 largest peaks:
43 999 | 74 673 | 45 602 | 71 368 | 103 324 |
87 249 | 42 237 | 59 225 | 61 208 | 29 94 |
Synonyms:
1.Methyl (S)-(+)-3-hydroxybutyrate
2.Butanoic acid, 3-hydroxy-, methyl ester, (3S)-
3.(+)-(3S)-3-Hydroxybutanoic acid methyl ester
4.(S)-3-Hydroxybutanoic acid methyl ester
5.(S)-Methyl 3-hydroxybutanoate
Estimated non-polar retention index (n-alkane scale):
Value: 848 iu
Confidence interval (Diverse functional groups): 89(50%) 382(95%) iu

(b)

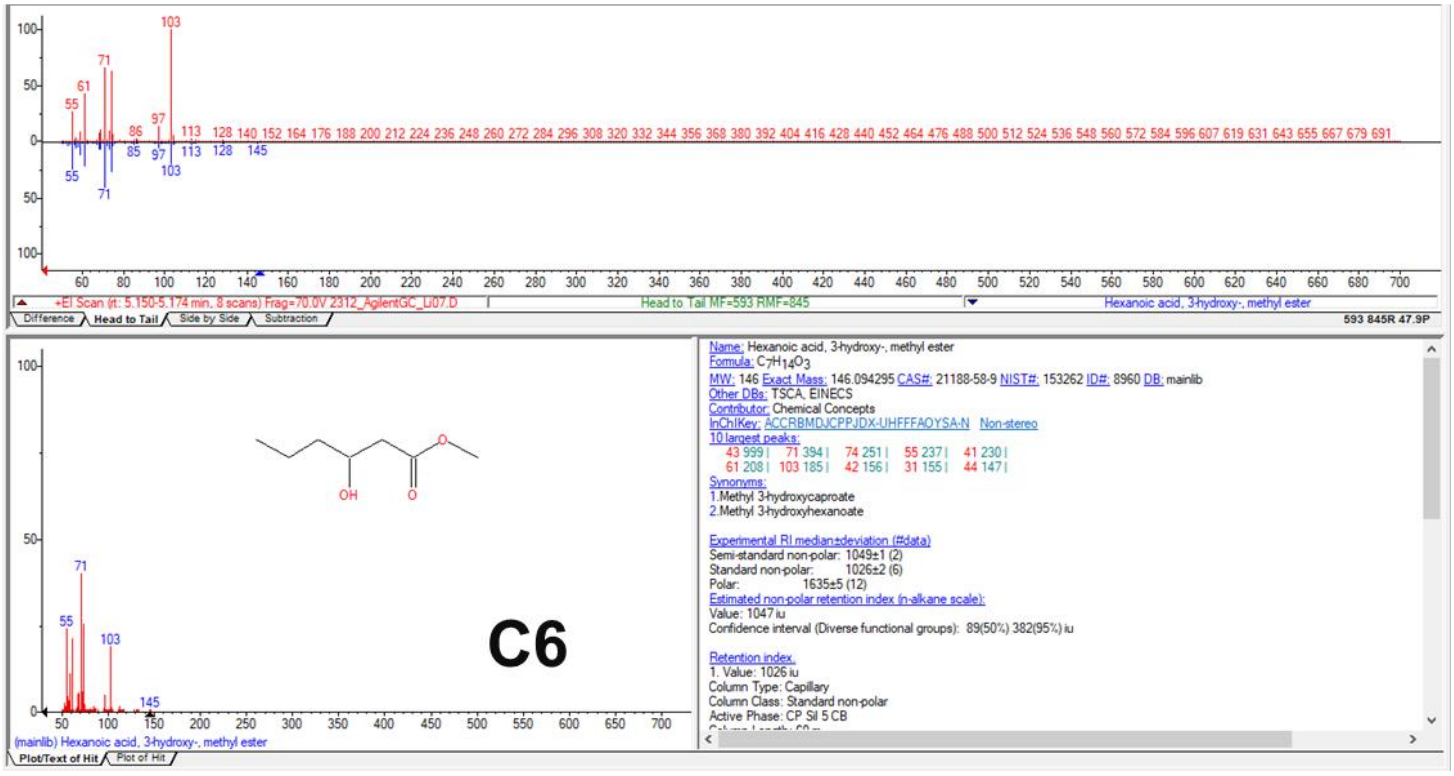
+EI Scan (rt: 5.150-5.174 min, 8 scans) Frag=70.0V 2312_AgilentGC_Li07.D
Head to Tail MF=593 RMF=845
Hexanoic acid, 3-hydroxy-, methyl ester
Difference
Head to Tail
Side by Side
Subtraction
593 845R 47.9P
C6
(mainlib) Hexanoic acid, 3-hydroxy-, methyl ester
Plot/Text of Hit
Plot of Hit
Name: Hexanoic acid, 3-hydroxy-, methyl ester
Formula: C7H14O3
MW: 146 Exact Mass: 146.094295 CAS#: 21188-58-9 NIST#: 153262 ID#: 8960 DB: mainlib
Other DBs: TSCA, EINECS
Contributor: Chemical Concepts
InChIKey: ACCRBMDJCPPJDX-UHFFFAOYSA-N Non-stereo
10 largest peaks:
43 999 | 71 394 | 74 251 | 55 237 | 41 230 |
61 208 | 103 185 | 42 156 | 31 155 | 44 147 |
Synonyms:
1.Methyl 3-hydroxycaproate
2.Methyl 3-hydroxyhexanoate
Experimental RI median±deviation (#data)
Semi-standard non-polar: 1049±1 (2)
Standard non-polar: 1026±2 (6)
Polar: 1635±5 (12)
Estimated non-polar retention index (n-alkane scale):
Value: 1047 iu
Confidence interval (Diverse functional groups): 89(50%) 382(95%) iu
Retention index
1. Value: 1026 iu
Column Type: Capillary
Column Class: Standard non-polar
Active Phase: CP Sil 5 CB

(c)

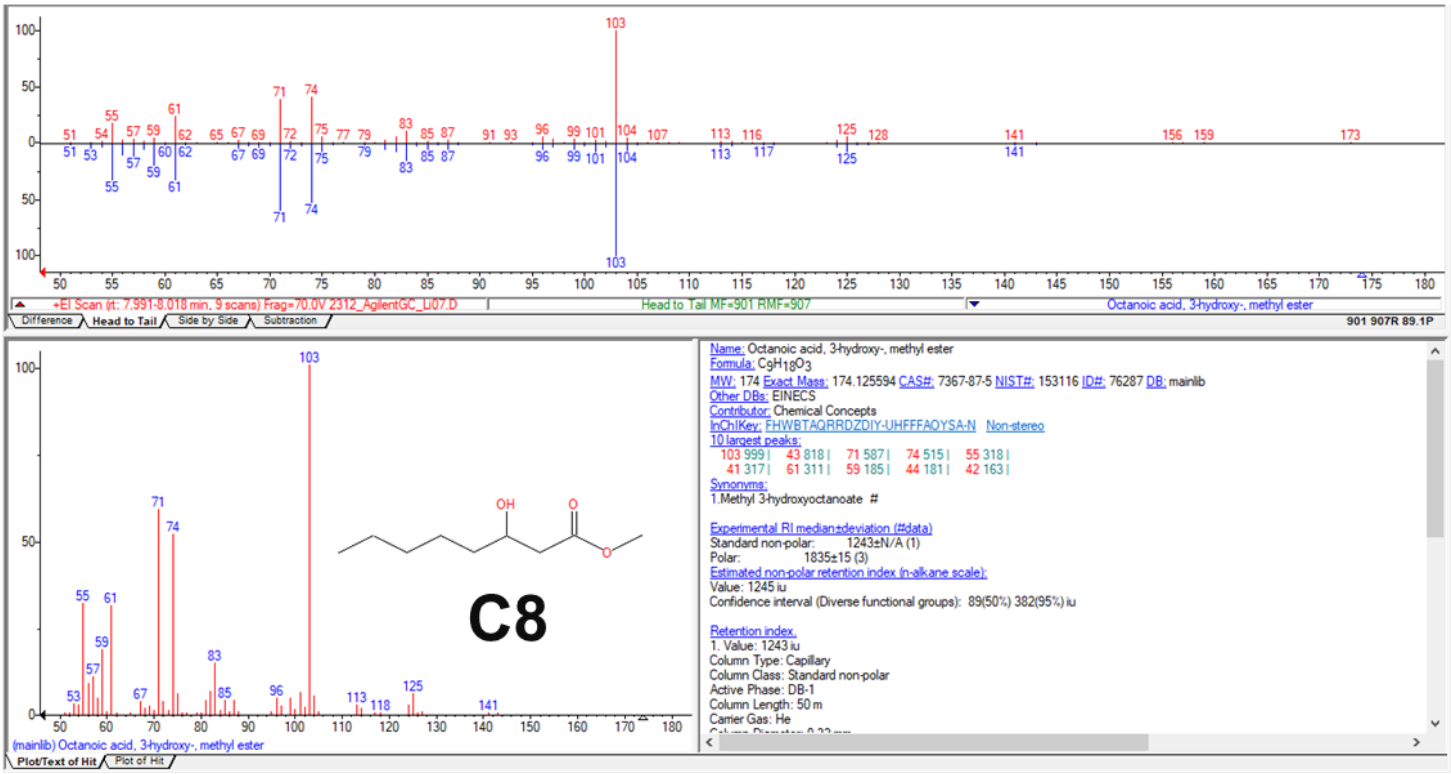
+EI Scan (rt: 7.991-8.018 min, 9 scans) Frag=70.0V 2312_AgilentGC_Li07.D
Head to Tail MF=901 RMF=907
Octanoic acid, 3-hydroxy-, methyl ester
Difference
Head to Tail
Side by Side
Subtraction
901 907R 89.1P
C8
(mainlib) Octanoic acid, 3-hydroxy-, methyl ester
Plot/Text of Hit
Plot of Hit
Name: Octanoic acid, 3-hydroxy-, methyl ester
Formula: C9H18O3
MW: 174 Exact Mass: 174.125594 CAS#: 7367-87-5 NIST#: 153116 ID#: 76287 DB: mainlib
Other DBs: EINECS
Contributor: Chemical Concepts
InChIKey: FHWBTAQRRDZDIY-UHFFFAOYSA-N Non-stereo
10 largest peaks:
103 999 | 43 818 | 71 587 | 74 515 | 55 318 |
41 317 | 61 311 | 59 185 | 44 181 | 42 163 |
Synonyms:
1.Methyl 3-hydroxyoctanoate #
Experimental RI median±deviation (#data)
Standard non-polar: 1243±N/A (1)
Polar: 1835±15 (3)
Estimated non-polar retention index (n-alkane scale):
Value: 1245 iu
Confidence interval (Diverse functional groups): 89(50%) 382(95%) iu
Retention index
1. Value: 1243 iu
Column Type: Capillary
Column Class: Standard non-polar
Active Phase: DB-1
Column Length: 50 m
Carrier Gas: He

(d)

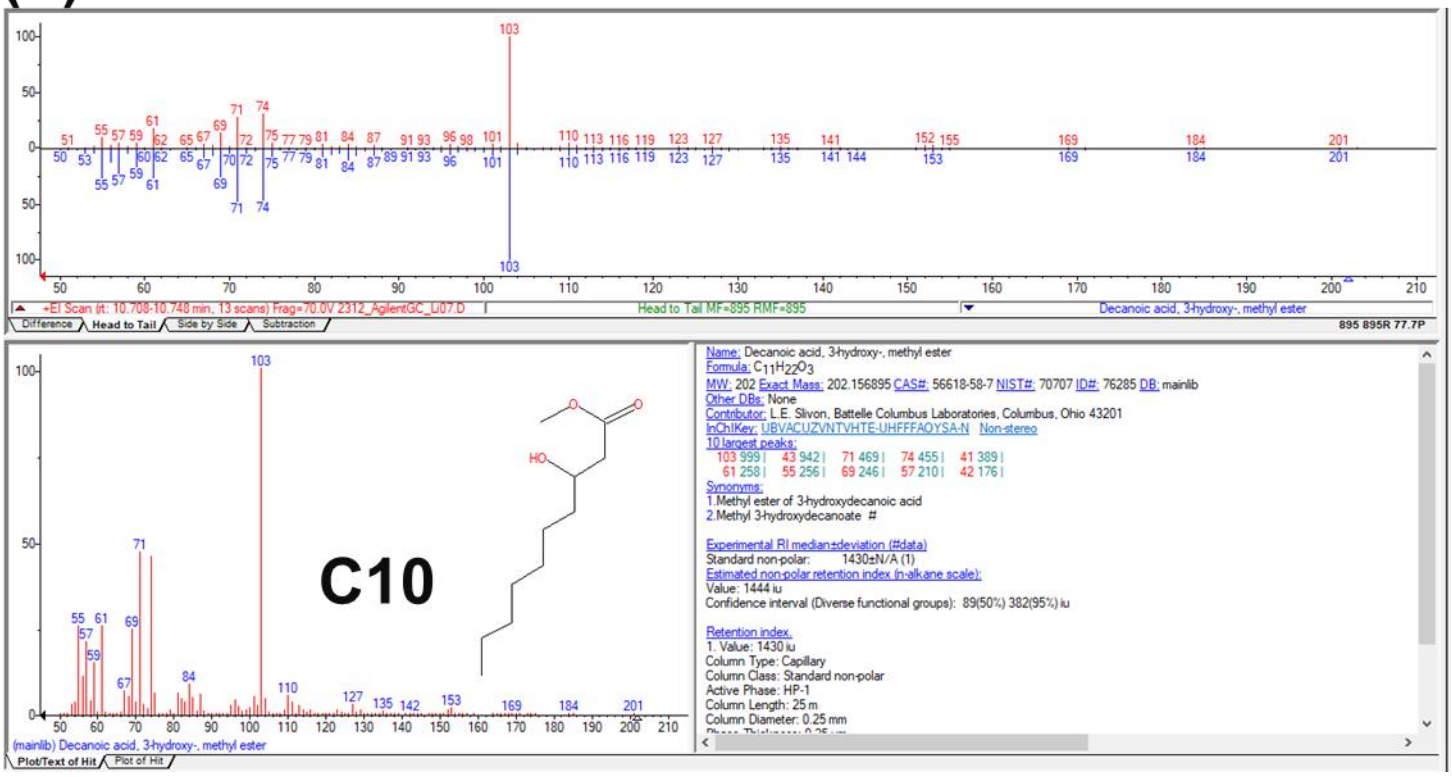
+EI Scan (rt: 10.708-10.748 min, 13 scans) Frag=70.0V 2312_AgilentGC_Li07.D
Head to Tail MF=895 RMF=895
Decanoic acid, 3-hydroxy-, methyl ester
Difference
Head to Tail
Side by Side
Subtraction
895 895R 77.7P
C10
(mainlib) Decanoic acid, 3-hydroxy-, methyl ester
Plot/Text of Hit
Plot of Hit
Name: Decanoic acid, 3-hydroxy-, methyl ester
Formula: C11H22O3
MW: 202 Exact Mass: 202.156895 CAS#: 56618-58-7 NIST#: 70707 ID#: 76285 DB: mainlib
Other DBs: None
Contributor: L.E. Slivon, Battelle Columbus Laboratories, Columbus, Ohio 43201
InChIKey: UBVACUZVNTVHTE-UHFFFAOYSA-N Non-stereo
10 largest peaks:
103 999 | 43 942 | 71 469 | 74 455 | 41 389 |
61 258 | 55 256 | 69 246 | 57 210 | 42 176 |
Synonyms:
1.Methyl ester of 3-hydroxydecanoic acid
2.Methyl 3-hydroxydecanoate #
Experimental RI median±deviation (#data)
Standard non-polar: 1430±N/A (1)
Estimated non-polar retention index (n-alkane scale):
Value: 1444 iu
Confidence interval (Diverse functional groups): 89(50%) 382(95%) iu
Retention index
1. Value: 1430 iu
Column Type: Capillary
Column Class: Standard non-polar
Active Phase: HP-1
Column Length: 25 m
Column Diameter: 0.25 mm

(e)

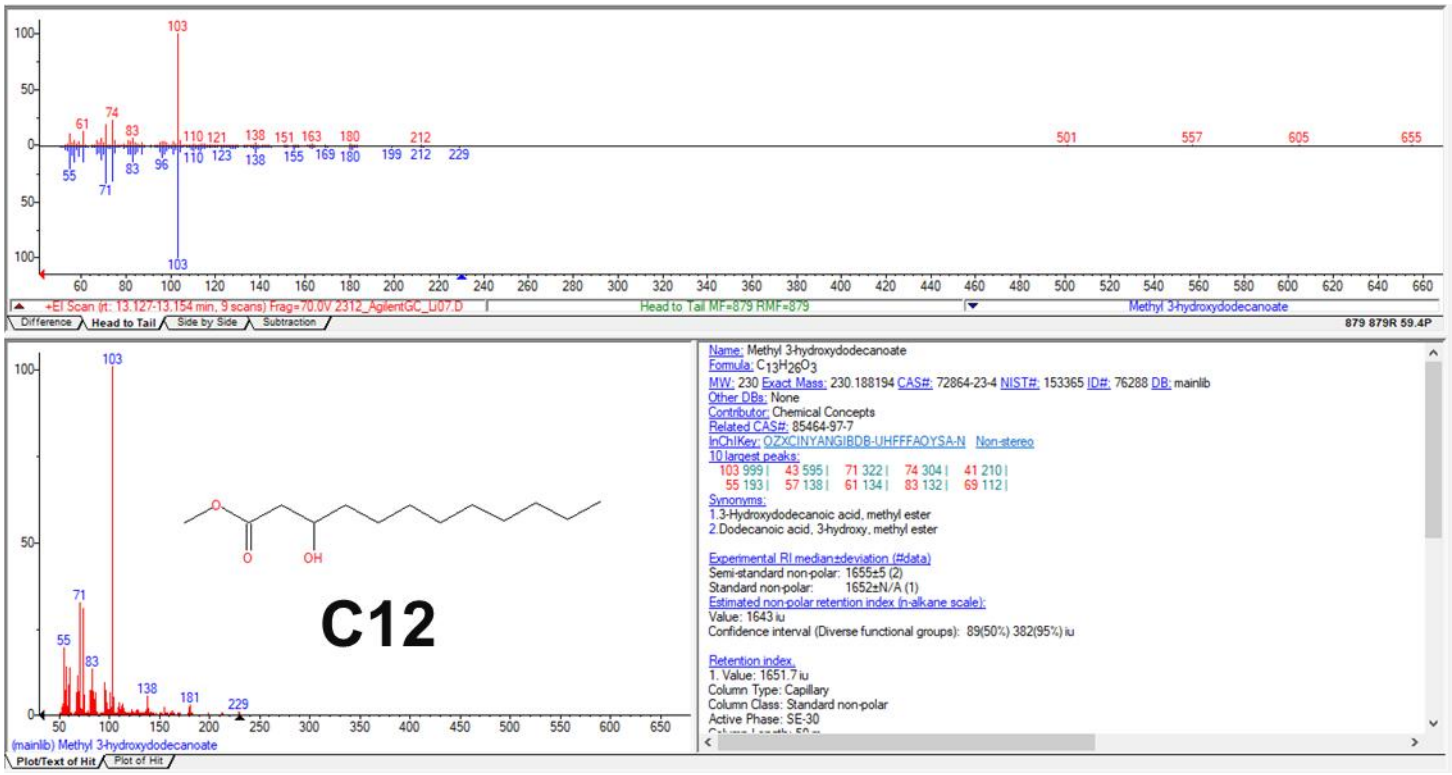
+EI Scan (rt: 13.127-13.154 min, 9 scans) Frag=70.0V 2312_AgilentGC_U07.D
Head to Tail MF=879 RMF=879
Methyl 3-hydroxydodecanoate
Difference
Head to Tail
Side by Side
Subtraction
879 879R 59.4P
C12
(mainlib) Methyl 3-hydroxydodecanoate
Plot/Text of Hit
Plot of Hit
Name: Methyl 3-hydroxydodecanoate
Formula: C13H26O3
MW: 230 Exact Mass: 230.188194 CAS#: 72864-23-4 NIST#: 153365 ID#: 76288 DB: mainlib
Other DBs: None
Contributor: Chemical Concepts
Related CAS#: 85464-97-7
InChIKey: QZXCINYANGIBDB-UHFFFAOYSA-N Non-stereo
10 largest peaks:
103 999 | 43 595 | 71 322 | 74 304 | 41 210 |
55 193 | 57 138 | 61 134 | 83 132 | 69 112 |
Synonyms:
1.3-Hydroxydodecanoic acid, methyl ester
2.Dodecanoic acid, 3-hydroxy, methyl ester
Experimental RI median±deviation (#data)
Semi-standard non-polar: 1655±5 (2)
Standard non-polar: 1652±N/A (1)
Estimated non-polar retention index (n-alkane scale):
Value: 1643 iu
Confidence interval (Diverse functional groups): 89(50%) 382(95%) iu
Retention index
1. Value: 1651.7 iu
Column Type: Capillary
Column Class: Standard non-polar
Active Phase: SE-30

(f)

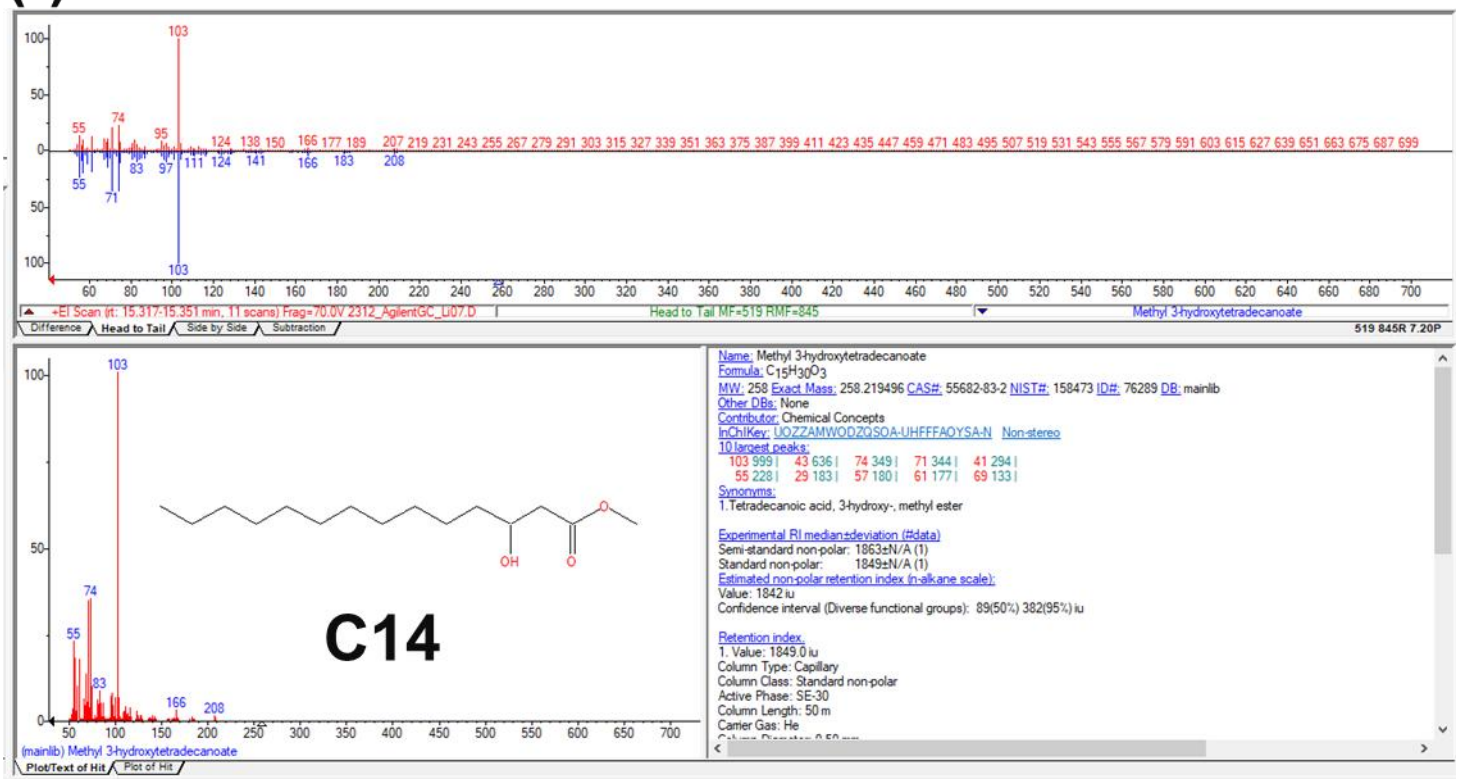
+EI Scan (rt: 15.317-15.351 min, 11 scans) Frag=70.0V 2312_AgilentGC_U07.D
Head to Tail MF=519 RMF=845
Methyl 3-hydroxytetradecanoate
Difference
Head to Tail
Side by Side
Subtraction
519 845R 7.20P
C14
(mainlib) Methyl 3-hydroxytetradecanoate
Plot/Text of Hit
Plot of Hit
Name: Methyl 3-hydroxytetradecanoate
Formula: C15H30O3
MW: 258 Exact Mass: 258.219496 CAS#: 55682-83-2 NIST#: 158473 ID#: 76289 DB: mainlib
Other DBs: None
Contributor: Chemical Concepts
InChIKey: UOZZAMWODZQSOA-UHFFFAOYSA-N Non-stereo
10 largest peaks:
103 999 | 43 636 | 74 349 | 71 344 | 41 294 |
55 228 | 29 183 | 57 180 | 61 177 | 69 133 |
Synonyms:
1.Tetradecanoic acid, 3-hydroxy-, methyl ester
Experimental RI median±deviation (#data)
Semi-standard non-polar: 1863±N/A (1)
Standard non-polar: 1849±N/A (1)
Estimated non-polar retention index (n-alkane scale):
Value: 1842 iu
Confidence interval (Diverse functional groups): 89(50%) 382(95%) iu
Retention index
1. Value: 1849.0 iu
Column Type: Capillary
Column Class: Standard non-polar
Active Phase: SE-30
Column Length: 50 m
Carrier Gas: He

Figure S4. GC-MS–based identification of PHA monomer methyl esters via mass spectral comparison. Mass spectra of methyl esters derived from the methanolysis of PHA samples were compared against reference spectra retrieved from the NIST database. Each panel (a–f) displays a pair of spectra: the top spectrum in red corresponds to the experimental MS data from the analyzed PHA sample, while the bottom spectrum in blue represents the reference spectrum of the corresponding methyl ester. Major fragment ions used for compound identification are labeled with their m/z values. Compound identities were confirmed based on agreement in both fragmentation patterns and retention time under identical GC-MS conditions. (a). 3-hydroxybutyrate (C4); (b). 3-hydroxyhexanoate (C6); (c). 3-hydroxyoctanoate (C8); (d). 3-hydroxydecanoate (C10); (e). 3-hydroxydodecanoate (C12); (f). 3-hydroxytetradecanoate (C14)

Additional Experimental Notes: Unexpected Misidentification of a Received *Rhodococcus jostii*

1. Background

At the beginning of my PhD project, the research objective was to genetically engineer *R. jostii* RHA1 for polyhydroxyalkanoate (PHA) production. The strain was obtained from a Spanish research group, contacted by my supervisor Dr. Kang Lan Tee. For simplicity, this strain is hereafter referred to as the Spanish strain.

All experimental work in the early phase of the PhD project was conducted using this strain, under the assumption that it was indeed *R. jostii* RHA1. It was not until the end of the second year that inconsistencies in experimental results prompted a formal identification of the strain, which ultimately revealed that it was not *R. jostii*, as initially believed. This misidentification had a significant impact on the early direction of the project.

2. Early Experiments

To avoid the use of hazardous organic solvents such as chloroform or dichloromethane for PHA extraction, we attempted an alternative method based on SDS-sonication

treatment (Arikawa et al., 2017). This method, originally developed for *Cupriavidus necator*, involves suspending lyophilized cells in an SDS solution followed by sonication to release intracellular PHA granules. The released material is subsequently washed with water and ethanol to remove impurities. According to the original study, PHA purity could reach up to 96%.

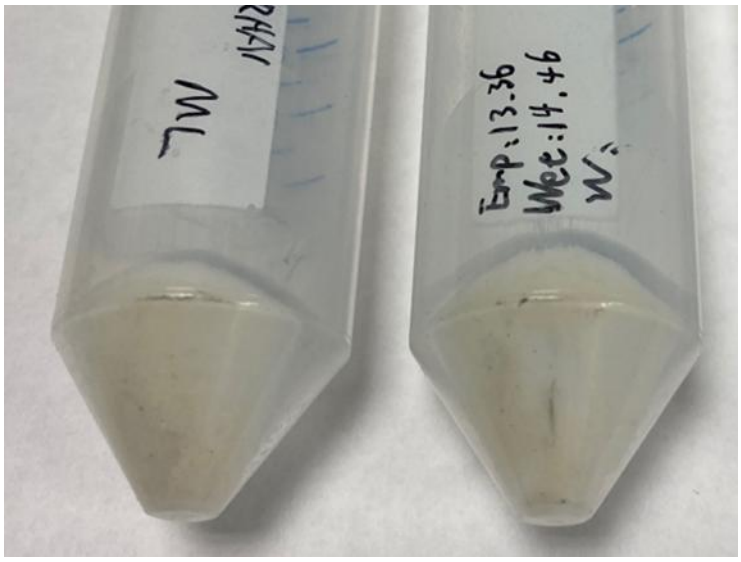

Figure S5. White solid extracted using SDS-sonication method from the Spanish strain.

We applied this method to the Spanish strain and successfully isolated a white solid material (**Figure S1**) from the cells, which we initially assumed to be PHA. However, at that time, the GC system in our laboratory was not fully installed, and we were unable to analyze the chemical composition of the extracted material.

3. Unexpected Findings and Troubleshooting

To preliminarily characterize the extracted material, we attempted NMR analysis. However, the samples exhibited extremely poor solubility in all commonly used solvents for NMR sample preparation, including chloroform, dichloromethane, acetone, methanol, and ethanol. This behavior led us to hypothesize that the white material might be high molecular weight PHA aggregates, although no literature reports supported such insolubility for PHA.

Genetic engineering work continued for over a year using the Spanish strain. After the GC system became fully operational and the PHA analysis protocol was established, we re-examined previously extracted samples. Surprisingly, GC analysis showed no detectable PHA monomers in the extracted material. Additional tests using lyophilized cells of the Spanish strain also failed to show any detectable PHA content.

Even more unexpectedly, these cells also lacked any detectable intracellular lipid content, as no fatty acid methyl ester were detected after methanolysis. This was highly unusual, as native *Rhodococcus* species are known for their ability to accumulate significant amounts of triacylglycerol and other lipophilic storage compounds. These results cast serious doubt on the identity of the strain. We subsequently sent the strain for 16S rRNA sequencing and full-genome identification.

4. Strain Identification and Conclusion

Sequencing results revealed that the predicted genus of the Spanish strain was *Escherichia–Shigella*, rather than *Rhodococcus*. This finding was supported by both whole-genome assembly and 16S rRNA classification analyses (**Figure S5**). Combined with the absence of PHA or lipid accumulation, as well as negative results from NMR and GC analyses, these results confirmed that the received strain had been misidentified and was not *Rhodococcus jostii* RHA1.

(a)

Sample	Expected assembly size	Assembly Size	Assembly size warning	Expected GC (%)	GC (%)	GC warning	16S warning
040206_Minglong1RjostiiSpain	9700000	10777253	High	66.97	59.83	Low	Yes

(b)

Expected Taxon	Contig	Coverage	Identity %	Warning	Predicted species	Predicted genus	Predicted family
Rhodococcus jostii	NODE_262	501	100	No match	Escherichia coli	Escherichia-Shigella	Enterobacteriaceae

Figure S6. Taxonomic identification of the Spanish strain based on genome and 16S rRNA sequence analysis. (a) Quality control (QC) metrics and classification results from whole-genome assembly, indicating that the closest genus-level match was Escherichia–Shigella. (b) 16S rRNA gene alignment and QC summary, supporting classification within the Escherichia–Shigella genus.

This discovery explains the anomalous experimental outcomes during the first 1.5 years of work with this strain. While the strain was eventually discontinued for further PHA studies, it served as a valuable model for testing plasmid-based expression systems. Interestingly, we found that genetically modified versions of the Spanish strain carrying various plasmids could produce detectable amounts of PHA. These results are summarized in **Table S8**, and they offer insight into the metabolic plasticity of this unidentified *Escherichia-Shigella* strain under synthetic pathway control.

Table S8. Summary of PHA production in plasmid-transformed Spanish strain (based on GC data).

Strain	Plasmid	CDW (g/L)	PHA content (wt% CDW)	PHA composition (mol%)
Escherichia-Shigella	pBBR1c-phaCAB	1.32	29.30%	100% C4

Strain	Plasmid	CDW (g/L)	PHA content (wt% CDW)	PHA composition (mol%)
	pBBR1c-CAG	1.18	4.47%	C8:C10:C12 = 33.85%:62.28%:3.87%

5. Evaluation of Carbon Sources, C/N Ratios, and SDS-Based Extraction

Before the misidentification of the strain was known, I performed extensive testing of culture conditions to optimize PHA production. This included evaluating various carbon sources (e.g., acetate, gluconate, glucose, fructose), adjusting carbon-to-nitrogen (C/N) ratios, and optimizing the SDS concentration used in the extraction process. However, as previously mentioned, the white material extracted from the Spanish strain was ultimately determined not to be PHA. As a result, the experimental data obtained under these conditions were rendered scientifically invalid and excluded from the main chapters of this thesis.

Due to the limited effectiveness of the SDS-sonication method, particularly in the context of extracting mcl-PHA, this approach was not used for any of the final PHA extraction procedures presented in the main body of this thesis. Despite repeated attempts, the white material obtained via SDS extraction could not be conclusively identified using standard analytical techniques such as GC or NMR.

These results suggest that the SDS-sonication method may have limited applicability when applied to non-model microorganisms, potentially due to differences in cell wall structure or intracellular composition. Consequently, only solvent-based extraction methods were adopted for the validated experiments reported in the main chapters. These findings underscore the importance of validating extraction methods for specific host strains and reinforce the decision to rely on solvent-based protocols for reliable PHA recovery.

6. Summary and Reflections

This case study illustrates how unverified assumptions in strain identity can profoundly impact the trajectory of research. The misidentification of the Spanish strain as *R. jostii* RHA1 led to over a year of exploratory work with misleading materials and results. Despite this setback, the experience provided several valuable lessons:

1. The critical importance of verifying strain identity, particularly when strains are received from external sources.
2. The limitations of alternative extraction methods, especially when applied to less-characterized PHA types.
3. The role of negative results in shaping future decisions, including a shift toward solvent-based extraction in this thesis.

Moreover, the process of troubleshooting, questioning assumptions, and ultimately resolving discrepancy served as a formative scientific experience. It highlighted the importance of scientific rigor and the value of method validation, particularly when developing new systems for microbial biosynthesis.

Reference

Arikawa, H., Sato, S., Fujiki, T. & Matsumoto, K. 2017. Simple and rapid method for isolation and quantitation of polyhydroxyalkanoate by SDS-sonication treatment. *Journal of Bioscience and Bioengineering,* 124**,** 250-254.